**Thesis**

# Expression Analysis of Eukaryotic Translation Initiation Factors in Pancreatic Ductal Adenocarcinoma


Submitted by

**Philip Puchas, BSc**


For the Academic Degree

**Doctor medicinae universae**

**(Dr. med. univ.)**


At the

**Medical University of Graz**

Performed at the

**Diagnostic & Research**

**Institute of Pathology**

Under Supervision of

**Univ.-Prof. Dr. med. univ. Dr. sc. nat. Johannes Haybaeck**

**Dr. scient. med. Nicole Golob-Schwarzl, MSc, BSc**


**April 18, 2019**

# Declaration of Authorship

*I hereby declare that this thesis and the work presented in it are my own and have been generated by the results of my original research. All contents primarily generated or stated by others have been properly marked as such and quoted thoroughly.*
*The contents of this thesis are subsequently submitted to peer-reviewed journals where they might be published in the future.*

*Graz, April 18, 2019* *Philip Puchas, BSc e.h.*

## Acknowledgements

First and foremost, I would like to sincerely thank my supervisor, *Prof. Johannes Haybaeck*, who made this research project possible for me. Not only through granting me the opportunity of working at his lab and providing the necessities, but also, and importantly, through his kind and contagiously positive attitude, he made this project and everything surrounding it a stimulating, great experience that further motivates me to pursue the scientific path I intended to follow.

Coinciding with and causatively implicated in all this, is also my co-supervisor, *Dr. Nicole Golob-Schwarzl*, whom I want to deeply thank. She guided me through all this and always knew what to do when I struggled with experiments.

Furthermore, I want to thank the whole lab group which so kindly received me. Thank you all for the great time, your help and your advice!

Besides this, I have to thank my dearest friends who accompanied me through the years at university and even earlier.

Last, and most of all, I want to thank my family.
My two sisters, *Claudia* and *Eva*, who somehow managed to not justifiably interrupt me every time I unceasingly spoke of some medical conditions nobody wanted to hear about, when we could indeed have spoken about social matters at family evenings instead.
And finally, my beloved parents. They imperturbably backed me up in every possible way and never stopped helping me in realizing the plans I made. All this would not have been possible without them and I owe them my biggest gratitude.

*To my parents*

# Abstract

**Introduction:**

Pancreatic cancer is one of the major causes of cancer related death worldwide. Its most important subtype is pancreatic ductal adenocarcinoma (PDAC). Deregulation of protein synthesis has been observed in various malignancies. Translation initiation is the rate-limiting step of protein synthesis which is regulated by eukaryotic translation initiation factors (eIFs). Differential expression of various eIFs has recently been reported in a range of malignancies. However, knowledge concerning eIF expression in PDAC remains scarce. The aim of this work was to provide insights into eIF expression patterns in PDAC and to analyze potential usefulness of eIFs as prognostic biomarkers.

**Methods:**

Immunohistochemistry (IHC) was used to characterize eIF expression in 174 cases of PDAC compared to 9 non-neoplastic pancreatic tissues (NNTs). *In vitro* expression analysis was performed on protein level using Immunoblots for PDAC (n = 56) and NNT (n = 28) and on mRNA level using qRT-PCR for PDAC (n = 38) and NNT (n = 22). Survival analysis was performed with protein expression data and *in silico* with The Cancer Genome Atlas (TCGA) public dataset (n = 125).

**Results:**

PDAC samples showed differential expression of various eIF subunits such as downregulation of eIF1, eIF2$\alpha$, eIF3C and eIF6 and upregulation of eIF3A in IHC. Immunoblot analysis confirmed the downregulation of eIF1, eIF2$\alpha$, eIF3C and eIF6 and further showed downregulation of eIF1A, phosphorylated eIF2$\alpha$ (p-eIF2$\alpha$), eIF3B and eIF4E. mRNA levels of *EIF1* and *EIF1AX* were found at lower levels in PDAC samples. High eIF2$\alpha$ protein level correlated with worse outcome. Additionally, high *EIF2A* and *EIF3C* mRNA levels correlated with poor prognosis, whereas high *EIF1* mRNA predicted better outcome.

**Conclusion:**

In this work, alterations in the expression of various eIFs in PDAC were demonstrated on protein and mRNA level, indicating their importance for pancreatic tumorigenesis.

Additionally, their relevance for tumor biology is supported by the findings, that *EIF1*, *EIF2A* and *EIF3C* mRNA as well as eIF2$\alpha$ protein levels significantly correlated with patient overall survival. They might therefore serve as prognostic biomarkers. However, further investigation is needed to fully understand the molecular mechanisms and implications of eIFs in PDAC tumorigenesis.

# Zusammenfassung

**Einleitung:**

Das Pankreaskarzinom ist eine der häufigsten Ursachen für Krebs-assoziierte Mortalität weltweit. Der häufigste histologische Subtyp ist das duktale Adenokarzinom (PDAC). Unter einer Vielzahl von anderen dysregulierten Prozessen wurde rezent die Relevanz alterierter Proteinbiosynthese in einigen Malignomen aufgezeigt. Der geschwindigkeitsbestimmende Schritt der Translation ist deren Initiation, welche durch eukaryotische Translationsinitiationsfaktoren (eIFs) gesteuert wird. Veränderungen der Expression unterschiedlicher eIFs und deren tumorbiologische Bedeutung wurden bereits in einigen Tumoren demonstriert. Im PDAC hingegen ist diesbezüglich bisher wenig bekannt. Das Ziel dieser Arbeit war daher, das Expressionsmuster der eIFs im PDAC und deren Evaluation hinsichtlich prognostischer Bedeutung zu erforschen.

**Methoden:**

Die Expression unterschiedlicher eIFs wurde mittels Immunhistochemie (IHC) in 174 PDACs ermittelt und mit 9 nicht-neoplastischen Kontrollgeweben (NNTs) verglichen. *In vitro* wurde auf Proteinebene mittels Immunoblot die eIF-Expression in PDACs (n = 56) bestimmt und mit NNTs (n = 28) verglichen, sowie auf RNA-Ebene in PDACs (n = 38) und NNTs (n = 22) mittels qRT-PCR. Überlebensanalysen wurden mit Proteindaten sowie mit öffentlich zugänglichen RNA-Daten (TCGA) durchgeführt.

**Ergebnisse:**

In den Tumorproben zeigten sich alterierte Expressionsmuster verschiedener eIFs wie beispielsweise die reduzierte Expression von eIF1, eIF2$\alpha$, eIF3C und eIF6 sowie die erhöhte Expression von eIF3A in der IHC. Die reduzierte Expression von eIF1, eIF2$\alpha$, eIF3C und eIF6 bestätigte sich im Immunoblot, welcher außerdem eine reduzierte Expression von eIF1A, phosphoryliertem eIF2$\alpha$ (p-eIF2$\alpha$), eIF3B und eIF4E zeigte. Auf mRNA Ebene zeigte sich eine reduzierte Expression von *EIF1* und *EIF1AX* in den Tumorproben. Hohe eIF2$\alpha$ Proteinexpression korrelierte mit schlechterem Gesamtüberleben. Hohe *EIF2A* und *EIF3C* mRNA Expression

korrelierte mit einer signifikant schlechteren Prognose, wohingegen hohe *EIF1* mRNA Expression mit einem günstigeren Verlauf korrelierte.

**Schlussfolgerung:**

In dieser Arbeit konnten Alterationen der Expression mehrerer eIFs im PDAC auf Protein und mRNA Ebene demonstriert werden, wodurch ihre potentielle Relevanz für die pankreatische Karzinogenese aufgezeigt wird. Verdeutlicht wird dies auch dadurch, dass beispielsweise die Expression von *EIF1*, *EIF2A* und *EIF3C* auf mRNA Ebene und die Expression von eIF2$\alpha$ auf Protein Ebene signifikant mit der Prognose der Patienten korrelierte. Nichtsdestotrotz ist zusätzliche Forschung auf dem Gebiet notwendig um die molekularen Mechanismen und die Implikationen der eIFs in der pankreatischen Tumorgenese gänzlich zu erklären.

# Contents

# Abbreviations

| | |
|---|---|
| 4E-BP | eIF4E-binding protein |
| ADM | acinar-to-ductal metaplasia |
| AJCC | american joint committee on cancer |
| APS | ammonium persulfate |
| ATM | ataxia-telangiectasia mutated |
| BRAF | B-rat fibrosarcoma |
| BRCA1/2 | breast cancer 1/2 |
| BSA | bovine serum albumin |
| CDKN2A | cyclin-dependent kinase inhibitor 2A |
| cDNA | complementary deoxyribonucleic acid |
| CT | computed tomography |
| DTT | dithiothreitol |
| DNA | deoxyribonucleic acid |
| e.g. | example given |
| eIF | eukaryotic translation initiation factor |
| EMT | epithelial-mesenchymal transition |
| ERK | extracellular regulated kinase |
| EUS | endoscopic ultrasound |
| FFPE | fresh-frozen paraffin-embedded |
| FPC | familial pancreatic cancer |
| GAP | GTPase-activating protein |
| GAPDH | glyceraldehyde-3-phosphate dehydrogenase |
| GEF | guanine exchange factor |
| GEM | genetically engineered mouse |
| GNAS | guanine nucleotide binding protein, alpha stimulating |
| GTP | guanosine triphosphate |
| HE | hematoxylin-eosin |
| HIER | heat-induced epitope retrieval |
| HKG | housekeeping gene |
| hTERT | human telomerase reverse transcriptase |
| IC | initiation complex |

| | |
|---|---|
| i.e. | id est |
| IHC | immunohistochemistry |
| IPMN | intraductal papillary mucinous neoplasm |
| IPO8 | importin 8 |
| kDa | kilo dalton |
| KRAS | kirsten rat sarcoma virus |
| mAb | monoclonal antibody |
| MAPK | mitogen-activated protein kinase |
| MCN | mucinous cystic neoplasm |
| MEK | MAPK/ERK kinase |
| Met-tRNA$_i$ | initiator-methionyl-tRNA |
| miRNA | micro ribonucleic acid |
| MLH1 | MutL homolog 1 |
| mRNA | messenger ribonucleic acid |
| MSH2/6 | MutS homolog 2/6 |
| mTOR | mammalian/mechanistic target of rapamycin |
| NET | neuroendocrine tumor |
| NNT | non-neoplastic tissue |
| ORF | open reading frame |
| PABP | poly-(A)-binding protein |
| PanIN | pancreatic intraepithelial neoplasia |
| PC | pancreatic cancer |
| PCR | polymerase chain reaction |
| PDAC | pancreatic ductal adenocarcinoma |
| PI3K | phosphoinositide 3-kinase |
| PIC | preinitiation complex |
| PVDF | poly vinylidene fluoride |
| PRSS1 | cationic trypsinogen |
| qRT-PCR | quantitative real-time polymerase chain reaction |
| RAF | rapidly accelerated fibrosarcoma |
| RNA | ribonucleic acid |
| RPL41 | ribosomal protein L41 |
| RT | reverse transcriptase |
| SDHA | succinate dehydrogenase complex subunit A |

| | |
|---|---|
| SDS-PAGE | sodium dodecyl sulfate polyacrylamide gel electrophoresis |
| SEM | standard error of the mean |
| SMAD4 | mothers against decapentaplegic homolog 4 |
| SPINK1 | serine protease inhibitor kazal type 1 |
| STK11 | serine/threonine kinase 11 |
| TBS(T) | tris-buffered saline (tween) |
| TC | ternary complex |
| TCGA | the cancer genome atlas |
| TEMED | tetramethylethylenediamine |
| TMA | tissue microarray |
| TP53 | tumor protein p53 |
| tRNA | transfer ribonucleic acid |
| UICC | union for international cancer control |
| UTR | untranslated region |
| YWHAZ | 14-3-3 protein zeta/delta |

# List of Figures

# List of Tables

# 1 Introduction

## 1.1 Pancreatic cancer

### 1.1.1 Epidemiology, etiology and risk factors

Pancreatic cancer (PC) is among the most fatal forms of cancer ranking fourth in cancer-related deaths in both sexes in 2018 (1). It is surpassed only by lung, colorectal and prostate cancer in men and by breast, lung and colorectal cancer in women (1). With an estimated 55,440 newly diagnosed cases in the United States in 2018 it comprises around 3.2% of all new cancer cases (2). Despite this relatively small proportion, it accounts for almost 7.3% of total cancer-related deaths with an estimated 44,330 deaths due to pancreatic cancer, markedly underlining its fatality compared to other forms of cancer (2). Similarly, high numbers are also reported for the European Union, where 44,500 deaths due to PC are estimated for 2018 with an unfavorable trend, marking a slight increase in mortality rates in women, in contrast to declining mortality rates observed in most other entities (3).

When analyzed on a global scale, there were an estimated 458,918 (2.5% of all diagnosed cancers) new cases of PC in 2018 and almost the same amount of deaths due to the disease (432,242, 4.5% of total cancer deaths) (4). Importantly, the incidence and the mortality rates due to PC will most likely increase, as the impact of most risk factors is rising due to the demographic and life-style development worldwide (5).

As the abovementioned numbers clearly demonstrate, PC is and continues to be a massive burden for global health. Therefore, numerous studies have tried to elucidate potential causes and risk factors for the disease. The most well-established, non-familial risk factors include cigarette smoking (as well as second-hand smoke), diabetes mellitus, chronic inflammation (chronic pancreatitis), diet, obesity and advancing age (5,6). Of the environmental factors, smoking is an etiologic factor for about 25% of PC cases and was also shown to negatively affect survival, with increasing hazard ratios for higher consumption (7,8). Taking all environmental factors into account, meta-analytical epidemiological studies found that almost two-thirds of PCs are potentially preventable (9).

Besides the modifiable risk factors, a broad range of inherited factors has been linked to PC. These include genetic alterations implied in well-known cancer-

predisposition syndromes such as Li-Fraumeni syndrome (*TP53*), Lynch Syndrome (mutations in mismatch repair genes such as *MLH1*, *MSH2* or *MSH6*), hereditary breast and ovarian cancer syndrome (*BRCA1/2*), Peutz-Jegher´s syndrome (*STK11*), Ataxia telangiectasia (*ATM*) and forms of hereditary pancreatitis (*PRSS1*, *SPINK1*) (10). In contrast to these genetically defined syndromes, there is yet another group of PC-susceptible patients without specific genetic mutation accounting for 4-10% of all cases, summarized as familial pancreatic cancer (FPC) with at least two first-degree-relatives affected by the disease (11).

### 1.1.2 Pathology of (pre)malignant pancreatic tumors

Malignant pancreatic tumors are mainly classified based on their microscopic appearance regarding cellular morphology, histoarchitecture and differentiation (either originating from ductal, acinar or islet/neuroendocrine cells) and their macroscopic characteristics (solid or cystic) (12). By far the most common malignancy, representing ~85% of cases, is pancreatic ductal adenocarcinoma (PDAC), followed by neuroendocrine tumors (NETs, ~5%) and other rarely encountered types such as acinar cell carcinoma, pancreatoblastoma and solid-pseudopapillary neoplasms (12). The focus herein will be on PDAC.

#### 1.1.2.1 Pancreatic ductal adenocarcinoma (PDAC)

PDAC is mainly located in the head of the pancreas and macroscopically appears as white, firm lesion with infiltrating character with a mean size of around 3 cm in resected specimens (Figure 1A) (13).

The histological characteristics of PDAC include glandular structures composed of atypical cells with adjacent strong desmoplastic reaction (14). The glandular histoarchitecture is successively lost during the process of dedifferentiation. Well- and moderately-differentiated tumors (G1 & G2) show medium- to small-sized glandular and duct-resembling structures with aberrant and irregular growth patterns (15). The nuclei can be multiple times larger than those of adjacent non-neoplastic cells (16). In well-differentiated tumors, the mitotic rate is usually low. High-grade tumors (G3), in contrast, display poorly-differentiated glands, tumor cells in solid nests as well as single infiltrating cells, loss of mucin production and often high numbers of mitoses (Figure 1B - E) (15).

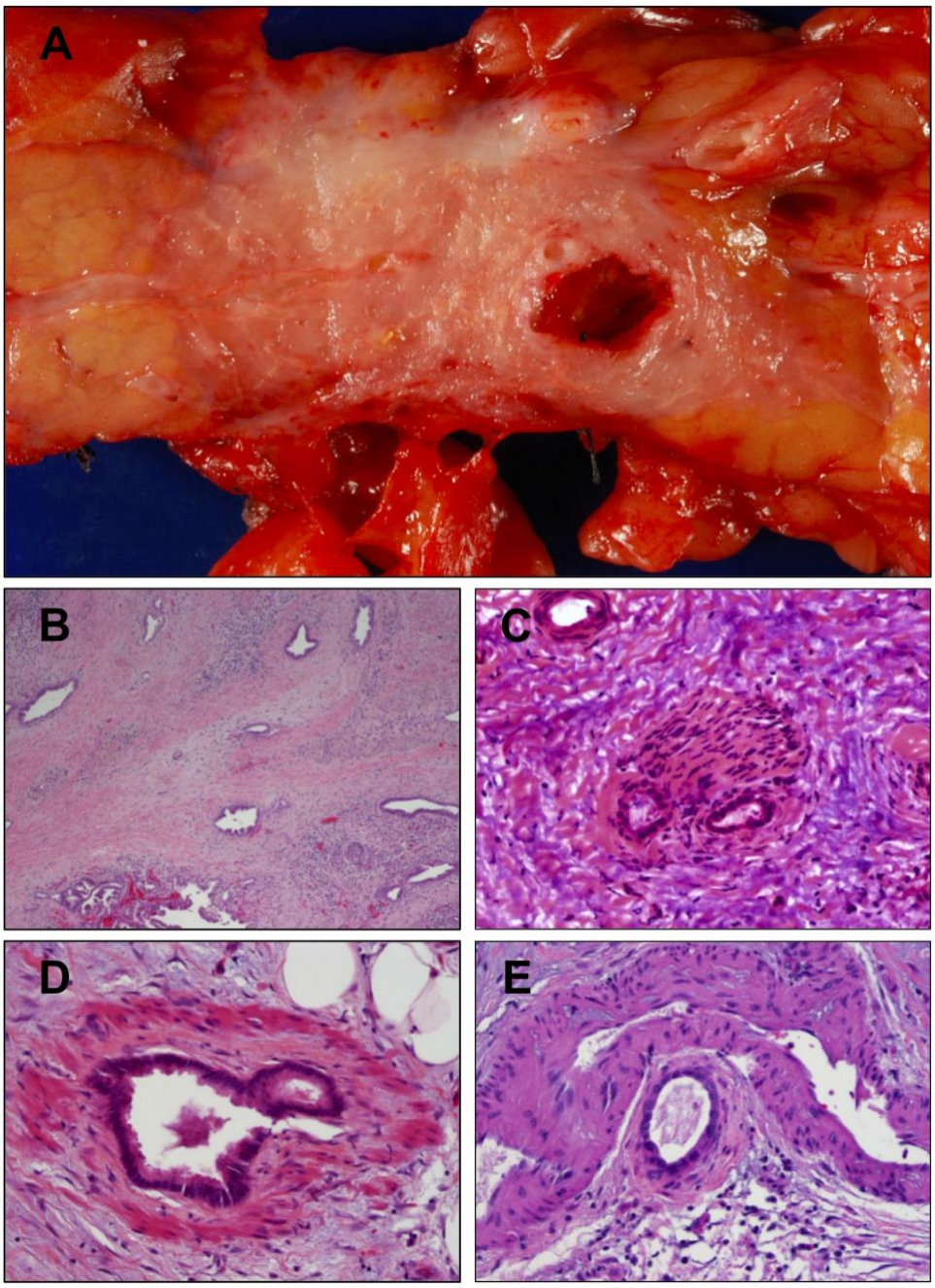


***Figure 1: Macroscopic and histological characteristics of pancreatic ductal adenocarcinoma.***
**(A)** Gros morphology of PDAC. **(B-E)** Key histological features of PDAC: **(B)** haphazard glandular structures, **(C)** perineural invasion, **(D)** venous invasion and **(E)** glandular structures directly adjacent to muscular arteries. (Figure reprinted from (13), with kind permission of the publisher)

Further common features of PDAC include perineural infiltration, lymph and blood vessel invasion and early metastatic spread to local lymph nodes. A large study including 1,175 ductal adenocarcinomas in pancreaticoduodenectomy specimens found a distribution of tumor differentiation of 3% well-, 56% moderately-, 46% poorly-differentiated and 0.2% undifferentiated/anaplastic tumors (17).

As histopathological differential diagnosis of PDAC can be challenging, Hruban and Klimstra summarized the key features of PDAC as opposed to reactive glands (Table 1) (13).

***Table 1: Histopathology of PDAC.***
Key features in histopathological diagnosis of PDAC compared to reactive changes. (Content adopted from (13), with kind permission of the publisher)

| **Ductal adenocarcinoma** | **Reactive glands (e.g. pancreatitis)** |
|---|---|
| Haphazard gland arrangement | Lobular gland arrangement |
| Perineural invasion | Neuroendocrine cells may be close to nerves |
| Vascular invasion | |
| Glands directly adjacent to muscular artery | Glands separated from vessels by acinar cells or connective tissue |
| Luminal necrosis | May have polymorph leucocytes but no necrotic epithelial cells |
| Incomplete lumina | Complete rings of epithelial cells form lumina |
| Four-to-one rule (nuclei vary in size within one gland more than four to one) | Nuclei sizes vary less than four to one in one gland |
| Glands without connective tissue in fat | Glands in fat are associated with connective tissue |

Immunohistochemically, most ductal adenocarcinomas show reactivity with site-unspecific epithelial markers such as different cytokeratins (cytokeratin 7,8,18,19 and partially 20), but also different mucins (mucin 1, 3, 5AC, 6) and general tumor markers, also currently used as serum tumor markers in clinical follow-up (carcinoembryonic antigen, carcinoma antigen 19-9) (18–20). Furthermore, most pancreatic adenocarcinomas show altered expression of p53 and loss of p16 and SMAD4 expression (21).

Besides the typical appearance described above, different variants of PDAC have been reported. These include adenosquamous carcinoma, colloid carcinoma, undifferentiated or anaplastic carcinoma, osteoclast-like giant cell tumor, signet-ring cell carcinoma, medullary carcinoma and hepatoid carcinoma (22–28).

#### 1.1.2.2 Precursor lesions

The model of step-wise tumorigenesis first arose in 1990, when Vogelstein and Fearon proposed the adenoma-carcinoma sequence for colorectal cancer, stating that malignant tumors develop through multiple, accumulating genetic events yielding premalignant lesions that later manage to acquire malignancy-defining traits (e.g. the ability to invade surrounding structures or the formation of distant metastases) (29). Models developed later-on have proposed that PDAC arises in very similar fashion: through successive dedifferentiation and malignant transformation of precursor lesions (Figure 2) (30). Ever since, multiple studies have demonstrated further evidence and broadened our understanding of these premalignant conditions, summarized in (31). The most common precursor lesion is pancreatic intraepithelial neoplasia (PanIN), followed by intraductal papillary mucinous neoplasm (IPMN) and mucinous cystic neoplasm (MCN) (32). Another recently identified pancreatic premalignant lesion is intraductal tubulopapillary neoplasm (ITPN), though its molecular profile differs from the majority of PDACs, suggesting alternative oncogenic pathways (33).

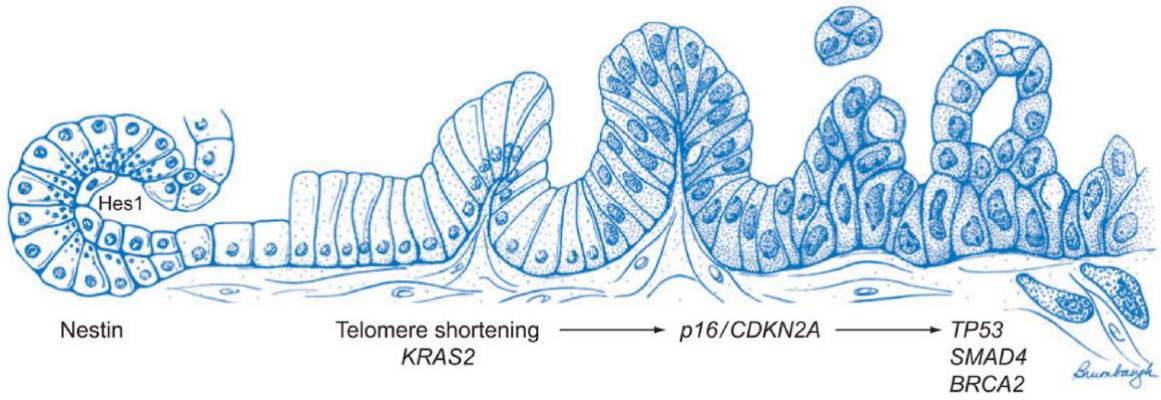


***Figure 2: Multi-step carcinogenesis of pancreatic cancer.***

Model of successive dedifferentiation of normal pancreatic epithelium from low and high grade PanIN to invasive carcinoma (left to right). Altered key regulators are listed as well. (Figure reprinted from (14), with kind permission of the publisher)

##### 1.1.2.2.1 Pancreatic intraepithelial neoplasms (PanINs)

PanINs are neoplastic lesions with ductal morphology (usually <0.5cm) and are currently separated into two grades (low and high grade) (34,35). Histological features of PanIN range from flat epithelial lesions with (micro)papillary or basally pseudostratified architecture, basal nuclei with mucin and none or minor signs of

atypia in low-grade lesions (former PanIN-1A and 1B) to highly atypical (macronucleoli, shift in nucleus-to-cell-size favoring the nucleus, atypical mitoses) epithelial cell clusters with necrotic cells protruding into the duct-lumen, cribriform gland structures and loss of cell polarity (basal-to-apical cell structure) in high-grade (former PanIN-3) lesions (Figure 3A, B) (36). However, as PanINs are defined as non-invasive precursor lesions, the basement membrane is still intact, prohibiting every kind of infiltrative or metastatic spread. In recent genetic studies, PanINs were shown to harbor similar genetic alterations that are also encountered in its end-stage, malignant variant – i.e. PDAC (37,38).

##### 1.1.2.2.2 Intraductal papillary mucinous neoplasms (IPMNs)

This distinct entity reflects a group of grossly visible lesions (usually >1cm) with papillary architecture and mucin-producing, hypersecreting, columnar cells in either the main pancreatic duct, the branch ducts or both (39,40). Based on more detailed histological characterization IPMNs have been classified to various subtypes: the gastric, intestinal, pancreatobiliary and oncocytic type (Figure 3C - F) (41,42). As pancreatic cysts are often identified incidentally in asymptomatic patients by magnetic resonance imaging (with a prevalence up to 19.9% (43)), the evaluation of their malignant potential is of great interest.

Molecular profiling of IPMNs revealed mutations commonly encountered in PDAC such as the *KRAS* point mutation in codon 12 but also, and importantly, characteristic mutations in the *GNAS* gene, discriminating it from other precursor lesions (44). The same study found that the mutation is also found in PDACs associated with IPMNs, but not in other cystic pancreatic neoplasms or PDACs without associated IPMNs, hinting to its role in malignant transformation of IPMNs and its potential in underpinning the causative precursor of a given invasive tumor (44). Various other commonly deregulated pathways such as the PI3K/AKT pathway, the hedgehog pathway and the expression of human telomerase reverse transcriptase (*hTERT*) were shown to be altered to different extent in IPMNs, summarized in (45).

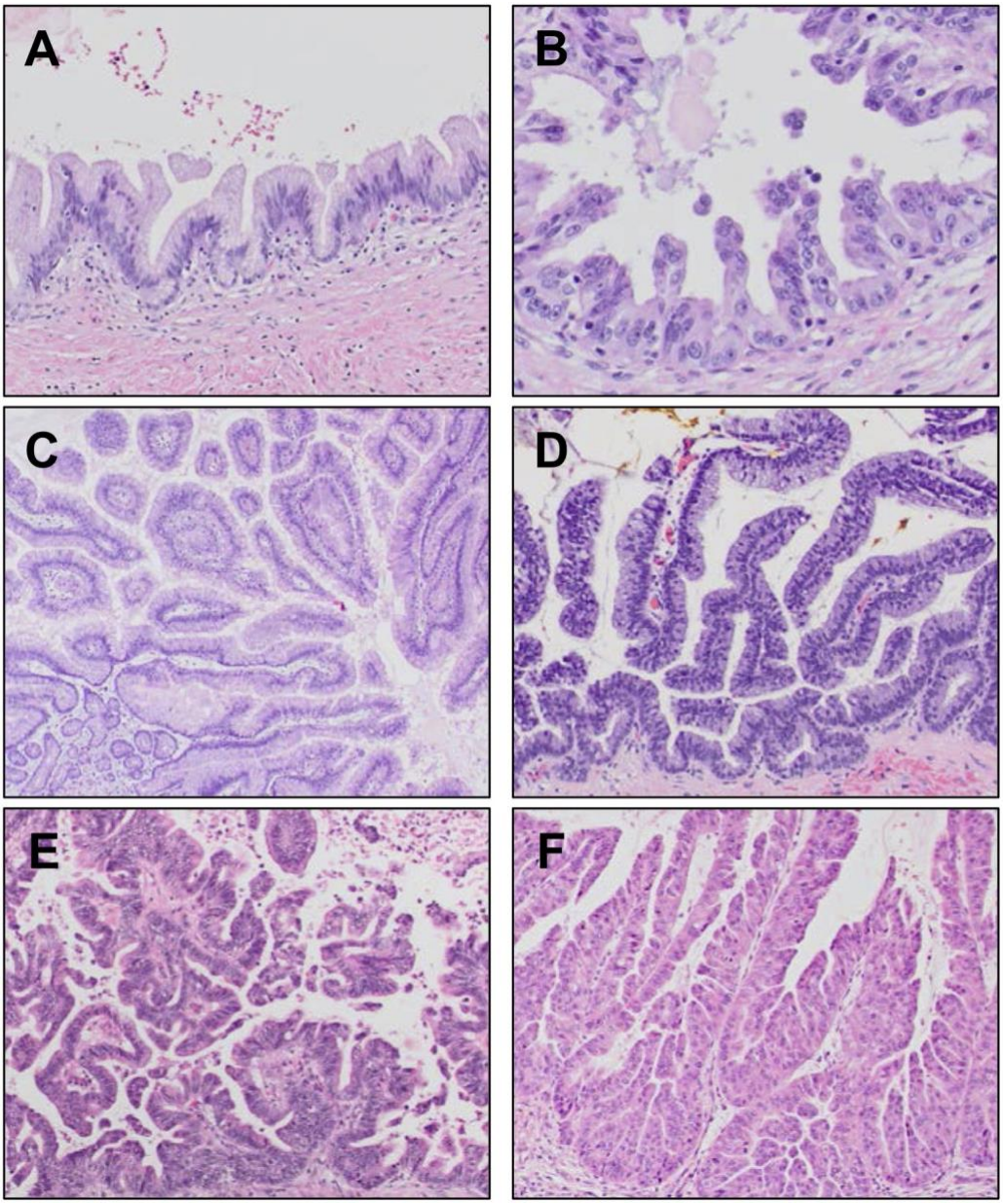


***Figure 3: Haematoxylin-Eosin (HE) staining of various precursor lesions of PDAC.***

Pancreatic intraepithelial neoplasia (PanIN) **(A)** low-grade and **(B)** high-grade. Intraductal papillary mucinous neoplasm **(C)** gastric type, **(D)** intestinal type, **(E)** pancreatobiliary type and **(F)** oncocytic type. (Figure reprinted from (46), with kind permission of the publisher)

#### 1.1.2.2.3 Mucinous cystic neoplasms (MCNs)

Mucinous cystic neoplasms (MCN) are cystic lesions with an ovarian-type stroma topped by a mucin-producing epithelial lining, almost exclusively affecting women (47). They are grossly visible with sizes > 1cm and do usually not, in contrast to IPMNs, communicate with larger pancreatic ducts (48). As in IPMNs and PanINs, MCNs do also harbor mutations that are encountered in invasive adenocarcinomas, some of which are: *KRAS*, *TP53* and *SMAD4* mutations (47). As demonstrated by

thorough pathological investigation, invasive carcinoma does occur focally in these lesions, making total resection a necessity to prevent malignant progression (49).

##### 1.1.2.2.4 Intraductal tubulopapillary neoplasms (ITPNs)

ITPNs are rare (< 1% of exocrine pancreatic neoplasms), recently identified pancreatic neoplasms characterized by grossly visible, nodular masses without mucin production (50). Histologically, they display tubulopapillary growth with cribriform glandular structures, high-grade atypia, focal necrosis and – in contrast to IPMNs – no supranuclear mucin (50). ITPNs are frequently associated with invasive cancers, with reports ranging from 30 to 81% (33,51). However, molecular profiling and modern sequencing techniques have revealed distinct mutation patterns in ITPNs and their associated epithelial malignancies, differing vastly from other precursor lesions and PDAC itself – e.g. *KRAS* and *BRAF* mutations did not occur in any ITPN samples (in 19 examined cases, respectively (51,52)) – indicating involvement of different oncogenic pathways. As their contribution to common PDAC carcinogenesis therefore seems rather negligible, ITPNs will not be further detailed here.

### 1.1.3 Molecular pathology of PDAC

#### 1.1.3.1 Key regulators in PDAC carcinogenesis

As indicated above, pancreatic carcinogenesis is a multi-step process resulting from accumulating genetic alterations, leading from normal epithelium, to non-invasive precursor lesions with increasing atypia to invasive carcinoma. The number and identity of involved genes and their respective pathways were identified through large-scale sequencing revealing that pancreatic cancers harbor 63 genetic alterations on average (53). Contextualizing the altered genes to cellular processes showed core pathways (e.g. DNA damage control, apoptosis, KRAS signaling, Wnt/Notch signaling) that are deregulated in pancreatic cancer to different extent (53). Among these, changes in four driver genes have turned out to be of critical importance: the *KRAS* oncogene mutation and *TP53*, *p16/CDKN2A* and *SMAD4* inactivation (the latter three functioning as tumor suppressor genes) (54).

*KRAS* activation occurs through an activating point mutation in around 90% of pancreatic cancers and is almost exclusively found in codon 12 of the oncogene (rarely also in 13 and 61), most commonly changing the normal glycine to aspartate (G12D) or valine (G12V) (55). The actively rendered pathway is involved in initiating tumorigenesis (as it occurs early in precursor lesions such as PanINs and was shown to induce PanIN formation in mouse models) and has a plethora of downstream effects such as activation of the MEK/ERK pathway via RAF and activation of the PI3K/AKT/mTOR pathway (Figure 4) (56–59).

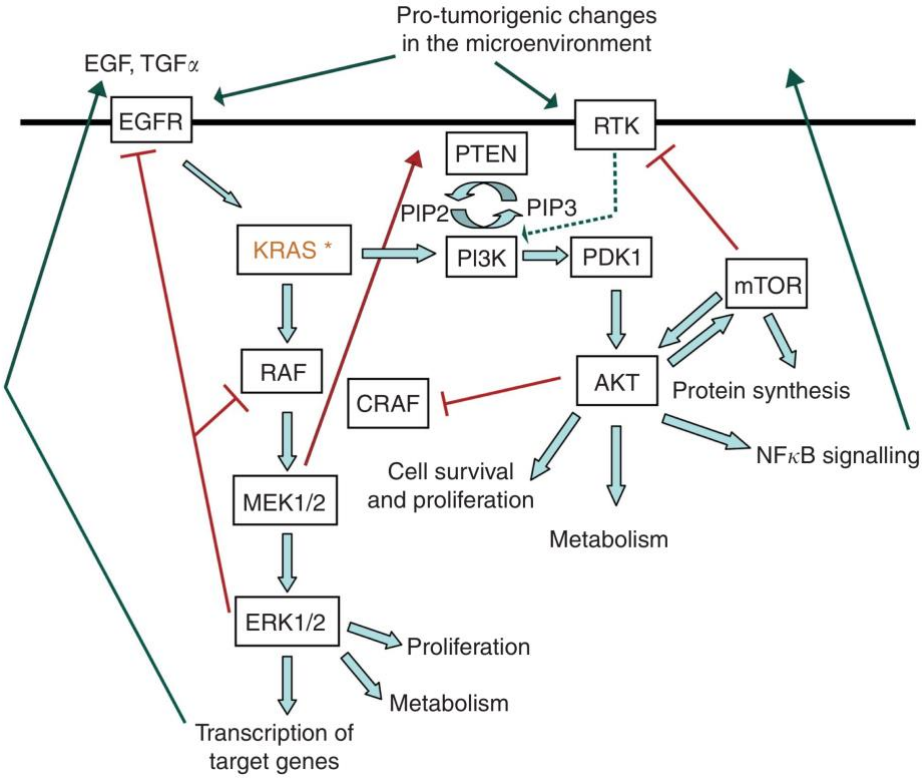


***Figure 4: KRAS signaling and downstream effectors.***

Depicted are the downstream effectors of the KRAS oncoprotein (asterisk indicates the mutational activation). Activation of the RAF/MEK/ERK cascade leads to enhanced proliferative signaling, whereas the PI3K/AKT/mTOR axis regulates protein synthesis, cellular metabolism and cell survival. Green arrows indicate activating signals, red arrows indicate anti-tumorigenic feedback-loops. (Figure reprinted from (59), reused under the creative commons license CC BY 4.0)

In case of the tumor suppressor genes mentioned above inactivation of both alleles is needed. This is achieved through combinations of either homozygous deletions or loss of heterozygosity. This leads to inactivation of *p16/CDKN2A* in > 90% (leading to loss of cell cycle control), *TP53* in around 75% (causing deregulation of cellular proliferation and impaired apoptosis upon DNA damage) and *SMAD4* in

around 55% (deregulating signal transduction of transforming growth factor β) of PDACs (54,60).

Besides these key factors encountered in the majority of tumors, novel analyses have tried subclassifying pancreatic cancers into distinct molecular and genetic subtypes. Whole genome-approaches have yielded classifications according to chromosomal structure and stability with first hints to clinical applicability in predicting chemotherapy response (61). Additionally, expression of transcriptional factors and pathway members were used to define four main subtypes of pancreatic cancers on a molecular basis: the squamous, pancreatic progenitor, immunogenic and aberrantly differentiated endocrine exocrine (ADEX) subtype (62). These promising results might allow for personalized therapeutic approaches in the future.

#### 1.1.3.2 Cells of origin in PDAC

Although vast knowledge on molecular characteristics and genetic aberrations in PDAC and its precursor lesions accumulated over the last few decades, the precise cell type giving rise to these neoplasms remains a topic of discussion (63). Early findings, based mainly on histomorphology, characterized most PDACs as being descendant directly from duct epithelium (64). Multiple studies have tried creating a more detailed model by using genetically engineered mouse (GEM) models, most of which rely on inducible $KRAS^{G12D}$ expression in certain pancreatic cell types to trace the origin of different precursors. The most convincing model to date is, that both the acinar cell and the duct epithelial cell can give rise to PDAC, but with different pathophysiology (65).

The majority seems to arise from acinar cells via transdifferentiation to duct-like cells through a process called acinar-to-ductal metaplasia (ADM), consecutively causing PanIN and PDAC formation (66–68). Notably, *NR5A2* encoding a key regulator of acinar cell function, was identified as PDAC-susceptibility locus and its conditional deletion in mice was shown to dramatically promote PanIN and PDAC formation, supporting the ADM-PanIN-PDAC model (69). Importantly, the transdifferentiation process was also shown to occur in cultured human cells, indicating that this pathway may also be prevalent in humans (70).

Nonetheless, the genuinely postulated cell of origin – as indicated above, the duct epithelial cell – was also shown to play an important role in PDAC carcinogenesis. The subset of tumors developing via IPMNs is hypothesized to descend from this

population (63). Evidence supporting this hypothesis came from multiple studies, one of which showed that loss of *BRG1*[1] reproducibly causes IPMN and PDAC formation as well as transformation of adult duct cells, but inhibits *KRAS*-driven PanIN development in acinar cells (71). Additionally, PDAC formation in a murine model was effectively recapitulated through expression of oncogenic *KRAS* and inactivation of *TP53* (whereas sole oncogenic *KRAS* expression did not suffice) in ductal epithelial cells, supporting their potential as effective cells of origin in PDAC (72).

While the dualistic acinar cell→PanIN→PDAC versus ductal cell→(IPMN→)PDAC model might be too simplistic to explain the actual process in its details, it poses an attractive framework to explain PDAC development as known to date (Figure 5).

Notably, attempts to differentiate the cellular origin in PDAC specimens revealed that AGR2 could be used as molecular marker, whose high expression points towards a ductal cell origin and low expression to an acinar cell origin (65).

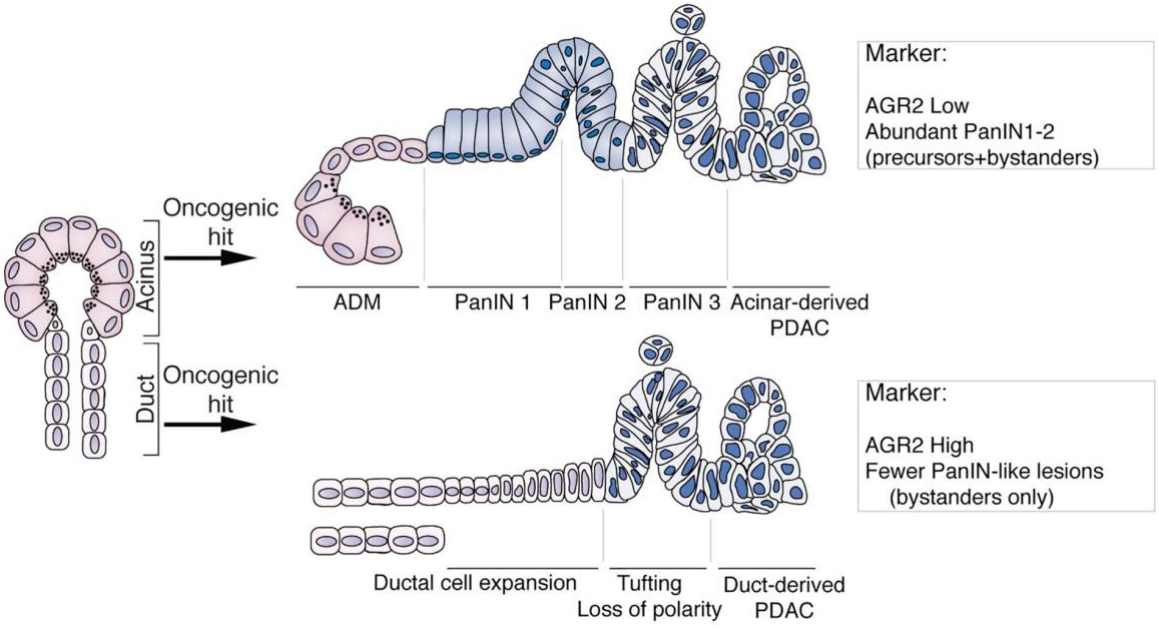


***Figure 5: Cells of origin in PDAC.***

Pathogenetic models of acinar-derived PDACs and duct-derived PDACs are indicated. PanIN precursors are typical for acinar-derived tumors, whereas PanIN-like bystander lesions can occur in both types. Also, AGR2 expression may allow for stratification concerning the cell of origin. (Reprinted from (65), reused under the creative commons license CC BY 4.0)

[1]A subunit of the SWI/SNF chromatin remodeling complex whose loss is implicated in KRAS-dependent formation of cystic pancreatic neoplasms.

### 1.1.4 TNM classification and stages of pancreatic cancer

The recently released, revised version of the UICC/AJCC Cancer Staging Manual, 8th Edition, classifies pancreatic cancer as indicated in Table 2 (73). The resulting prognostic stages are shown in Table 3.

***Table 2: TNM classification of pancreatic cancer according to the UICC and AJCC Cancer Staging Manual, 8th Edition (2017).***

| **Primary tumor (T)** | |
|---|---|
| TX | Primary tumor cannot be assessed |
| T0 | No evidence of primary tumor |
| Tis | Carcinoma in situ (including high-grade PanINs, IPMNs, MCNs, ITPNs) |
| T1 | Tumor ≤ 2 cm |
| T1a | Tumor ≤ 0.5 cm |
| T1b | Tumor > 0.5 cm and < 1 cm |
| T1c | Tumor 1 to 2 cm |
| T2 | Tumor > 2 and ≤ 4 cm |
| T3 | Tumor > 4 cm |
| T4 | Tumor involves celiac axis, superior mesenteric artery and/or common hepatic artery, regardless of size |
| **Regional lymph nodes (N)** | |
| NX | Regional lymph nodes cannot be assessed |
| N0 | No regional lymph node metastasis |
| N1 | Metastasis in 1-3 regional lymph nodes |
| N2 | Metastasis in 4 or more regional lymph nodes |
| **Distant metastasis (M)** | |
| M0 | No distant metastasis |
| M1 | Distant metastasis |

***Table 3: Prognostic stages in pancreatic cancer according to the UICC and AJCC Cancer Staging Manual, 8th Edition (2017).***

| **Stage** | **T** | **N** | **M** |
|---|---|---|---|
| 0 | Tis | N0 | M0 |
| IA | T1 | N0 | M0 |
| IB | T2 | N0 | M0 |
| IIA | T3 | N0 | M0 |
| IIB | T1-3 | N1 | M0 |
| III | Any T | (N1 if T4) N2 | M0 |
| IV | Any T | Any N | M1 |

### 1.1.5 Diagnosis, treatment and prognosis

The diagnosis of PDAC is usually made at an advanced stage, as the disease lacks specific early symptoms (74). Due to the dismal prognosis resulting from this constellation, Keane et al. aimed to reveal alarming symptoms occurring within 2 years prior to diagnosis (75). In their cohort (n = 2,790), the patients experienced the following symptoms: abdominal pain (44%), jaundice (31%), change in bowel habit (27%), dyspepsia (20%), nausea/vomiting (17%), back pain (16%), new-onset diabetes (14%), non-cardiac chest pain (12%), weight loss (11%) and lethargy (11%). Notably, in a subgroup analysis, among 296 patients 268 (91%) presented to primary health care providers with relevant symptoms within the same period. Evaluation is initiated through either clinical suspicion if some of the abovementioned symptoms are presented or because of incidental findings in abdominal radiologic examinations due to other reasons.

The recommendations of the European Society for Medical Oncology for diagnostic work-up of a pancreatic mass starts with computed tomography (CT) and branches upon the initial findings (76): Non-metastatic, resectable and locally advanced disease should be further investigated using endoscopic ultrasound (EUS). Magnetic resonance imaging might be considered in non-characterizable lesions. Fine-needle aspiration biopsy of either the primary lesion via EUS or metastatic lesions (e.g. in the liver) in advanced disease should be performed in all tumors except confirmed non-metastatic, resectable lesions (15-20%) where immediate surgery without biopsy is recommended. Histopathological work-up of either the biopsy or the resected specimen confirms the diagnosis. The only prognostic biomarker currently in use is the serum level of carbohydrate antigen 19-9 (CA 19-9), whose applicability lies in the measure of disease burden, possible treatment guidance and as prognostic parameter (high preoperative levels indicate a worse prognosis).

Treatment options depend on the staging results, classifying disease as either resectable, borderline resectable, locally advanced or metastatic disease (76): Whereas treatment in resectable disease primarily consists of surgery followed by adjuvant chemotherapy or (within trials) chemoradiotherapy, neoadjuvant chemoradiotherapy should be used in patients with borderline resectable disease to enable consecutive surgery. In contrast, treatment of locally advanced and

metastatic disease relies exclusively on chemotherapy (plus possible radiotherapy in locally advanced disease).

The prognosis of pancreatic cancer is strongly associated with the AJCC stage at time of diagnosis. The median overall survival drops with increasing stage, as indicated by survival data for surgically resected disease: for stage IA it was 38 months, stage IB 24 months, stage IIA 17 months, stage IIB 17 months and stage III 14 months when stratified by the 8$^{th}$ Edition staging system (77).

As resection especially increases survival for early-stage disease, this effect decreases with higher stage-disease, so that the median overall survival for stage IV disease – whether resected or non-resected – is 2.5 months and 5-year overall survival is 0.7% (78)[2]. Furthermore, as stage IV disease accounts for the majority of patients making up 55.2% in this study (with $n_{total}$ = 121,713), the collective median overall survival across all stages is a disastrous 3.5 months (78).

[2] The stage IV survival data refer to the 6$^{th}$ edition of the staging manual. However, definition of stage IV disease is identical to the recent 8$^{th}$ edition.

## 1.2 Translation initiation and its relevance for PDAC

### 1.2.1 Translation in eukaryotes

Translation is the process of protein synthesis from RNA by deciphering its nucleotide sequence, yielding polypeptide chains (79,80). Altered protein synthesis is a main characteristic of human tumors resulting from the fact that many oncogenic pathways regulate translation as one of their most downstream effects (81). Translation is subdivided into four steps: initiation, elongation, termination and ribosome recycling. The rate-limiting step and consequently, the most tightly regulated one, is the initiation process, concerted by a plethora of eukaryotic translation initiation factors (eIFs), acting in manifold ways to generate the fully functional ribosomal apparatus (82). Thus, translation initiation with its major players is also the process most implicated in tumorigenesis and progression and has therefore received growing attention over the last few decades, harnessing a large body of knowledge concerning its relevance in human cancers (83).

Generally, translation initiation consists of five distinct steps. First, the 43S preinitiation complex (PIC) is formed. Simultaneously, the messenger RNA (mRNA) is activated through attachment of eIF4F via an eIF4F-cap complex, followed by recruitment of this mRNA complex to the prepared 43S PIC, forming the 48S initiation complex (IC) (84). This results in scanning of the mRNA to localize the initiation codon. Lastly, the 60S ribosome joins, causing peptide synthesis to commence (82). After this brief overview, the process and the involved eIFs will be detailed in the following chapters and is schematically outlined in Figure 6.

#### 1.2.1.1 Translation initiation

##### 1.2.1.1.1 Assembly of the 43S preinitiation complex (PIC)

In order to prepare the small, 40S subunit of the ribosome for translation, several factors must be recruited to it. As translation starts at an AUG and happens through complementary, transfer RNAs (tRNAs) acting as adaptors with specific amino acids bound to them, the respective first tRNA, i.e. the initiator-methionyl-tRNA (Met-$tRNA_i$) needs to be directed to the small subunit. For this purpose, it is bound by eIF2 and GTP, forming the ternary complex (TC) (85). eIF2 is a heterotrimeric complex, consisting of three subunits (eIF2$\alpha$, $\beta$ and $\gamma$) (86).

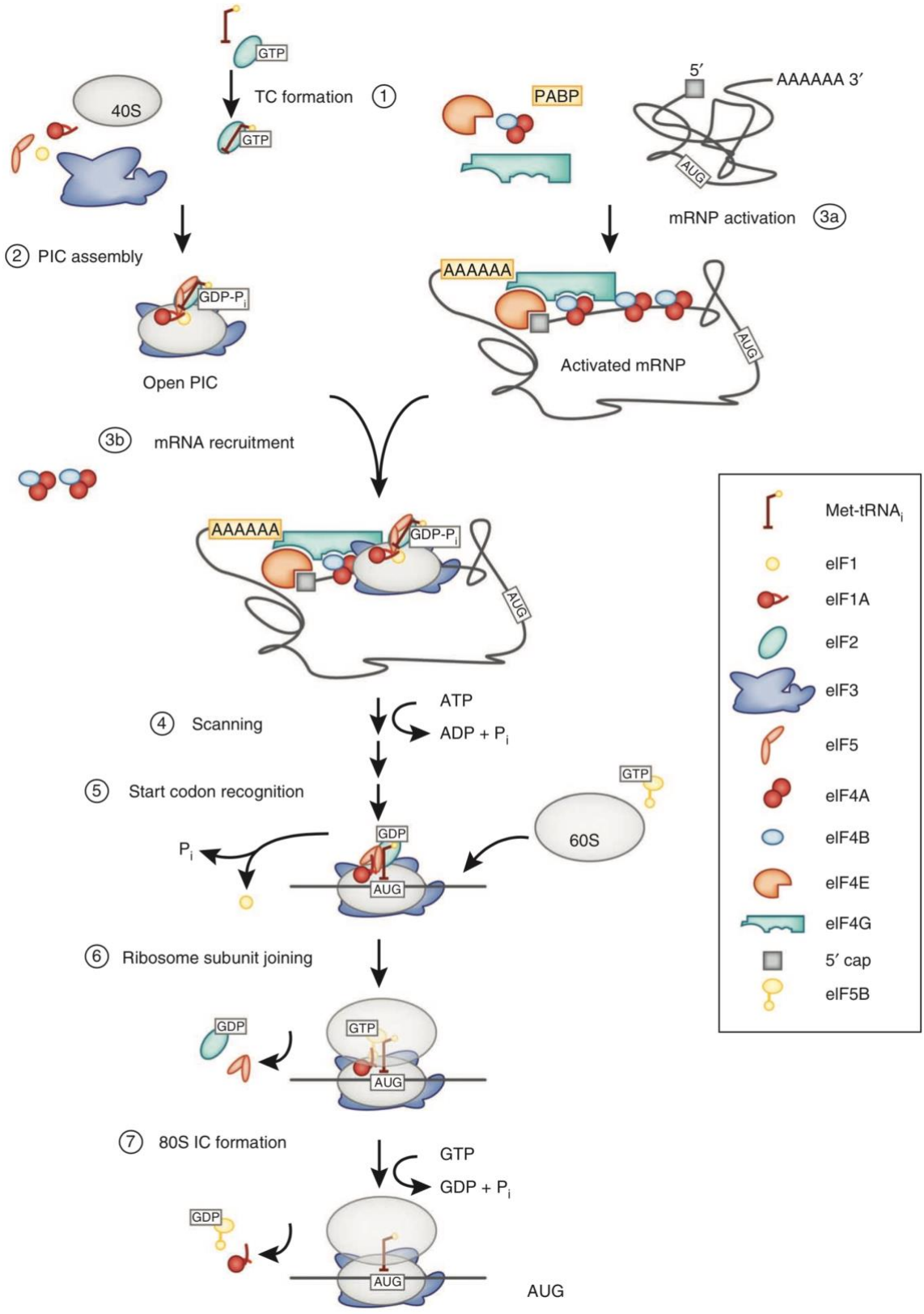


***Figure 6: Translation initiation in eukaryotes.***

**(1 + 2)** 43S preinitiation complex assembly starts with formation of the ternary complex. **(3a)** mRNA activation is enabled by various interaction partners and is followed by **(3b)** mRNA recruitment to the PIC. **(4)** The PIC scans the mRNA until **(5)** start codon recognition. **(6)** Joining of the large subunit (60S). **(7)** GTP hydrolysis and factor dissociation yields the functional 80S initiation complex and enables elongation. For details about involved eIFs see main text. (Reprinted from (85), with kind permission of the publisher)

Importantly, translational activity is negatively regulated through phosphorylation of eIF2$\alpha$, as it blocks eIF2B, the guanine-exchange factor (GEF) of eIF2 from exchanging its hydrolyzed GDP to an active GTP, fixing it in an inactive state (87). Global protein synthesis is regulated through this process by integrating diverse pathways upon various stimuli such as nutritional stress, endoplasmic reticulum stress or during antiviral response (88). However, in case of non-phosphorylated eIF2$\alpha$ the TC is abundantly formed and consecutively bound to the 40S subunit by eIF1, eIF1A, eIF3 and eIF5 to initiate translation (89,90).

#### 1.2.1.1.2 Preparation of the mRNA – eIF4F binding

Following transcription, eukaryotic mRNAs undergo two important modifications that act to prevent degradation: addition of a 5´ 7-methyl-guanosine cap and a 3´ poly(A) tail (91). Both modifications are crucially needed for the canonical[3], cap-dependent pathway of translation initiation, which is regarded as the standard mechanism in eukaryotes (85). The 5´ cap is recognized by eIF4F, a multi-subunit factor consisting of eIF4E, eIF4A and eIF4G (92). Binding of the cap is mediated through eIF4E, whereas eIF4A acts as a helicase unwinding secondary structures in the 5´ untranslated region (5´ UTR) (92). eIF4G, the largest subunit, tethers the subunits and the mRNA together by acting as a molecular scaffold, having attachment sites for eIF4A, eIF4E, poly-(A)-binding protein (PABP1) and eIF3 (93). PABP attaches to the 3´ poly(A) tail of the mRNA, thereby enabling circularization of the mRNA through interaction with eIF4G – a mechanism implied in stabilization and translation regulation through facilitating reinitiation on the same mRNA after ribosomal termination (94–96). Finally, the interaction site with eIF3 is needed for mRNA recruitment to the 43S PIC (97).

#### 1.2.1.1.3 mRNA recruitment – 48S IC formation

As mentioned above, the interaction of eIF3 as part of the 43S PIC and eIF4G bound to the activated mRNA is crucial for mRNA binding to the small ribosomal subunit, leading to the formation of the 48S IC. The responsible eIF3 subunits for this interaction were shown to be eIF3C, eIF3D and eIF3E (97). Furthermore, besides

[3]As opposed to non-canonical initiation through various mechanisms, e.g. internal ribosomal entry sites (IRES).

mapping the interaction sites, the activity of this interaction was studied and was shown to be stimulated *in vivo* by activation of the PI3K/AKT/mTOR pathway (98). To date, multiple other bridging contacts between the 43S PIC, the mRNA and phosphorylation sites on various eIF3 subunits have been identified (99). Loading of the activated mRNA onto the 43S PIC causes the latter to undergo multiple structural rearrangements to fit the mRNA into its binding channel and to form the functional 48S IC (84). However, the specific location and interaction of all involved factors including their regulation remains to determined.

#### 1.2.1.1.4 Scanning and start codon selection

Following the formation of the 48S IC at the 5´ end of the mRNA, the former starts scanning the mRNA in 5´→ 3´ direction until an AUG initiation codon is encountered (100). eIF1 and eIF1A seem to play a crucial role in stabilizing the scanning competent conformation and in start site recognition fidelity (82,101,102). Additionally, the eIF4F complex and eIF4B seem to aid the scanning process through unwinding of secondary structures in the 5´ UTR (82). A key event in halting the scanning process is the dissociation of eIF1 from its binding site upon base pairing of the initiating codon and the complementary initiator tRNA, keeping the small ribosomal subunit in its position (103). This conformational change causes eIF5, the GTPase-activating protein (GAP) of eIF2, to activate eIF2-GTP hydrolysis and release of organic $P_i$, the latter marking the irreversible step in start codon selection (104).

#### 1.2.1.1.5 48S IC and 60S subunit joining

Formation of a fully functional ribosome is enabled by joining of the large 60S subunit, carrying the peptidyl-transferase activity (105). The process is regulated by eIF6, which is bound to the 60S subunit and prevents premature association. Multiple cellular signaling pathways integrate towards eIF6 affinity to the large subunit, mediating its dissociation (105). Besides eIF6 dissociation from the 60S subunit, the remaining eIFs from the 40S subunit must dissociate to enable subunit joining. This is mediated through eIF5B, causing eIF1, eIF2-GDP and eIF5 to dissociate from the inter-subunit cleft (106). After subunit joining, GTPase activity of eIF5B is stimulated by eIF1A, resulting in its dissociation from the newly formed 80S

ribosome (107). In a final step, eIF1A dissociates and the elongation-competent 80S ribosome starts translation (107).

### 1.2.2 eIFs and their implications in cancer

The role of various eIFs and their differential expression in numerous entities has recently been reviewed in (108,109). Therefore, the following will only cover the eIFs discussed in this work.

#### 1.2.2.1 eIF1 and eIF1A

eIF1 (encoded by *EIF1*, also *sui1* on chromosome 17) is a protein with a length of 113 amino acids (12.7 kDa) cooperating with eIF1A (encoded by *EIF1AX*, as it resides on chromosome X), measuring 144 amino acids (16.5 kDa), to enhance start codon selection fidelity (108,110). eIF1 furthermore seems to play a role in response to genotoxic stress, as it is induced upon treatment with genotoxic stimuli such as UV light (111). Besides its role in translation initiation, eIF1A has recently been shown to affect miRNA processing by stimulating AGO2, a protein implicated in biogenesis through cleavage of miRNA-precursors (112). However, knowledge concerning the involvement of eIF1 and eIF1A in carcinogenesis remains scarce.

#### 1.2.2.2 eIF2$\alpha$ and phospho-eIF2$\alpha$

eIF2$\alpha$ (encoded by *EIF2S1*) is a 315 amino acids (36.1 kDa) long subunit of the heterotrimeric eIF2 complex, acting through providing the Met-tRNA$_i$ to the 40S subunit and by enabling start codon recognition through hydrolyzing the eIF2-associated GTP (86). Importantly, regulation of eIF2 occurs through phosphorylation of eIF2$\alpha$ to p-eIF2$\alpha$, causing higher affinity to its GEF eIF2B, but inhibiting the GTP-GDP exchange activity, which in turn significantly reduces TC abundance, leading to inhibition of global protein synthesis (88). However, presence of p-eIF2$\alpha$ has been shown to selectively favor translation of activating transcription factors involved in cellular response to various stressors, also referred to as “integrated stress response” (113). Though several studies implicated this pathway as anti-neoplastic and pro-apoptotic, also high levels eIF2$\alpha$-phosphorylation in human tumors were described (114,115). Besides the phosphorylation status, other roles of eIF2$\alpha$ in tumorigenesis have been described. Overexpression was found in

a plethora of tumors, which seems to be the most common eIF2 alteration (108). However, eIF2$\alpha$ mutants that evade phosphorylation (eIF2$\alpha^{S51A}$) have been shown to facilitate transformation of normal cells (116). Hence, eIF2$\alpha$ and its regulation seem to play a role in tumor formation.

#### 1.2.2.3 eIF3A

eIF3A (encoded by *EIF3A*, also *EIF3S10*, *p170* or *p150*) is the largest subunit, consisting of 1,382 amino acids (170 kDa), of the multimeric eIF3 complex (108,117). Its relevance for tumor biology has been well established and its overexpression has been implicated in an array of malignancies, such as colon (118), lung (119) and urothelial carcinoma (120) among other cancer entities.

#### 1.2.2.4 eIF3C

eIF3C (encoded by *EIF3C*) is a 913 amino acid long (110 kDa) subunit of the eIF3 complex and resides on the p-arm of chromosome 16 (108,121). eIF3C specifically interacts with eIF1 (110). It was shown to act pro-oncogenic, as artificial overexpression in NIH 3T3 cells leads to enhanced proliferation, anchorage-independent growth and attenuated apoptosis (122).

#### 1.2.2.5 eIF4E

eIF4E (encoded by *EIF4E*[4]) is composed of 237 amino acids (25 kDa) and is responsible for 7-methylguanosine cap recognition and binding of the eIF4F complex, therefore being critical for translation initiation (123). Besides this cap recognition function, it also acts through stimulation of the helicase activity of eIF4A enhancing transcription of mRNAs with highly structured 5´UTRs as encountered in many pro-oncogenic mRNAs (124). Consistent with these findings, overexpression of eIF4E hardly affects translation of the vast majority of cellular genes, including housekeeping genes, but rather selectively increases translation of key regulatory and malignancy-promoting genes (125). However, other mechanisms of regulating eIF4E activity and availability are also of great importance. eIF4E-binding proteins (4E-BPs, with three known isoforms referred to as 4E-BP1, 2 and 3), act through

[4] Multiple paralogues have been described, such as *EIF4E2* and *EIF4E3* encoding the identically-named proteins. However, as eIF4E1 is the biologically most relevant protein product, it will herein be referred to as eIF4E, as commonly done in the literature.

binding of eIF4E, thereby inhibiting its activity (126). Thus, 4E-BPs function as tumor suppressors. Loss of 4E-BPs or inactivation through phosphorylation have been shown to dramatically promote tumorigenesis and to be of prognostic relevance in various tumors (127,128). Lastly, eIF4E itself is also subject to phosphorylation by mitogen-activated protein kinase (MAPK)-interacting kinases, termed MNK1 and 2 (129). Unsurprisingly, phosphorylated eIF4E has been shown to promote tumorigenesis in a variety of studies, acting through selective translation of pro-tumorigenic mRNAs (130–132).

#### 1.2.2.6 eIF4G

eIF4G (encoded by *EIF4G1*) is the largest eIF4F subunit, composed of 1,606 amino acids (175 kDa) (108). As indicated above, its main function is to act as a molecular scaffold, recruiting and coordinating an abundance of factors (82). Overexpression of eIF4G was found in various entities, such as squamous cell lung carcinoma (133) and breast cancer (134), and was shown – similar to eIF4E – to selectively enhance translation of survival-related genes upon DNA damage *in vitro*, implicating its relevance in tumorigenesis (135).

#### 1.2.2.7 eIF5

eIF5 (encoded by *EIF5*) is a 431 amino acid long (49 kDa) protein acting in the final stages of translation initiation by promoting GTP hydrolysis prior to subunit joining (108,136). Some evidence implicates eIF5 in tumor biology, with one study hinting to oncogenic *ATF4* induction upon eIF5 overexpression (137). Notably, eIF5 knockdown was shown to reduce overall translation and to alter cellular behavior in colorectal cancer cell lines by inducing apoptotic markers and by impeding proliferation *in vitro* (138).

#### 1.2.2.8 eIF6

Last, eIF6 (encoded by *EIF6*), with a length of 245 amino acids (27 kDa), regulates cytoplasmic availability of the 60S subunit, thereby affecting the last step of initiation, i.e. subunit joining (82,108). Additionally, it is required for ribosome biogenesis in the nucleus (83,139). Nucleolar overexpression was found in various tumors, including head and neck cancers (140) and colorectal carcinomas (141). However,

the cytoplasmic relevance, function and contribution of eIF6 in tumorigenesis are a less straight-forward matter. As would be expected from the anti-association factor activity indicated above, eIF6 overexpression in various cell lines was shown to cause strong translational inhibition (142). Conversely, a haploinsufficiency mouse-model ($eIF6^{+/-}$) demonstrated impaired $G_1$/S cycle progression, defective translation initiation and reduction of transformational response upon oncogenic stimuli (143). Interestingly, eIF6 was also found to play a role in microRNA-mediated posttranscriptional silencing of various genes and its depletion alters regulation of target protein and mRNA levels (144). Hence, differential expression of eIF6 *in vivo* may affect cellular behavior in either way, depending on the altered miRNAs and their respective targets. Adding to this notion, eIF6 and Drosha[5] were found to be co-overexpressed in ovarian cancer (145). Confusingly, the same study also showed that low eIF6 expression correlates with worse outcome, somewhat contrasting to its pro-tumorigenic properties implied through overexpression. Hence, the relevance of eIF6 in tumorigenesis seems to be context-dependent and remains to be fully elucidated.

### 1.2.3 eIFs in PDAC

Relatively little is known about the role of eIFs in PDAC so far. However, some hints about their involvement in PDAC biology have been reported in recent years.

#### 1.2.3.1 eIF3A overexpression

Wang et al. demonstrated eIF3A overexpression on mRNA level in 30 PDAC cases and on protein level, via immunohistochemistry, in 140 cases (146). They found no correlation of eIF3A expression with age of onset, gender, tumor size, location of differentiation (146). However, significant correlation of eIF3A expression was observed with nodal positivity and TNM stage (146). Furthermore, they demonstrated functional relevance of eIF3A in PDAC biology, as knockdown in several cell lines caused inhibition of cell motility and proliferation (146).

[5] A protein regulating miRNA biogenesis to their active forms, which then continue to exert their functions in a RNA induced silencing complex (RISC).

#### 1.2.3.2 Enhanced eIF4E activity

As described above, eIF4E activity may be enhanced through several mechanisms including hyperphosphorylation of eIF4E or regulation of its binding protein (4E-BP1 and 2). Indeed, such alterations have also been shown in PDAC. eIF4E phosphorylation was shown to be implicated in irradiation response of PDAC cell lines through mediating a SOX2-dependent response (147). Additionally, eIF4E phosphorylation mediates ZEB1-dependent epithelial-mesenchymal transition (EMT) and targeting of eIF4E-phosphorylating kinases leads to growth inhibition of human PDAC organoids (148).

Besides direct modifications of eIF4E, its regulator, 4E-BP, was also shown to be altered in PDAC. Martineau et al. reported downregulation of 4E-BP1 in human PDAC samples and demonstrated successive loss of 4E-BP1 in a mouse model of PDAC (149). This loss consequently rendered eIF4E available for activation via phosphorylation and was shown to enhance tumor growth in mice (149).

#### 1.2.3.3 eIF5A overexpression

eIF5A, a factor found to undergo a very specific posttranslational modification called hypusination, was shown to be upregulated in PDAC (150). This alteration was recently shown to alter metastatic behavior of pancreatic tumors (151) and to affect protein expression and cell growth through regulation of various transcription factors (152). Notably, inhibition of hypusination of eIF5A reduced PDAC cell growth (150). Hence, this might be used as potential therapeutic target.

#### 1.2.3.4 eIF3f loss

Lastly, eIF3f, a factor thought to act as tumor suppressor and thought of as negative regulator of translation, was shown to be downregulated in PDAC (153). Accordingly, overexpression of eIF3f causes inhibition of global protein synthesis and reduces cell proliferation (154).

## 1.3 Aims of the study

Recent years have seen a tremendous increase in our understanding of the molecular details of translation and its relevance for health and disease. The major players implicated in its regulation, namely eIFs, have been analyzed in many cancer entities. However, the knowledge concerning eIFs in PDAC remains very limited. Based on findings in other tumors and pathophysiological ideas accompanying protein synthesis in transformed cells, we hypothesized that eIFs might also be of great relevance in PDAC.

We aimed at elucidating the expression of various eIFs in PDAC sections via immunohistochemistry and tissue specimens via immunoblotting. Additionally, we correlated expression scores with various clinicopathological data to find potential diagnostic or prognostic associations. Besides expression analysis on protein level, we also characterized mRNA levels of promising eIFs.

Finally, gene expression and survival data from the publicly accessible The Cancer Genome Atlas (TCGA) data base were analyzed to reveal any important associations of eIF gene expression with clinical outcome, hinting to biological implications of the respective factors.

Consequently, we tried to uncover findings that might shed light upon novel therapeutic targets or potential new biomarkers to facilitate diagnosis and to improve the dismal prognosis associated with this highly malignant disease.

# 2 Materials and Methods

## 2.1 Immunohistochemistry

### 2.1.1 Patient samples

We examined a total of 174 PDAC cases on tissue microarrays (TMAs) provided by the Institute of Pathology at the Technical University of Munich, Munich, Germany. Each case was represented by three cones on the TMA slides. Patient data and clinicopathological classification are summarized in Table 4. As a control, non-neoplastic pancreatic tissue was collected at the Institute of Pathology at the Medical University of Graz, Graz, Austria. A total of 9 formalin-fixed, paraffin-embedded (FFPE) control samples classified by two board-certified pathologists (J.H. and I.B.) were collected. Sample collection and use were done under approval of the local ethics committee (Nr. 28-294 ex 15/16).

***Table 4: Clinicopathological data of 174 PDAC cases on TMAs.***
Absolute numbers (and % of total) of the cohort used in this study.

| | **Total (%)** | **Male (%)** | **Female (%)** |
|---|---|---|---|
| **n** | 174 (100) | 98 (56.3) | 76 (43.7) |
| **Mean age** | 64.14 | 62.44 | 66.33 |
| **pT** | | | |
| 1/2 | 35 (20.1) | 15 (15.3) | 20 (26.3) |
| 3/4 | 139 (79.9) | 83 (84.7) | 56 (73.7) |
| **pN** | | | |
| 0 | 42 (24.1) | 22 (22.4) | 20 (26.3) |
| 1 | 132 (75.9) | 76 (77.6) | 56 (73.7) |
| **pM** | | | |
| 0 | 168 (96.6) | 93 (94.9) | 75 (98.7) |
| 1 | 6 (3.4) | 5 (5.1) | 1 (1.3) |
| **Grading** | | | |
| 1 | 7 (4) | 4 (4.1) | 3 (3.9) |
| 2 | 92 (52.9) | 51 (52) | 41 (54) |
| 3 | 75 (43.1) | 43 (43.9) | 32 (42.1) |

### 2.1.2 Immunohistochemical staining

TMAs and non-neoplastic FFPE samples were stained for expression of eIF1, eIF2α, eIF3A, eIF3C, eIF4E, eIF4G, eIF5 and eIF6. FFPE samples were cut into slices of 4 μm thickness, attached to adhesive-coated glass slides and fixed at 65°C for 60 minutes. Staining was done with a Ventana Immunostainer XT (Ventana Medical Systems, Tucson, USA) using an ultra-VIEW universal DAB Detection Kit (Ventana Medical Systems, Tucson, USA) and cell-conditioning solution for 30 minutes via heat-induced epitope retrieval (HIER). The primary antibodies and dilutions used are listed in Table 5. Antibodies were incubated for 30 minutes at room temperature.

***Table 5: Antibodies used for immunohistochemical staining.***

| Primary Antibody | Company | Dilution | Secondary Antibody |
|---|---|---|---|
| eIF1 | Sigma Aldrich (HPA043003) | 1:30 | Rabbit |
| eIF2α (D7D3) XP | Cell Signaling (#5324) | 1:100 | Rabbit |
| eIF3A | Cell Signaling (#2538) | 1:50 | Rabbit |
| eIF3p110 (B-6) (eIF3C) | Santa Cruz (sc-74507) | 1:2000 | Mouse |
| eIF4E | Cell Signaling (#9742) | 1:100 | Rabbit |
| eIF4G | Cell Signaling (#2498) | 1:25 | Rabbit |
| eIF5 | Gene Tex | 1:100 | Rabbit |
| eIF6 | Gene Tex(GTX63642) | 1:250 | Rabbit |

### 2.1.3 Expression evaluation/ scoring

Staining was evaluated for its intensity and the amount of positively stained cells. Staining intensity was classified using an intensity score ranging from 0-3 (0: no staining, 1: weak staining, 2: moderate staining, 3: strong staining), whereas the amount of positive cells was quantified using a proportion score ranging from 0-4 (0%: 0, 1-10%: 1, 11-49%: 2, 50-79%: 3, 80-100%: 4). By multiplication, an overall tissue intensity score (TIS) taking both parameters into account was calculated ranging from 0-12; final expression was classified as follows: 0 no expression, 1-4 weak expression, 5-8 moderate expression, 9-12 strong expression.

### 2.1.4 Statistical analysis

Graphical analysis and statistical testing were done using GraphPad Prism V8.0.2 software (GraphPad software Inc., La Jolla, CA, USA). All data are presented as means ± standard of the mean (SEM). Significance level was set as $p < 0.05$; all data were analyzed with descriptive statistics and Mann-Whitney-U-test. Significance is depicted in the graphics as follows: * $p < 0.05$, ** $p < 0.01$, *** $p < 0.001$, **** $p < 0.0001$.

## 2.2 Western Blot analysis

### 2.2.1 Patient samples

A total of 56 tumor samples and 28 non-neoplastic pancreatic tissues (NNTs), serving as controls, were collected at the Institute of Pathology in Magdeburg, Magdeburg, Germany and used for this study. The tissue samples were cryopreserved after collection and stored at -80°C until analysis. Sampling and use of the tissue were done under the approval of the local ethics committees in Graz (Nr. 28-294 ex 15/16) and in Magdeburg (Nr. 08/18). The in- and exclusion criteria for patient samples used in this study were:

**Inclusion criteria:**

-Age: 18-100 years
-Sex: male and female
-Disease status:
- Histologically verified neoplasm of the pancreas (all types of adenocarcinomas, neuroendocrine tumours (NETs), adenomas) of all grades and clinicopathological stages
- Hematogenic or lymphogenic metastatic pancreatic tissue (e.g. in the liver or lymph nodes)
- Pre/postsurgically treated (adjuvant/neoadjuvant) and untreated patients (solely surgery as pimary approach)

-Surgery material cryopreservable/obtainable < 24h after surgery

**Exclusion criteria:**

-Age: < 18; > 100
-Histologically unidentifyable origin of neoplastic tissue (cancer of unknown primary = CUP-syndrome)

The in- and exclusion criteria for the NNTs were:

**Inclusion criteria:**

-Age: 18-100 years

-Sex: male and female

-Disease status:

- Morphologically/macroscopically normal tissue obtained during surgery

-Surgery material cryopreservable/obtainable < 24h after surgery

**Exlcusion criteria:**

-Age: < 18; > 100

-Disease status:

- Autoimmunpancreatitis
- Chronic pancreatitis
- Acute pancreatitis

### 2.2.2 Protein extraction and Immunoblot (Western Blot)

Homogenization of frozen tissue samples was performed using a MagNA Lyser homogenizer (Roche Diagnostics, Risch-Rotkreuz, Switzerland) in NP-40 Lysis buffer (0.05M Tris-HCl, 5M NaCl, 0.5% NP-40, 0.1M Pefabloc, 1M DTT, complete Mini, PhosSTOP). Protein concentration of the lysate was determined using the Bradford protein assay (Biorad Protein Assay Dye Reagent, BioRad Laboratories GmbH, Munich, Germany). Every sample was diluted with NP-40 Lysis buffer to yield an end concentration of 3 µg/µl. 30 µg protein were loaded onto 12.5% SDS-PAGE gels (30% Acrylamid / Bisacrylamid stock solution, ROTH, Karlsruhe, Germany). Gel composition is stated in Table 6. Electrophoresis was performed in mini-vertical electrophoresis units (Hoefer Inc., Richmond, USA). PVDF membranes (Immobilin-P transfer membrane, Millipore, Massachusetts, USA) were used for blotting in a Semi Dry Blotting Unit (SCIE-PLAS, Cambridge, England) for 90 minutes with 80 mA per gel. Primary antibodies are shown in Table 7. The stated dilutions were prepared in 0.1% tris-buffered saline tween (TBST) with 5% bovine serum albumin (BSA). Primary antibody incubation was done overnight at 4°C. Secondary antibodies were horseradish peroxidase-conjugated anti-mouse (1:3000 dilution) and anti-rabbit (1:5000 dilution) antibodies (GE Healthcare Life Sciences, Buckinghamshire, England) and were incubated for 60 minutes at room temperature. Visualization was done in the Image Quant LAS 500 detection system (GE Healthcare, Little Chalfont, UK) by chemiluminescence using Amersham ECL

Western Blotting Detection Reagent (GE Healthcare Life Sciences, Buckinghamshire, England). Immunoblot analysis and quantification was performed using the software Image J (National Institutes of Health, USA). Signals were normalized to glyceraldehyde-3-phosphate dehydrogenase (GAPDH).

***Table 6: Immunoblot gel composition.***

The indicated amounts were used for generating 4 gels. SDS = Sodium dodecylsulfate, APS = ammonium persulfate, TEMED = Tetramethylethylenediamine.

| | **Separating Gel** | **Collecting Gel** |
|---|---|---|
| Aqua dest. | 9.84 ml | 12.5 ml |
| Tris 1.5M | 7.5 ml (pH 8.8) | 5 ml (pH 6.6) |
| Acrylamid | 12.18 ml | 2 ml |
| 10% SDS | 300 µl | 200 µl |
| APS | 300 µl | 100 µl |
| TEMED | 22.5 µl | 30 µl |

***Table 7: Primary antibodies used for Immunoblot analysis.***

| **Primary Antibody** | **Company** | **Dilution** |
|---|---|---|
| eIF1 | Sigma Aldrich | 1:1000 |
| eIF1A | Abcam | 1:1000 |
| eIF2α (D7D3) XP | Cell Signaling | 1:1000 |
| Phospho-eIF2α (Ser51)(D9G8) | Cell Signaling | 1:1000 |
| eIF3B (= eIF3η (D-9)) | Santa Cruz | 1:1000 |
| eIF3C | Cell Signaling | 1:1000 |
| eIF4E | Cell Signaling | 1:1000 |
| eIF4G | Cell Signaling | 1:1000 |
| eIF5 | Gene Tex | 1:1000 |
| eIF6 | Cell Signaling | 1:1000 |
| GAPDH | Sigma-Aldrich | 1:1000 |

### 2.2.3 Statistical analysis

Immunoblot data are represented as means ± standard error of the mean (SEM). Statistical testing was performed using a Mann-Whitney-U test for overall expression and one-way ANOVA for multiple comparisons. Signifance levels were set to $p < 0.05$. Means of duplicates were used for generation of results. Tumor samples with highly diverging duplicates (standard deviation > 1) were excluded from analysis due to inacurracy. All analyses and graphs were genereated in GraphPad Prism software V8.0.2 (GraphPad software Inc., La Jolla, CA, USA). Significance is depicted in the graphics as follows: * $p < 0.05$, ** $p < 0.01$, *** $p < 0.001$, **** $p < 0.0001$.

## 2.3 RNA analysis

### 2.3.1 RNA isolation

Fresh-frozen tissue from PDAC and NNT specimens was used to isolate total RNA using a Trizol-based protocol. 70-100 mg of tissue were used per sample and homogenized with MagNA Lyser Green Beads (Roche Diagnostics, Risch-Rotkreuz, Switzerland) in 1ml Trizol reagent (Life Technologies, Carlsbad, California, USA). The MagNA Lyser (Roche Diagnostics, Risch-Rotkreuz, Switzerland) was set to 6,500 rpm for 30 seconds. After the lysate was incubated at room temperature for 10 minutes, 200 µl chloroform was added, followed by another 3 minutes of incubation at room temperature. The sample was then centrifuged at 10,000 rpm for 15 minutes at 4°C. After phase-separation, the upper, RNA-containing phase was pippeted into 500 µl isopropanol and consecutively centrifuged at 10,000 rpm for 15 minutes at 4°C. The supernatant was then discarded. The RNA pellet was washed 2 - 3 times with 1 ml of 80% ethanol. The pellet was then dried for 5 minutes at 37°C. The dried pellet was dissolved in 50 – 200 µl RNase free water (upon pellet size estimation). Afterwards, incubation at 58°C for 10 minutes was done. RNA purity and quantity were assessed at a NanoDrop spectrophotometer (Thermo Scientific, Waltham, Massachusetts, USA). The sample was then stored at -80°C until utilization.

### 2.3.2 Reverse transcription

Reverse transcription was performed using the High-Capacity cDNA Reverse Transcription Kit (Applied Biosystems, Foster City, California, USA) according to the manufacturer´s instruction. Accordingly, 20 µg RNA was added to 10 µl of 2x RT master mix (Table 8). Nuclease free $H_2O$ was added to an end volume of 20 µl. PCR was done using a PCR GeneAmp9700 thermocycler (Applied Biosystems, Foster City, California, USA). The programm settings are described in Table 9. 1:10 and undiluted cDNAs were stored at -20°C until further utilization.

***Table 8: Components of the 2x Reverse Transcriptase Master Mix.***

| **Component** | **Volume [µL]** |
|---|---|
| 10x RT Buffer | 2.0 |
| 25x dNTP Mix (100 mM) | 0.8 |
| 10x RT Random Primers | 2.0 |
| MultiScribe™ Reverse Transcriptase | 1.0 |
| RNase Inhibitor | 1.0 |
| Nuclease-free H2O | 3.2 |
| **Total Volume per Reaction** | **10.0** |

***Table 9: Program settings used for reverse transcription.***

| | **Temperature [°C]** | **Time [min]** |
|---|---|---|
| **Step 1** | 25 | 10 |
| **Step 2** | 37 | 120 |
| **Step 3** | 85 | 5 |
| **Step 4** | 4 | ∞ |

### 2.3.3 Quantitative real-time PCR

For quantitative real-time PCR (qRT-PCR) the Power SYBR Green PCR Master Mix Kit (Applied Biosystems, Foster City, California, USA) was utilized. Primers were self-designed using Primer-Blast and synthesized by Eurofins MWG operon (Germany). Detailed primer information is given in Table 10. qRT-PCR was performed with 30 ng of cDNA in a reaction volume of 10 µl, pippeting was done utilizing a Hamilton Microlab STAR (Hamilton Germany GmbH – Robotics, Germany). The programs were set according to the manufacturer´s instructions.

***Table 10: Primers used for qRT-PCR.***
Forward (Fwd) and reverse (Rev) primers including their sequence, length and melting temperature (Tm) are shown.

| Gene | Primer | Sequence (5'-3') | Length | Tm [°C] |
|---|---|---|---|---|
| **EIF1** | Fwd | GAAACGGCAGGAAGACCCTTA | 21 | 60 |
| | Rev | CGGATGCTCAATTACAGTACCAT | 23 | 59 |
| **EIF1AX** | Fwd | AACAGACGCAGGGGTAAGAAT | 21 | 61 |
| | Rev | CCTGAGCATACTCCTGACCAT | 21 | 61 |
| **EIF2A** | Fwd | TGGTGAATGTCAGATCCATTGC | 22 | 60 |
| | Rev | TAGAACGGATACGCCTTCTGG | 21 | 61 |
| **RPL41** | Fwd | AAGATGAGGCAGAGGTCCAA | 20 | 58 |
| | Rev | TCCAGAATGTCACAGGTCCA | 20 | 58 |
| **YWHAZ** | Fwd | ACTTTTGGTACATTGTGGCTTCAA | 24 | 60 |
| | Rev | CCGCCAGGACAAACCAGTAT | 20 | 60 |

### 2.3.4 Statistical analysis

Expression analysis was done by relative quantification using the $2^{-\Delta\Delta Ct}$-method. Normalization was done to ribosomal protein L41 (RPL41) and 14-3-3 protein zeta/delta (YWHAZ) as internal housekeeping genes (HKGs). All samples were determined in triplicates, the $C_t$ values were averaged for further analysis. X-fold expression calculation was done by dividing the averaged $2^{-\Delta\Delta Ct}$-values of the tumor samples by $2^{-\Delta\Delta Ct}$-values of NNTs. Addtionally, statistical testing for significance was done after log-transformation of $2^{-\Delta\Delta Ct}$ values using a t-test. Variance equality was tested by F test.

## 2.4 *In Silico* expression and survival analysis

125 PDAC subjects from The Cancer Genome Atlas (TCGA) database were analyzed to reveal associations between eIF expression and survival. Using the R survival package, Kaplan-Meier curves were generated. Association was tested via log-rank test. $p < 0.05$ was set as significance threshold.

# 3 Results

## 3.1 Expression analysis via Immunohistochemistry and Western Blot

### 3.1.1 Housekeeping gene (HKG) testing

Prior to analyzing various eIFs in the entire cohort via Western Blot, small-scale testing for the most stably expressed housekeeping gene (HKG) was performed in 4 NNTs and 5 PDAC samples (Figure 7). The tested proteins were importin 8 (IPO8), succinate dehydrogenase complex subunit A (SDHA), actin and GAPDH. As GAPDH expression was the most stable across all tested samples, it was chosen as reference HKG for all subsequent analyses. As experimental pre-test, eIF4E was also analyzed to test for method applicability for eIF analysis.

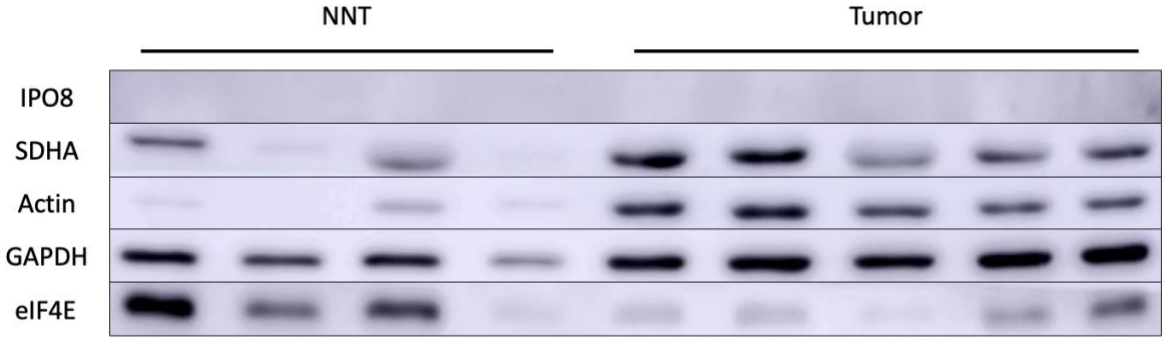


***Figure 7: Housekeeping gene testing for Western Blot analysis.***
4 NNTs and 5 PDAC samples were tested for IPO8, SDHA, actin and GAPDH signal intensity. Additionally, eIF4E was visualized to test if experimental settings were appropriate for eIF detection.

### 3.1.2 eIF1

#### 3.1.2.1 Immunohistochemistry

169 PDAC specimens were evaluated for their eIF1 expression and compared to 9 NNT specimens. Representative sections are shown in Figure 8A. Among the 169 samples, 97 were G1/2 and 72 were G3. eIF1 was downregulated in PDAC samples in the overall comparison (NNT vs. tumor of all grades, $p < 0.0001$, Figure 8B, C) and in the subgroup analysis (NNT vs. G1/2 and NNT vs. G3, both $p < 0.0001$) with no significant difference between different groups of differentiation (G1/2 vs. G3, $p = 0.4260$, Figure 8D, E).

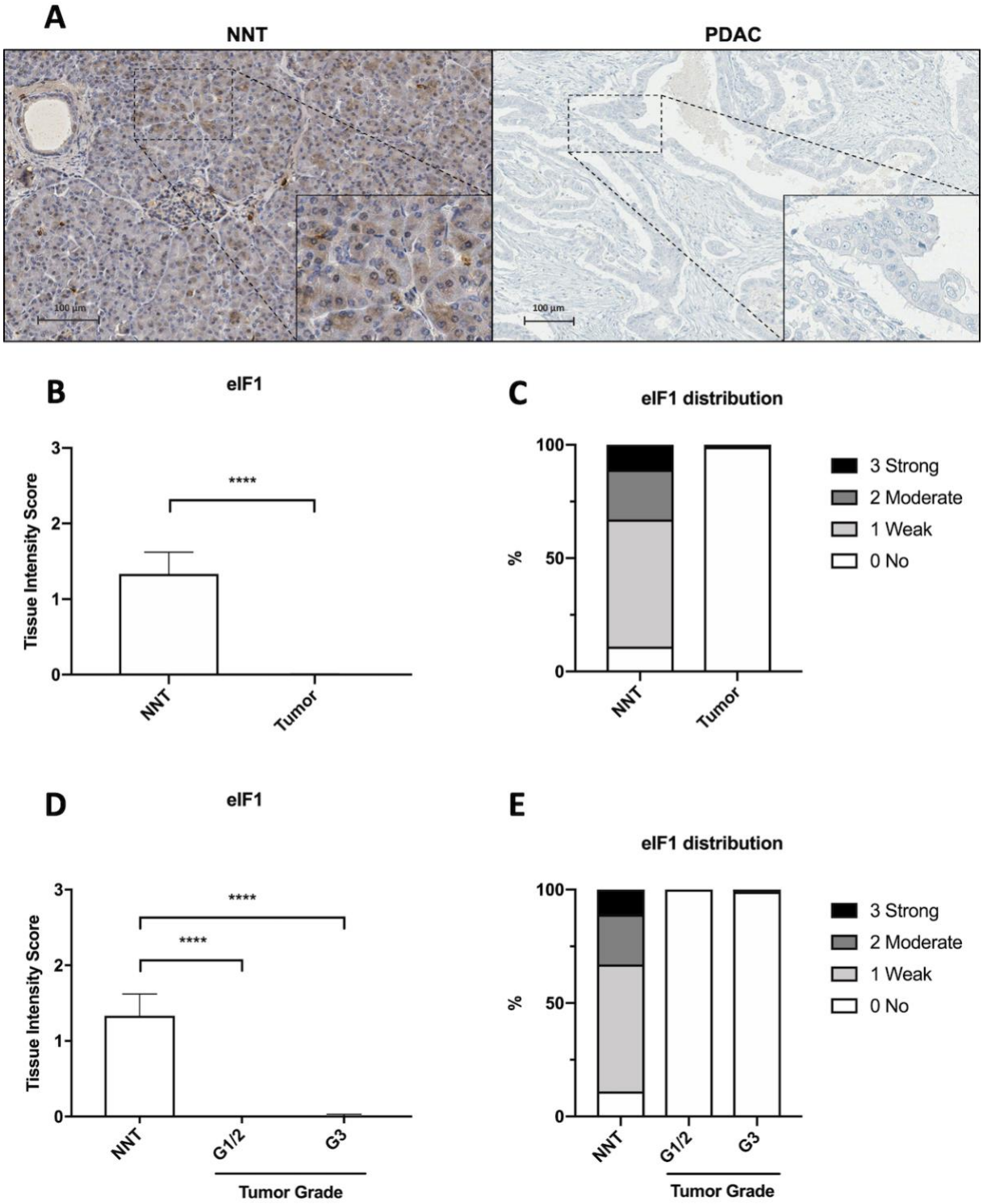


***Figure 8: Immunohistochemical evaluation of eIF1 expression in PDAC compared to NNT.***

**(A)** Representative sections of eIF1 staining in NNT and PDAC. Scale bar indicates 100 µm. **(B)** Downregulation of eIF1 expression in NNT versus PDAC samples (all grades), $p < 0.0001$. **(C)** Distribution of expression in NNT compared to PDAC samples. **(D)** Downregulation of eIF1 expression in NNT versus PDAC samples, subgrouped by differentiation. NNT vs. G1/2, $p < 0.0001$. NNT vs. G3, $p < 0.0001$ **(E)** Distribution of expression in NNT compared to PDAC samples, subgrouped by differentiation (G1/2 and G3). *($n_{NNT} = 9$, $n_{tumor} = 169$, $n_{G1/2} = 97$, $n_{G3} = 72$)*

#### 3.1.2.2 Western Blot

56 PDAC specimens were analyzed and compared to 28 NNT specimens. Representative blots are shown in Figure 9A. Downregulation was observed in tumor samples compared to NNTs (p = 0.0029, Figure 9B). A subgroup analysis of 28 NNTs and 26 PDAC samples where information on tumor grade was available showed significant downregulation of eIF1 in G3 tumors compared to NNT (p = 0.0488) and no significant difference for G1/2 tumors (Figure 9C). No significant difference was present between G1/2 and G3 tumors. However, for eIF1 the replicate experiment yielded no analyzable blots, the depicted results are therefore single measures.

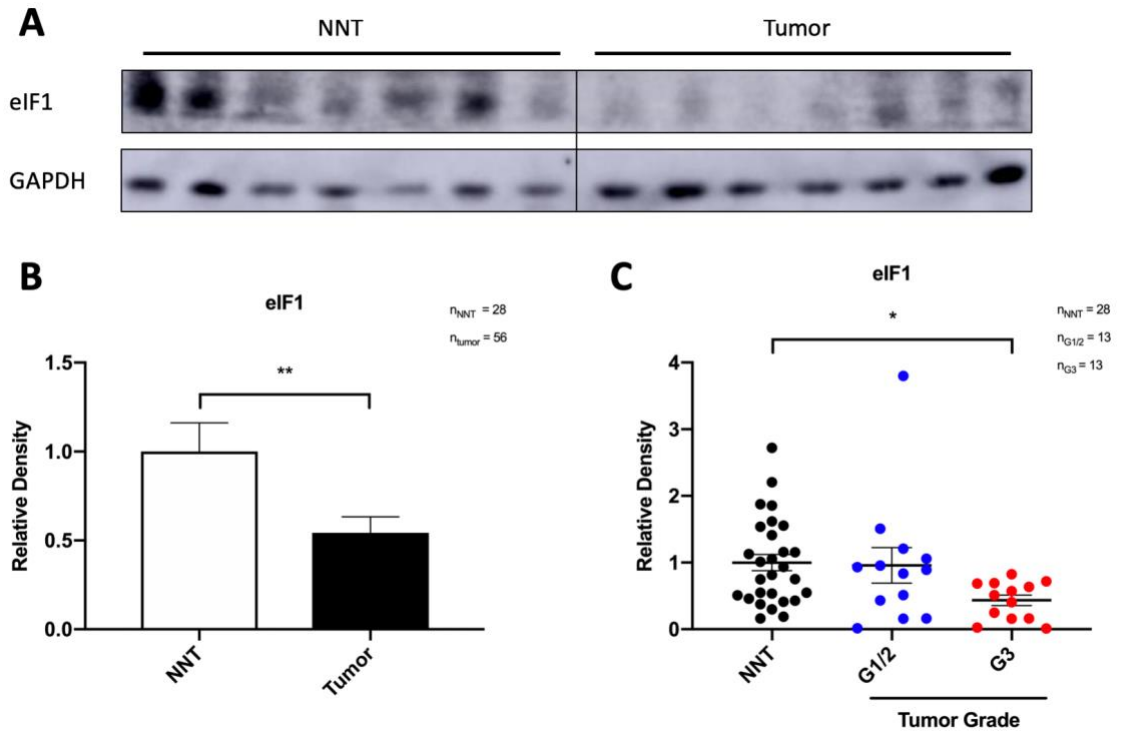


***Figure 9: Western Blot analysis of eIF1 expression.***

**(A)** Representative blots of eIF1 and GAPDH as HKG. **(B)** Downregulation of eIF1 in PDAC (n = 56) compared to NNT (n = 28), p = 0.0029. **(C)** Subgroup analysis of PDACs with available differentiation status (n = 26). G3 PDACs show significant reduction of eIF1 expression (p = 0.0488).

### 3.1.3 eIF2α

#### 3.1.3.1 Immunohistochemistry

165 PDAC specimens were evaluated for their eIF2α expression and compared to 9 NNT specimens. Representative sections are shown in Figure 10A. Among the 165 samples, 95 were G1/2 and 70 were G3. eIF2α was downregulated in PDAC samples in the overall comparison (NNT vs. tumor of all grades, $p < 0.0001$, Figure 10B, C) and in the subgroup analysis (NNT vs. G1/2 and NNT vs. G3, both $p < 0.0001$, Figure 10D, E). Additionally, significant differences were detectable between differentiation states, with higher expression in poorly differentiated tumors compared to well and moderately differentiated ones (G1/2 vs. G3, $p = 0.0119$, Figure 10D, E).

#### 3.1.3.2 Western Blot

53 PDAC specimens were analyzed and compared to 28 NNT specimens. Representative blots are shown in Figure 11A. Downregulation was observed in tumor samples compared to the controls ($p < 0.0001$, Figure 11B). A subgroup analysis of 28 NNTs and 26 PDAC samples where information on tumor grade was available showed that the observed downregulation is present across all differentiation states (NNT vs. G1/2, $p = 0.0065$, NNT vs. G3, $p = 0.0002$) with no significant differences within these groups (G1/2 vs. G3, $p = 0.9620$) (Figure 11C). Additionally, p-eIF2α expression was determined via Western Blot (Figure 12A). Overall expression was significantly reduced in PDAC samples ($n = 52$) compared to NNTs ($n = 28$) ($p = 0.0005$, Figure 12B). Subgroup analysis showed that this downregulation is primarily attributable to downregulation in G1/2 tumors ($n = 11$), where a significant difference compared to NNT ($n = 28$) was present ($p = 0.0184$, Figure 12C). No significant difference was present between NNT and G3 ($n = 12$, $p = 0.3474$), and between differentiation subgroups ($p = 0.8034$).

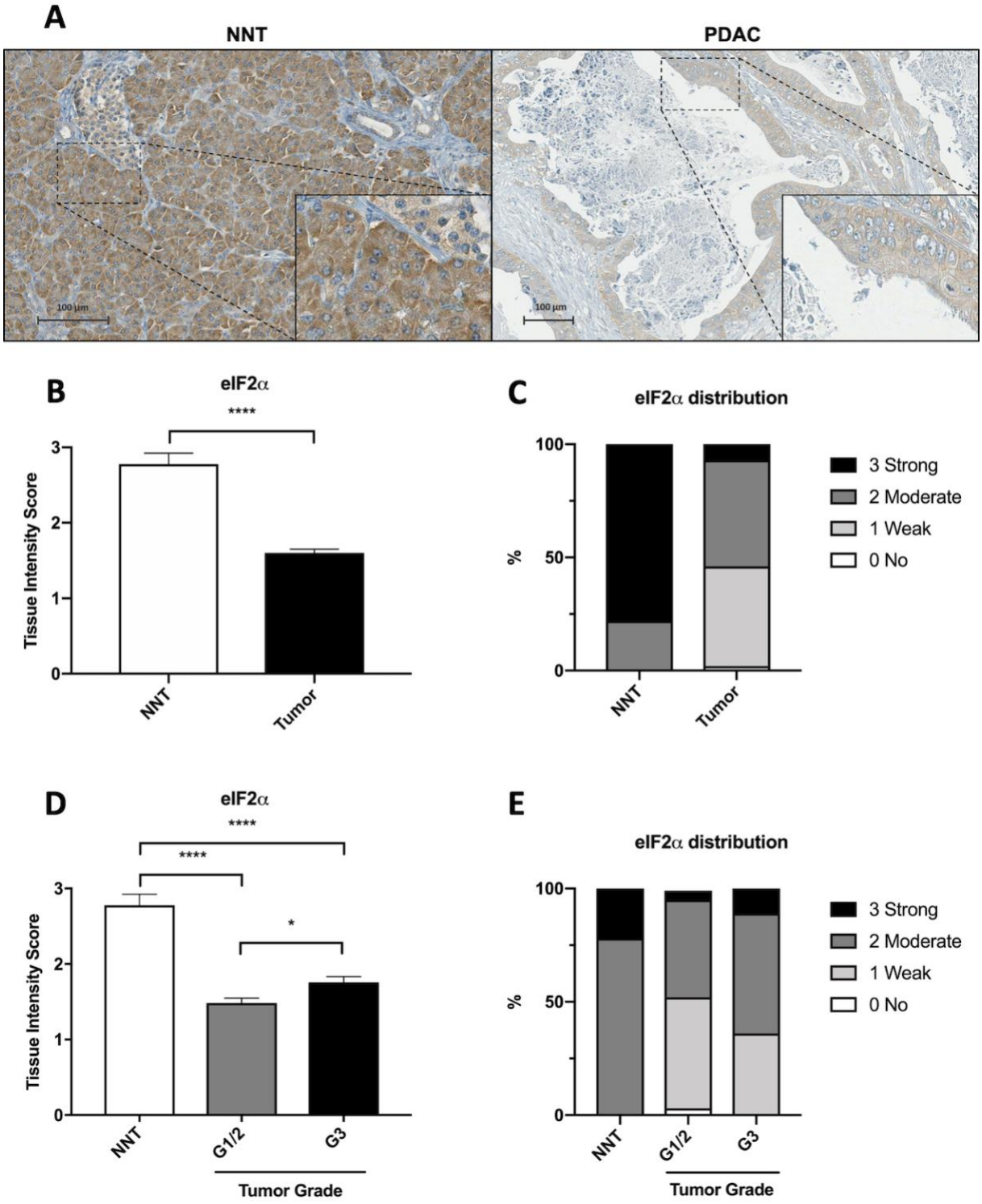


***Figure 10: Immunohistochemical evaluation of eIF2α expression in PDAC compared to NNT.***

**(A)** Representative sections of eIF2α staining in NNT and PDAC. Scale bar indicates 100 µm. **(B)** Downregulation of eIF2α expression in NNT versus PDAC samples (all grades), $p < 0.0001$. **(C)** Distribution of expression in NNT compared to PDAC samples. **(D)** Downregulation of eIF2α expression in NNT versus PDAC samples, subgrouped by differentiation. NNT vs. G1/2, $p < 0.0001$. NNT vs. G3, $p < 0.0001$. G1/2 vs. G3, $p = 0.0119$. **(E)** Distribution of expression in NNT compared to PDAC samples, subgrouped by differentiation (G1/2 and G3). *($n_{NNT} = 9$, $n_{tumor} = 165$, $n_{G1/2} = 95$, $n_{G3} = 70$)*

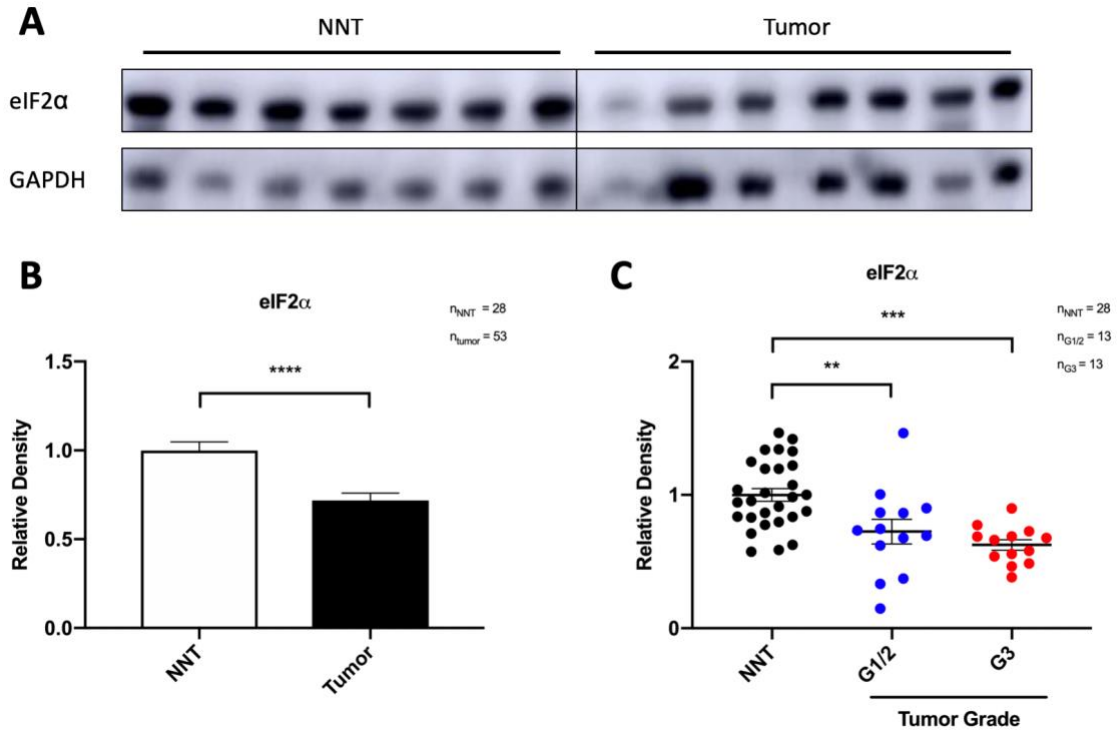


***Figure 11: Western Blot analysis of eIF2α expression.***

**(A)** Representative blots of eIF2α and GAPDH as HKG. **(B)** Downregulation of eIF2α in PDAC (n = 53) compared to NNT (n = 28), p > 0.0001. **(C)** Subgroup analysis of tumors with available differentiation status (n = 26). Significant reduction of eIF2α expression in G1/2 (p = 0.0065) and G3 tumors (p = 0.0002).

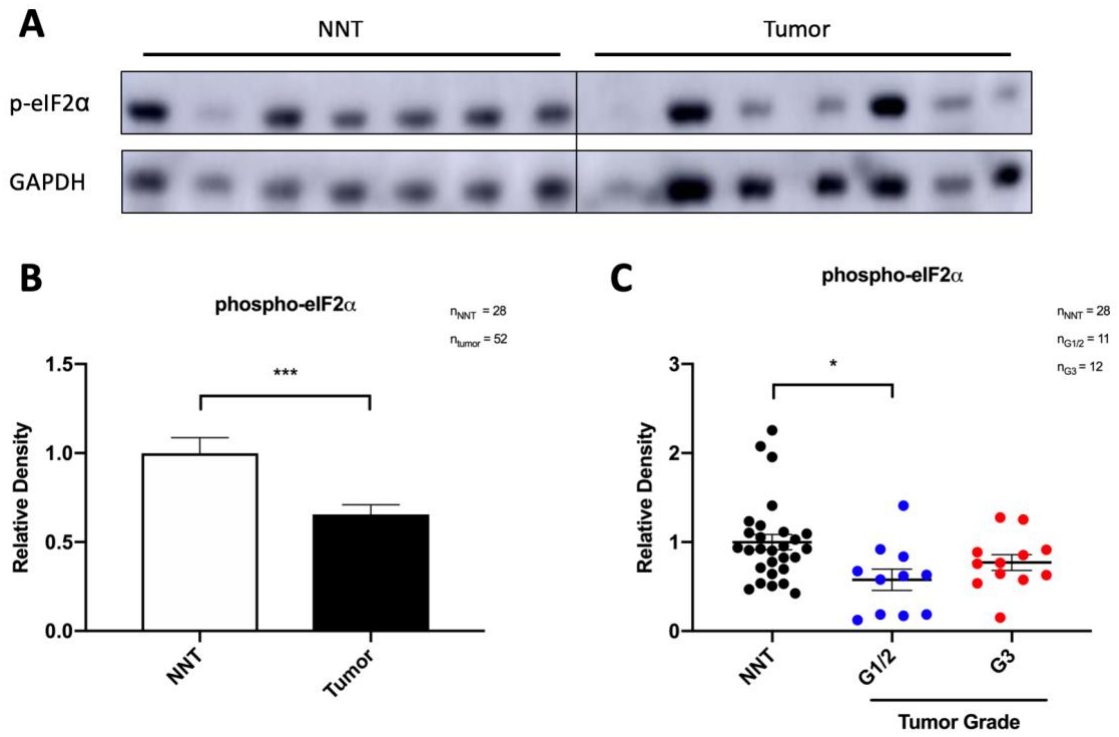


***Figure 12: Western Blot analysis of phospho-eIF2α expression.***

**(A)** Representative blots of p-eIF2α and GAPDH as HKG. **(B)** Downregulation of p-eIF2α in PDAC (n = 52) compared to NNT (n = 28), p = 0.0005. **(C)** Subgroup analysis of PDACs with available differentiation status (n = 23). G1/2 tumors show significant reduction of p-eIF2α expression (p = 0.0184).

### 3.1.4 eIF3A

#### 3.1.4.1 Immunohistochemistry

173 PDAC specimens were evaluated for their eIF3A expression and compared to 9 NNT specimens. Representative sections are shown in Figure 13A. Among the 173 samples, 99 were G1/2 and 74 were G3. eIF3A was upregulated in PDAC samples in the overall comparison (NNT vs. tumor of all grades, $p = 0.0132$, Figure 13B, C) and in the subgroup analysis (NNT vs. G1/2, $p = 0.0318$ and NNT vs. G3, $p = 0.0107$, Figure 13D, E). No significant differences were detectable between differentiation states (G1/2 vs. G3, $p = 0.2197$).

### 3.1.5 eIF3C

#### 3.1.5.1 Immunohistochemistry

168 PDAC specimens were evaluated for their eIF3C expression and compared to 9 NNT specimens. Representative sections are shown in Figure 14A. Among the 168 samples, 96 were G1/2 and 72 were G3. eIF3C was downregulated in PDAC samples in the overall comparison (NNT vs. tumor of all grades, $p < 0.0001$, Figure 14B, C) and in the subgroup analysis (NNT vs. G1/2 and NNT vs. G3, both $p < 0.0001$, Figure 14D, E). No significant differences were detectable between differentiation states (G1/2 vs. G3, $p = 0.7858$).

#### 3.1.5.2 Western Blot

47 PDAC specimens were analyzed and compared to 28 NNT specimens. Representative blots are shown in Figure 15A. Downregulation was observed in tumor samples compared to the controls ($p = 0.0048$, Figure 15B). A subgroup analysis of 28 NNTs and 22 PDAC samples where information on tumor grade was available indicated that the observed downregulation is only present in G1/2 tumors ($n = 12$, $p = 0.0009$, Figure 15C). No significant differences were detectable between NNT and G3 tumors ($n = 10$, $p = 0.2058$) or between different groups of differentiation (G1/2 vs. G3, $p = 0.3947$, Figure 15C).

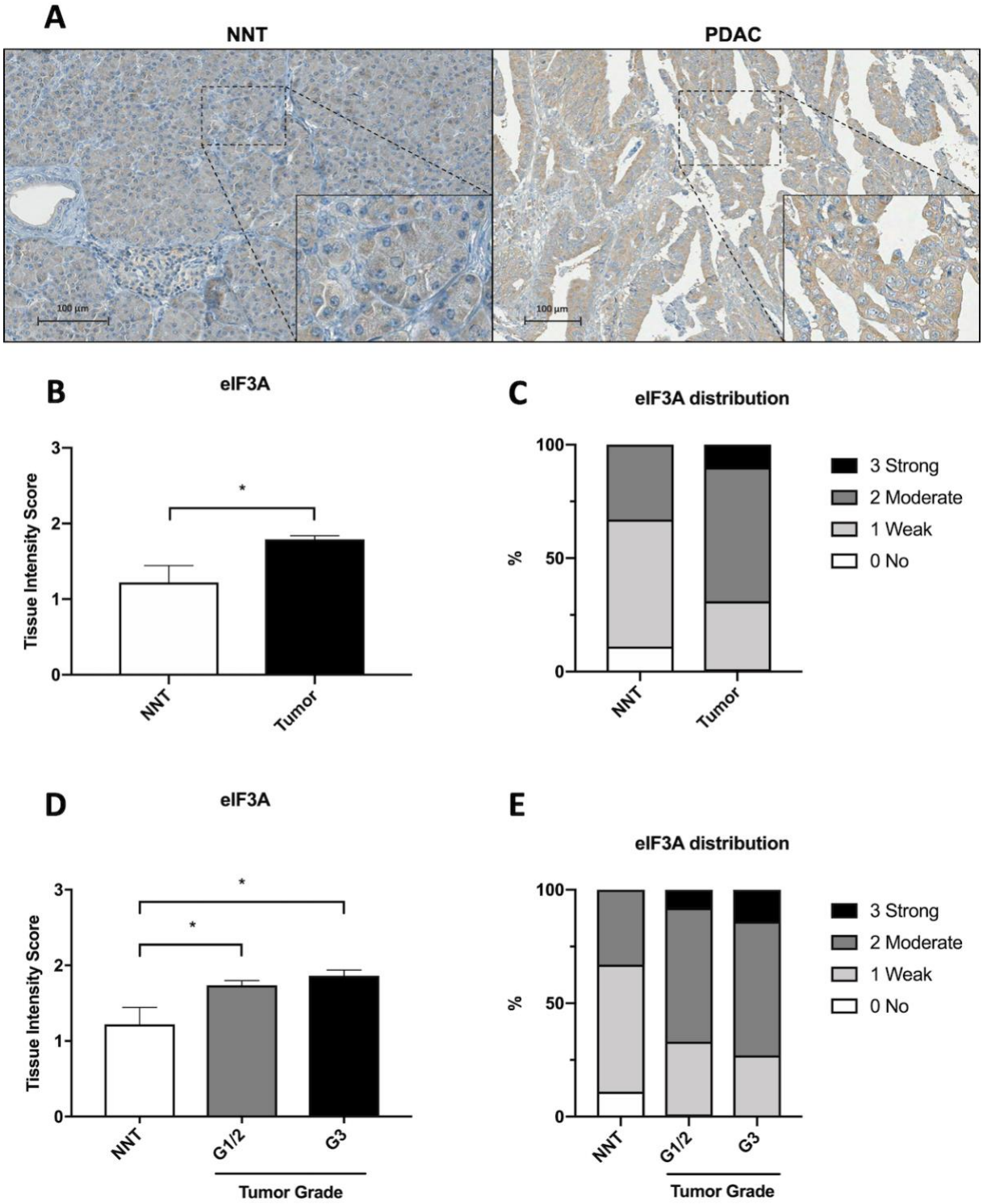


***Figure 13: Immunohistochemical evaluation of eIF3A expression in PDAC compared to NNT.***

**(A)** Representative sections of eIF3A staining in NNT and PDAC. Scale bar indicates 100 µm. **(B)** Upregulation of eIF3A expression in NNT versus PDAC samples (all grades), p = 0.0132. **(C)** Distribution of expression in NNT compared to PDAC samples. **(D)** Upregulation of eIF3A expression in NNT versus PDAC samples, subgrouped by differentiation. NNT vs. G1/2, p = 0.0318. NNT vs. G3, p = 0.0107. **(E)** Distribution of expression in NNT compared to PDAC samples, subgrouped by differentiation (G1/2 and G3). *($n_{NNT}$ = 9, $n_{tumor}$ = 173, $n_{G1/2}$ = 99, $n_{G3}$ = 74)*

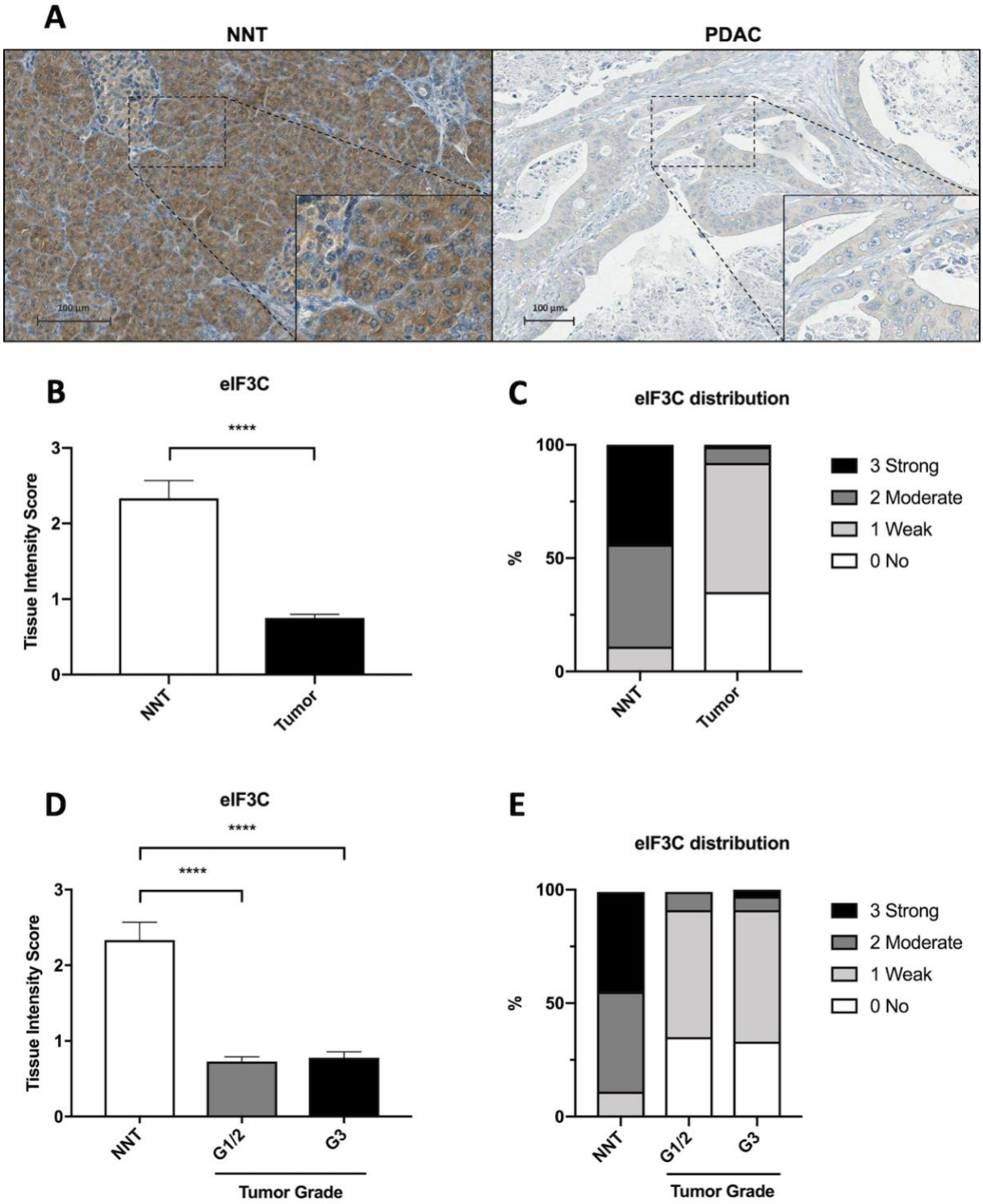


***Figure 14: Immunohistochemical evaluation of eIF3C expression in PDAC compared to NNT.***

**(A)** Representative sections of eIF3C staining in NNT and PDAC. Scale bar indicates 100 µm. **(B)** Downregulation of eIF3C expression in NNT versus PDAC samples (all grades), $p < 0.0001$ **(C)** Distribution of expression in NNT compared to PDAC samples. **(D)** Downregulation of eIF3C expression in NNT versus PDAC samples, subgrouped by differentiation. NNT vs. G1/2, $p < 0.0001$. NNT vs G3, $p < 0.0001$. **(E)** Distribution of expression in NNT compared to PDAC samples, subgrouped by differentiation (G1/2 and G3). *($n_{NNT} = 9$, $n_{tumor} = 168$, $n_{G1/2} = 96$, $n_{G3} = 72$)*

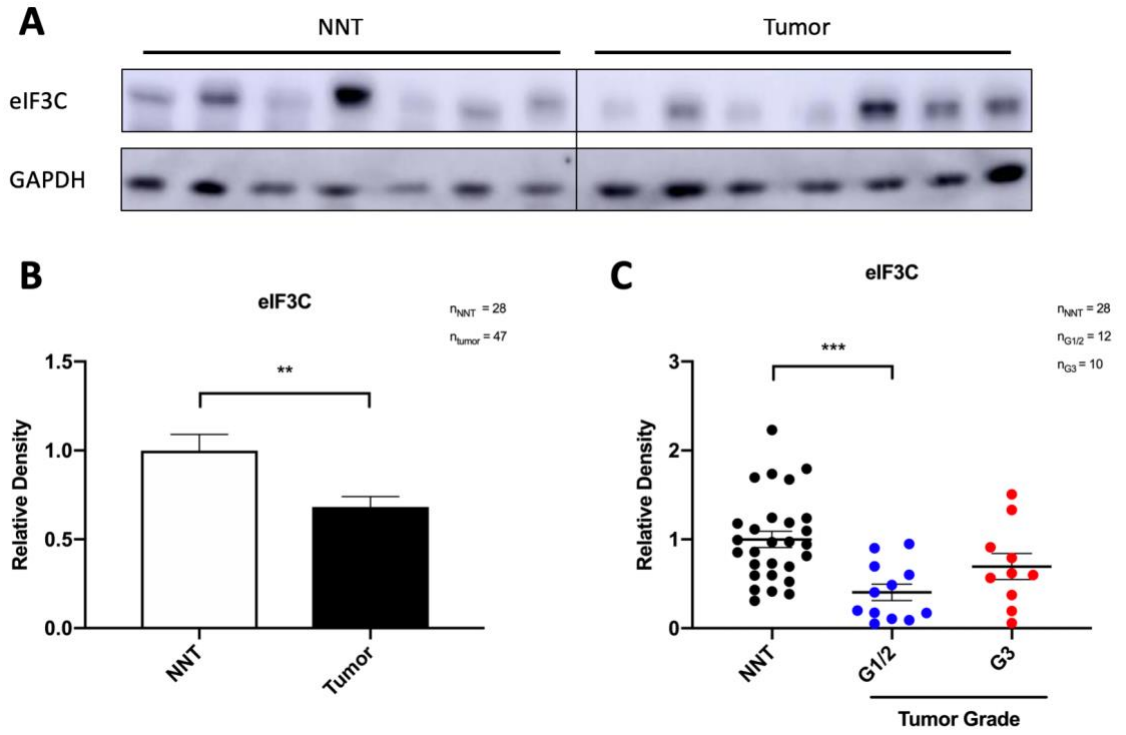


***Figure 15: Western Blot analysis of eIF3C expression.***

**(A)** Representative blots of eIF3C and GAPDH as HKG. **(B)** Downregulation of eIF3C in PDAC (n = 47) compared to NNT (n = 28), p = 0.0048. **(C)** Subgroup analysis of PDACs with available differentiation status (n = 22). G1/2 tumors show significant reduction of eIF3C expression compared to NNT (p = 0.0009).

### 3.1.6 eIF4E

#### 3.1.6.1 Immunohistochemistry

171 PDAC specimens were evaluated for their eIF4E expression and compared to 9 NNT specimens. Representative sections are shown in Figure 16A. Among the 171 samples, 98 were G1/2 and 73 were G3. eIF4E expression was not significantly altered in PDAC samples compared to NNT (p = 0.1168, Figure 16B, C). The subgroup analysis revealed no significant differences in neither of the groups (NNT vs. G1/2, p = 0.1064, NNT vs. G3, p = 0.2367, G1/2 vs. G3, p = 0.1989, Figure 16D, E).

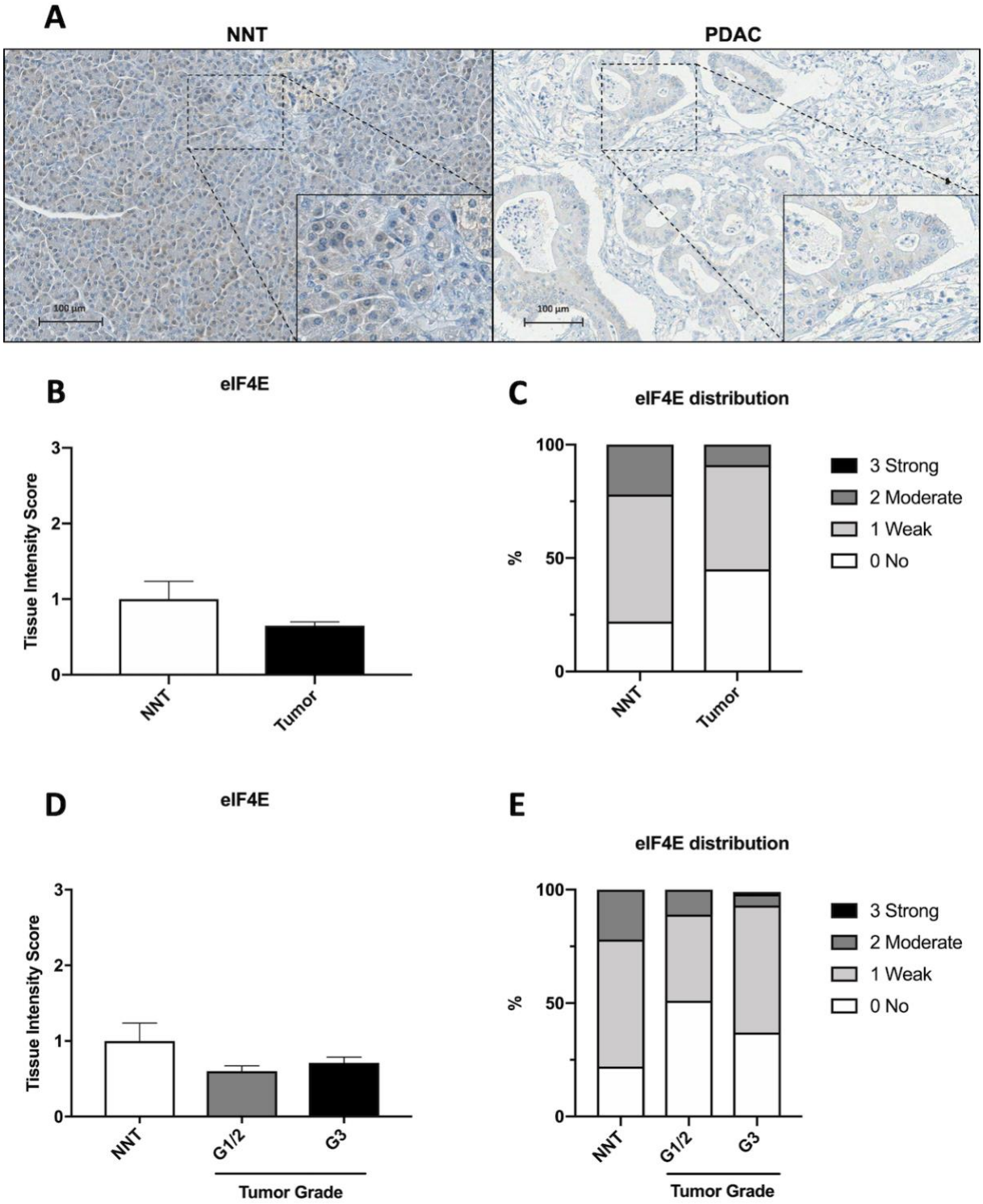


***Figure 16: Immunohistochemical evaluation of eIF4E expression in PDAC compared to NNT.***

**(A)** Representative sections of eIF4E staining in NNT and PDAC. Scale bar indicates 100 µm. **(B)** No significant differences in eIF4E expression in NNT versus PDAC samples (all grades) were detected. **(C)** Distribution of expression in NNT compared to PDAC samples. **(D)** No significant differences in eIF4E expression in NNT versus PDAC samples, subgrouped by differentiation (G1/2 and G3) were detected. **(E)** Distribution of expression in NNT compared to PDAC samples, subgrouped by differentiation (G1/2 and G3). *($n_{NNT}$ = 9, $n_{tumor}$ = 171, $n_{G1/2}$ = 98, $n_{G3}$ = 73)*

#### 3.1.6.2 Western Blot

53 PDAC specimens were analyzed and compared to 28 NNT specimens. Representative blots are shown in Figure 17A. Downregulation was observed in tumor samples compared to the controls ($p < 0.0001$, Figure 17B). A subgroup analysis of 28 NNTs and 26 PDAC samples where information on tumor grade was available showed that the downregulation is present in both groups of differentiation (NNT vs. G1/G2, n = 13 and NNT vs G3, n = 13, both $p < 0.0001$, Figure 17C). No significant differences were detectable between different groups of differentiation (G1/2 vs. G3, $p > 0.99$, Figure 17C).

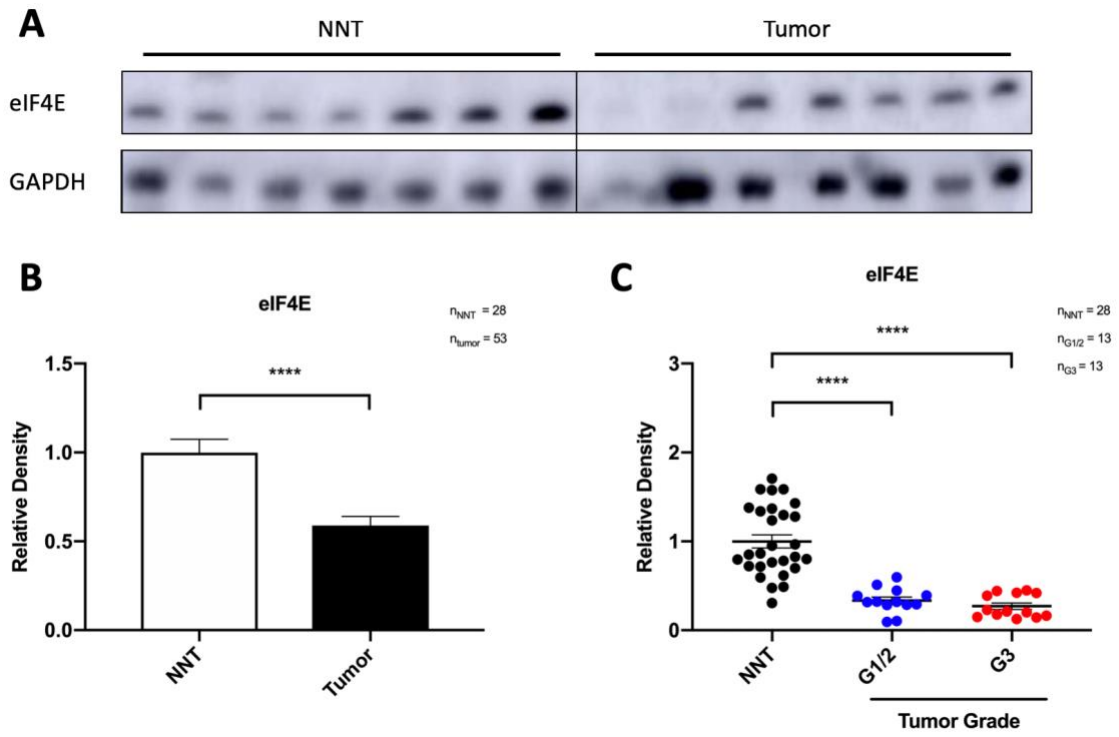


***Figure 17: Western Blot analysis of eIF4E expression.***

**(A)** Representative blots of eIF4E and GAPDH as HKG. **(B)** Downregulation of eIF4E in PDAC (n = 53) compared to NNT (n = 28), $p < 0.0001$. **(C)** Subgroup analysis of PDACs with available differentiation status (n = 26). Both differentiation groups show decreased eIF4E expression compared to NNT, both $p < 0.0001$.

### 3.1.7 eIF4G

#### 3.1.7.1 Immunohistochemistry

167 PDAC specimens were evaluated for their eIF4G expression and compared to 9 NNT specimens. Representative sections are shown in Figure 18A. Among the 167 samples, 95 were G1/2 and 72 were G3. eIF4G expression was not significantly altered in PDAC samples compared to NNT ($p = 0.8154$, Figure 18B, C). Significant alterations in eIF4G expression compared to NNT were not detected in any of the differentiation groups (NNT vs. G1/2, $p = 0.5169$, NNT vs. G3, $p = 0.8779$, Figure 18D, E). However, G3 tumors showed higher eIF4G expression compared to G1/2 tumors ($p = 0.0266$, Figure 18D, E).

### 3.1.8 eIF5

#### 3.1.8.1 Immunohistochemistry

168 PDAC specimens were evaluated for their eIF5 expression and compared to 9 NNT specimens. Representative sections are shown in Figure 19A. Among the 168 samples, 96 were G1/2 and 72 were G3. eIF5 expression was not significantly altered in PDAC samples compared to NNT ($p = 0.3867$, Figure 19B, C). Significant alterations in eIF5 expression compared to NNT were not detected in any of the differentiation groups (NNT vs. G1/2, $p = 0.3710$, NNT vs. G3, $p = 0.4633$, Figure 19D, E). Furthermore, no significant difference in eIF5 expression between differentiation groups was present ($p = 0.6785$, Figure 19D, E).

### 3.1.9 eIF6

#### 3.1.9.1 Immunohistochemistry

164 PDAC specimens were evaluated for their eIF6 expression and compared to 9 NNT specimens. Representative sections are shown in Figure 20A. Among the 164 samples, 92 were G1/2 and 72 were G3. eIF6 was downregulated in PDAC samples in the overall comparison (NNT vs. tumor of all grades, $p = 0.0093$, Figure 20B, C) and in the subgroup analysis (NNT vs. G1/2, $p = 0.0083$ and NNT vs. G3, $p = 0.0252$, Figure 20D, E). No significant differences were detectable between differentiation states (G1/2 vs. G3, $p = 0.4047$).

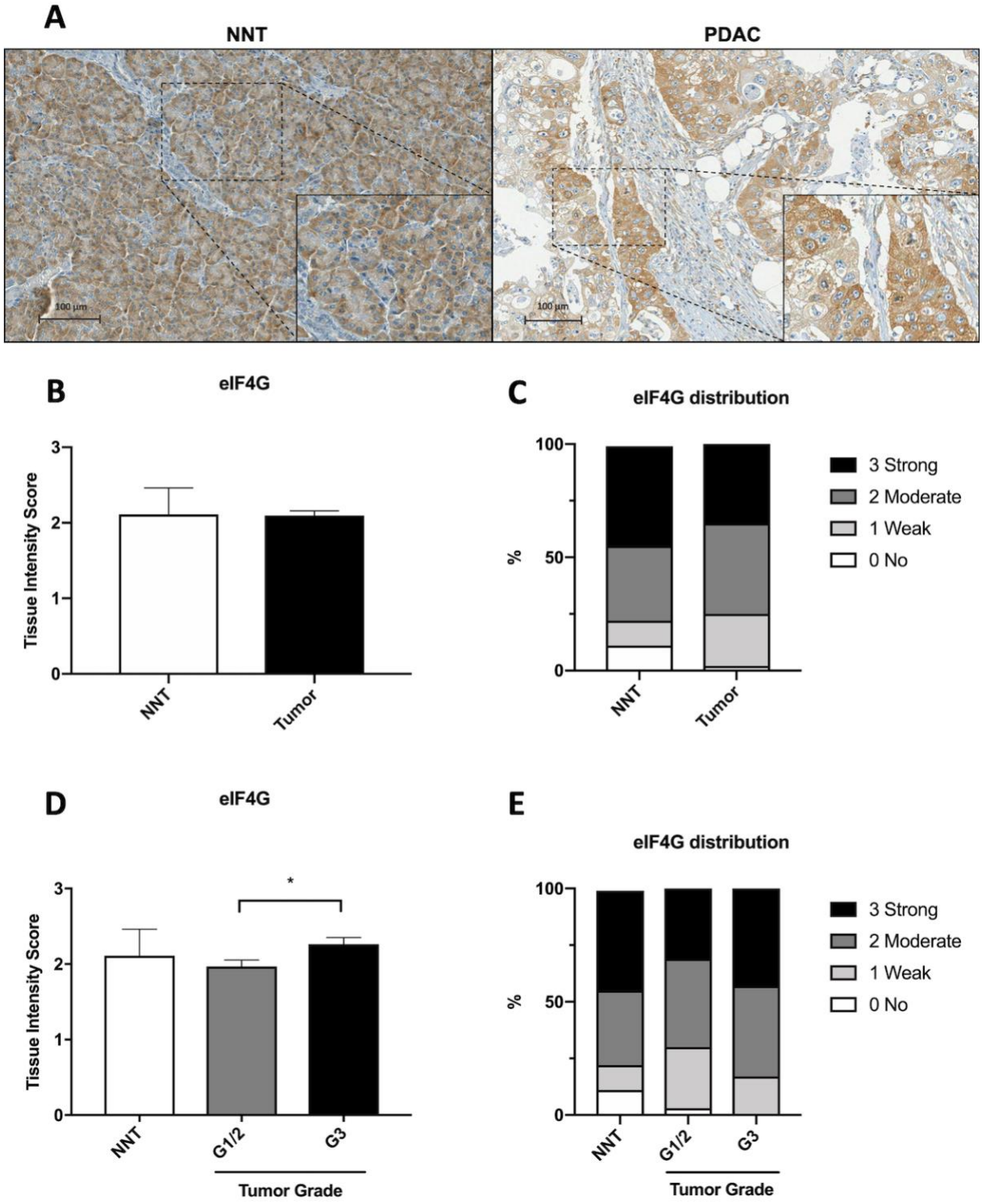


***Figure 18: Immunohistochemical evaluation of eIF4G expression in PDAC compared to NNT.***

**(A)** Representative sections of eIF4G staining in NNT and PDAC. Scale bar indicates 100 µm. **(B)** No alteration in eIF4G expression in NNT versus PDAC samples (all grades) was detectable. **(C)** Distribution of expression in NNT compared to PDAC samples. **(D)** No significant differences in eIF4G expression in NNT versus PDAC samples, subgrouped by differentiation (G1/2 and G3) were present. G3 tumors showed higher eIF4G expression compared to G1/2 tumors, p = 0.0266 **(E)** Distribution of expression in NNT compared to PDAC samples, subgrouped by differentiation (G1/2 and G3). *($n_{NNT}$ = 9, $n_{tumor}$ = 167, $n_{G1/2}$ = 95, $n_{G3}$ = 72)*

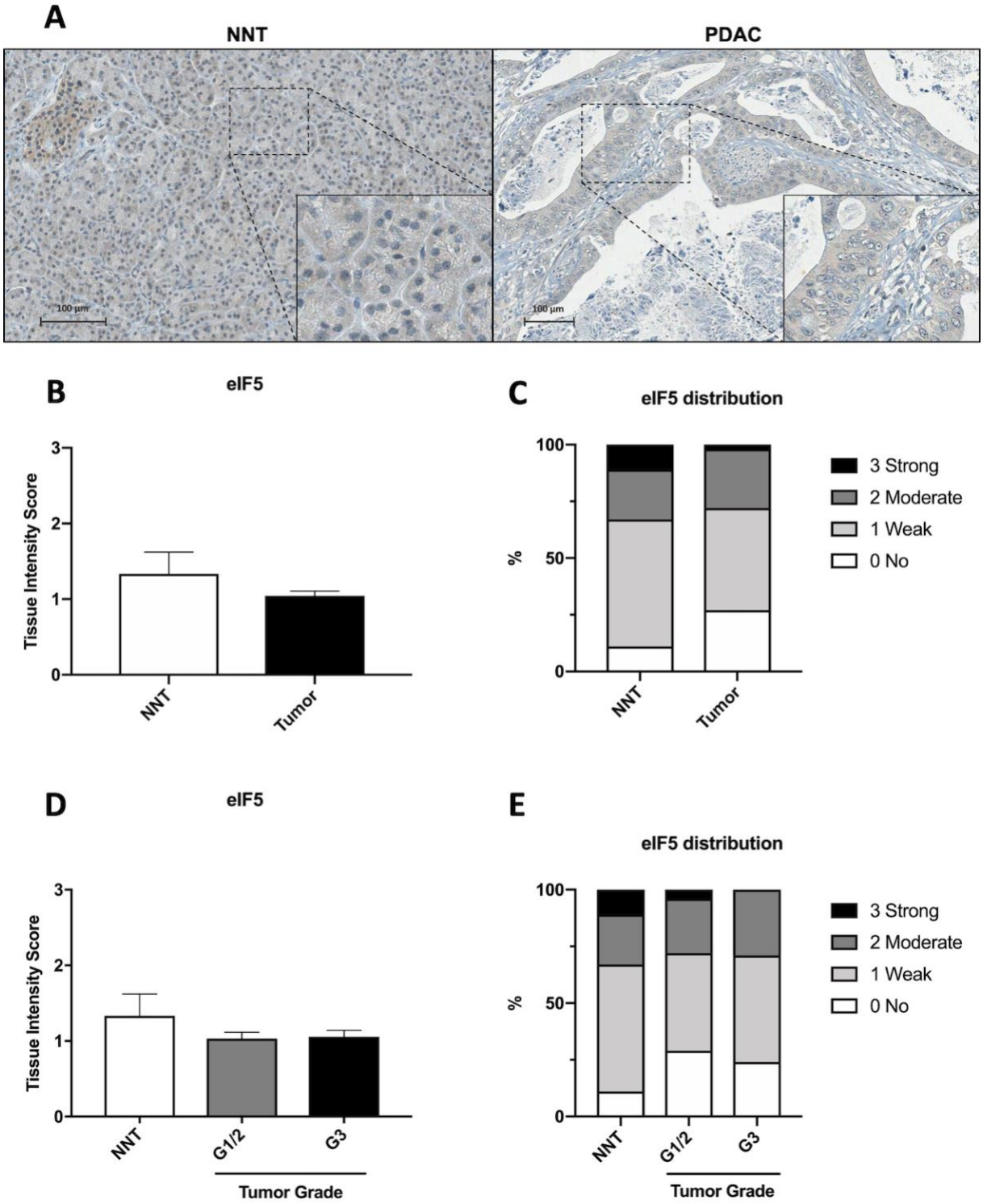


***Figure 19: Immunohistochemical evaluation of eIF5 expression in PDAC compared to NNT.***

**(A)** Representative sections of eIF5 staining in NNT and PDAC. Scale bar indicates 100 µm. **(B)** No alteration in eIF5 expression in NNT versus PDAC samples (all grades) was detectable. **(C)** Distribution of expression in NNT compared to PDAC samples. **(D)** No significant differences in eIF5 expression in NNT versus PDAC samples, subgrouped by differentiation (G1/2 and G3) were present. Different tumor grades showed no significant differences. **(E)** Distribution of expression in NNT compared to PDAC samples, subgrouped by differentiation (G1/2 and G3). *($n_{NNT}$ = 9, $n_{tumor}$ = 168, $n_{G1/2}$ = 96, $n_{G3}$ = 72)*

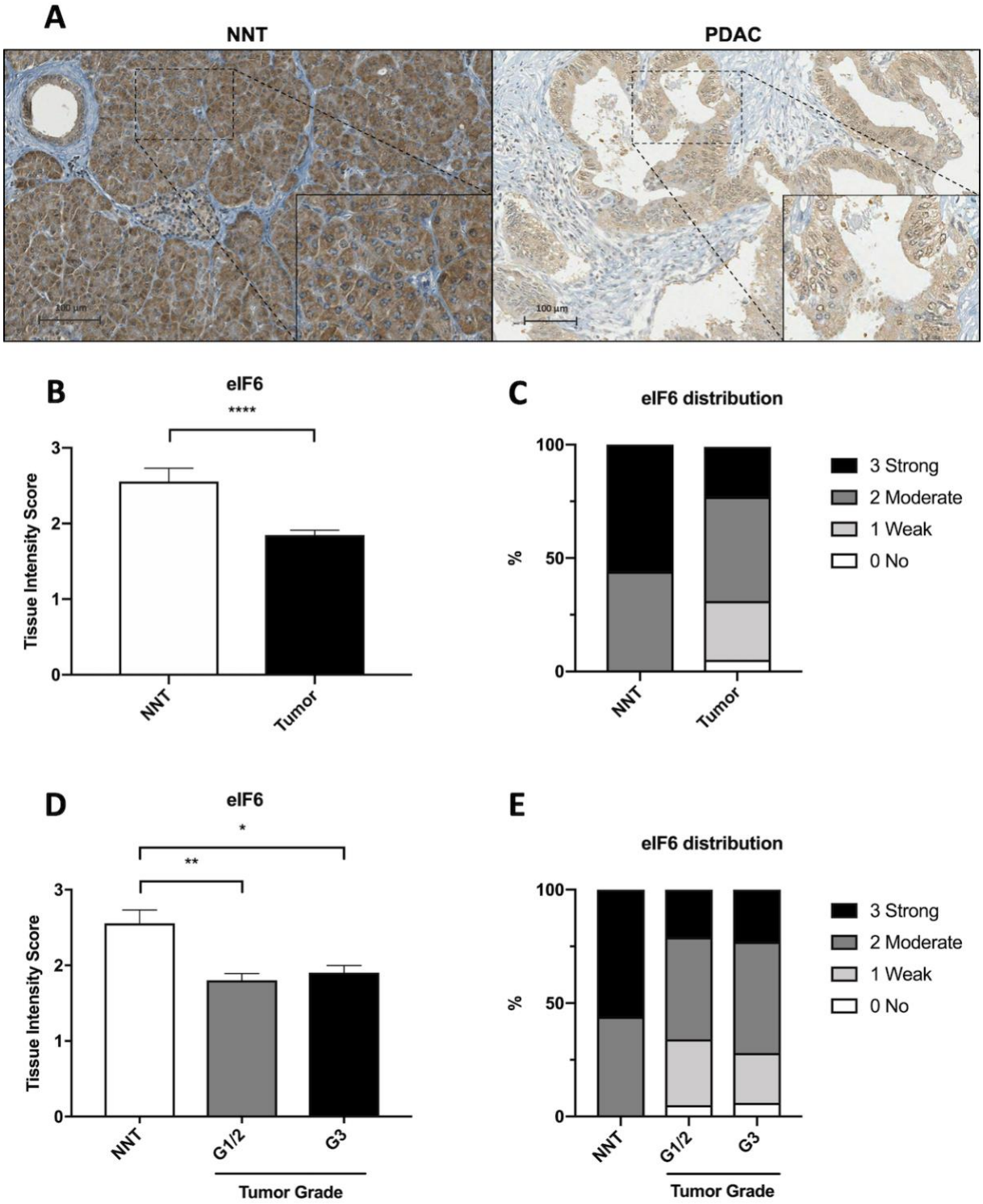


***Figure 20: Immunohistochemical evaluation of eIF6 expression in PDAC compared to NNT.***

**(A)** Representative sections of eIF6 staining in NNT and PDAC. Scale bar indicates 100 µm. **(B)** Downregulation of eIF6 expression in NNT versus PDAC samples (all grades), p = 0.0093. **(C)** Distribution of expression in NNT compared to PDAC samples. **(D)** Downregulation of eIF6 expression in NNT versus PDAC samples, subgrouped by differentiation. NNT vs. G1/2, p = 0.0083. NNT vs G3, p = 0.0252. **(E)** Distribution of expression in NNT compared to PDAC samples, subgrouped by differentiation (G1/2 and G3). *($n_{NNT}$ = 9, $n_{tumor}$ = 164, $n_{G1/2}$ = 92, $n_{G3}$ = 72)*

#### 3.1.9.2 Western Blot

53 PDAC specimens were analyzed and compared to 28 NNT specimens. Representative blots are shown in Figure 21A. Downregulation was observed in PDAC samples compared to NNT (p = 0.0052, Figure 21B). A subgroup analysis of 28 NNTs and 26 tumor samples where information on tumor grade was available revealed no significant differences in eIF6 expression between either of the groups (p > 0.99 for all groups, Figure 21C).

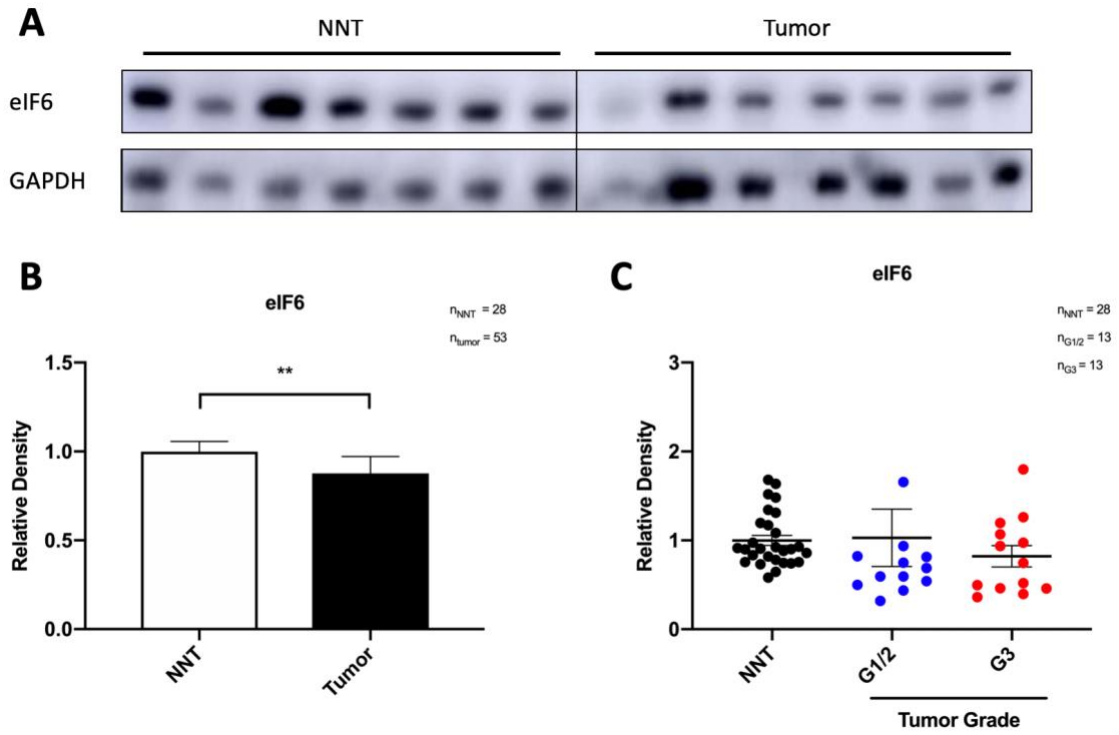


***Figure 21: Western Blot analysis of eIF6 expression.***

**(A)** Representative blots of eIF6 and GAPDH as HKG. **(B)** Downregulation of eIF6 in PDAC (n = 53) compared to NNT (n = 28), p = 0.0052. **(C)** Subgroup analysis of PDACs with available differentiation status (n = 26). No significant differences in eIF6 expression were detected (p > 0.99 for all groups).

### 3.1.10 Additional factors analyzed by Western Blot

#### 3.1.10.1 eIF1A

54 PDAC specimens were analyzed and compared to 28 NNT specimens. Representative blots are shown in Figure 22A. Downregulation was observed in PDAC samples compared to NNT ($p < 0.0001$, Figure 22B). A subgroup analysis of 28 NNTs and 26 PDAC samples where information on tumor grade was available showed significant downregulation for the G3 group compared to NNT ($p = 0.0013$), whereas the other groups showed no significant differences (Figure 22C).

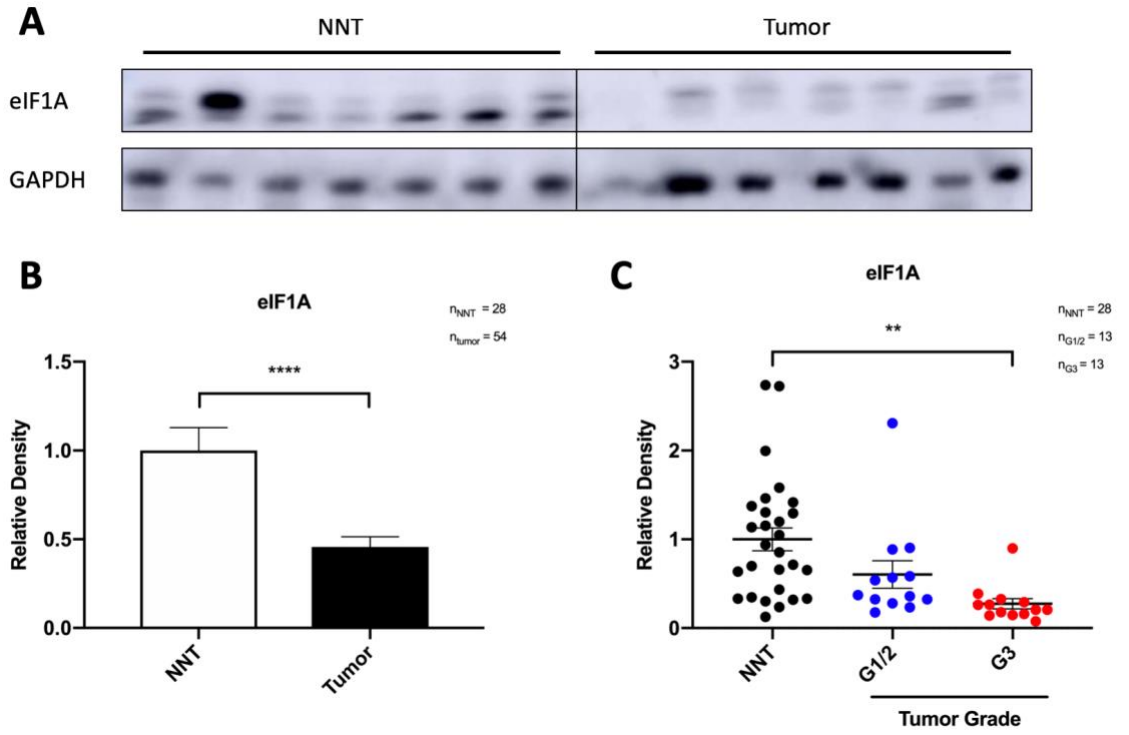


***Figure 22: Western Blot analysis of eIF1A expression.***

**(A)** Representative blots of eIF1A and GAPDH as HKG. **(B)** Downregulation of eIF1A in PDAC (n = 54) compared to NNT (n = 28), $p < 0.0001$. **(C)** Subgroup analysis of PDACs with available differentiation status (n = 26). Significant differences were detected in G3 tumors compared to NNT ($p = 0.0013$).

#### 3.1.10.2 eIF3B

52 PDAC specimens were analyzed and compared to 28 NNT specimens. Representative blots are shown in Figure 23A. Downregulation was observed in PDAC samples compared to NNT ($p = 0.0037$, Figure 23B). A subgroup analysis of 28 NNTs and 24 PDAC samples where information on tumor grade was available showed significant differences in the G1/2 (n = 12) group compared to NNT ($p = 0.0004$, Figure 23C). G3 vs. NNT ($p = 0.1261$) and G1/2 vs. G3 ($p = 0.2771$) showed no significant differences.

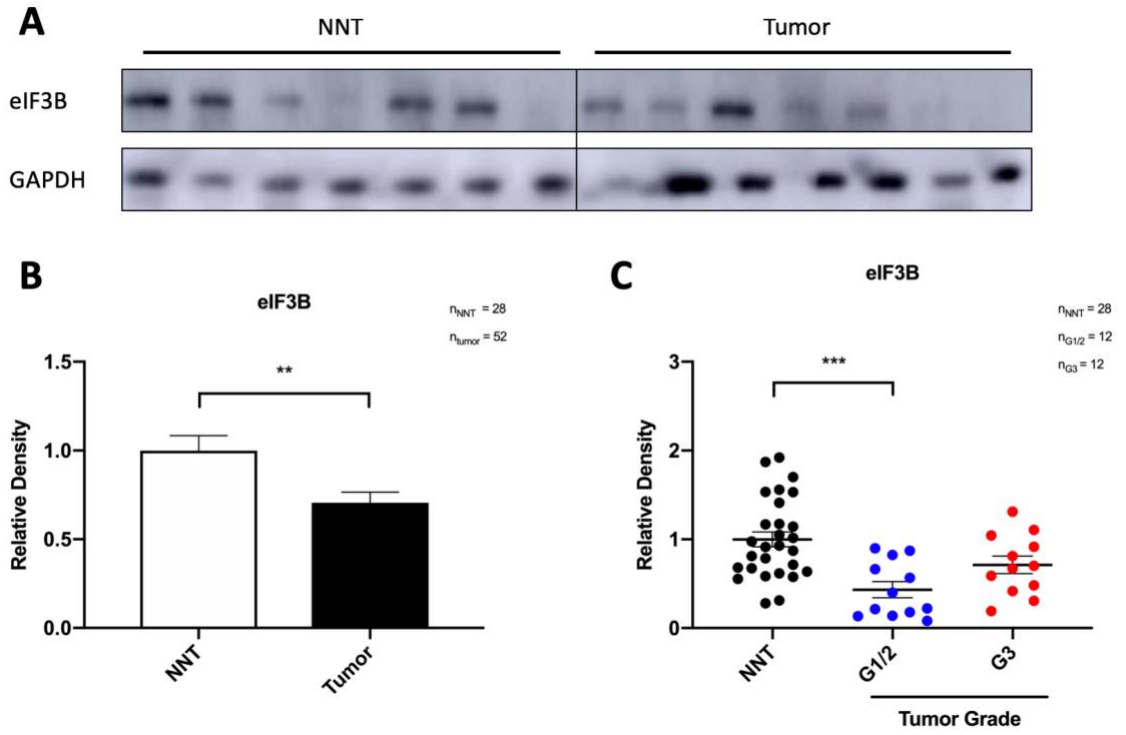


***Figure 23: Western Blot analysis of eIF3B expression.***

**(A)** Representative blots of eIF3B and GAPDH as HKG. **(B)** Downregulation of eIF3B in PDAC (n = 52) compared to NNT (n = 28), p = 0.0037. **(C)** Subgroup analysis of PDACs with available differentiation status (n = 24). Significant downregulation was detected in the G1/2 group compared to NNT (p = 0.0004).

## 3.2 mRNA expression analysis – qRT-PCR

For mRNA expression analysis, total RNA from 22 NNTs and 38 PDAC samples was isolated and subjected to reverse transcription to generate cDNA as described in the methods part. As HKG, mean $C_t$ values of *RPL41* and *YWHAZ* were used, as they were the most stably expressed HKGs and yielded specific products (Figure 24A - D).

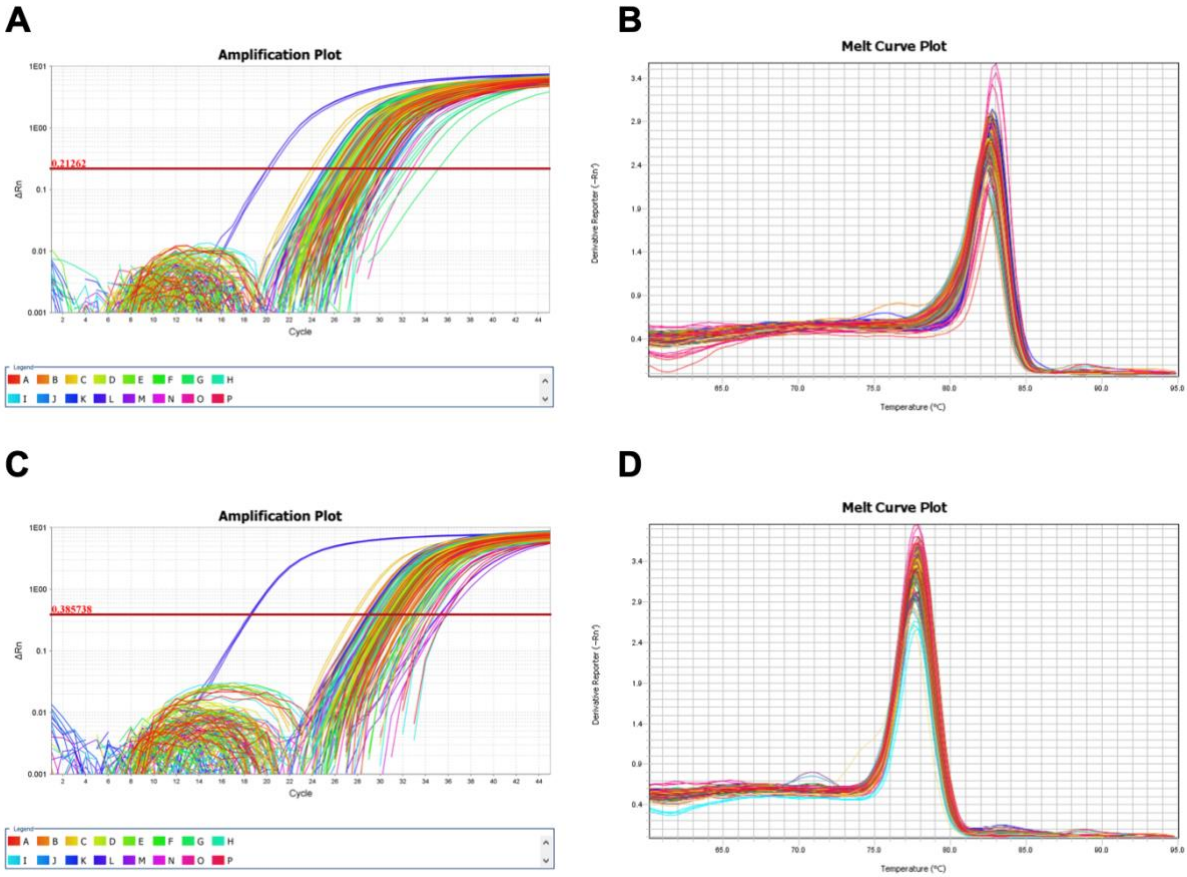


***Figure 24: Amplification plots and melt curves of utilized HKGs (RPL41 and YWHAZ).***

**(A)** Amplification plot of RPL41. **(B)** Melt curve plot of RPL41. The amplicon-specific peak is visible at 82.5°C. **(C)** Amplification plot of YWHAZ. **(D)** Melt curve plot of YWHAZ. The amplicon-specific peak is visible at 77.5°C.

### 3.2.1 *EIF1* mRNA expression

*EIF1* mRNA expression was reduced 0.710-fold in PDAC (n = 34) compared to NNT (n = 19) (Figure 25A). Statistical analysis after log-transformation revealed that this decrease was significant (p = 0.0338, Figure 25B). Amplification and melting curve plots were assessed to ensure specificity (Figure 25C, D). Samples with unspecific amplification products were excluded from data analysis.

### 3.2.2 *EIF1AX* mRNA expression

*EIF1AX* mRNA expression was reduced 0.413-fold in PDAC (n = 30) compared to NNT (n = 16) (Figure 26A). Statistical analysis after log-transformation revealed that this decrease was significant (p = 0.0002, Figure 26B). Amplification and melting curve plots were assessed to ensure specificity (Figure 26C, D). Samples with unspecific amplification products were excluded from data analysis.

### 3.2.3 *EIF2S1* mRNA expression

*EIF2S1* mRNA expression was reduced 0.753-fold in PDAC (n = 35) compared to NNT (n = 19) (Figure 27A). However, statistical analysis after log-transformation revealed that this decrease was not significant (p = 0.2829, Figure 27B). Amplification and melting curve plots were assessed to ensure specificity (Figure 27C, D). Samples with unspecific amplification products were excluded from data analysis.

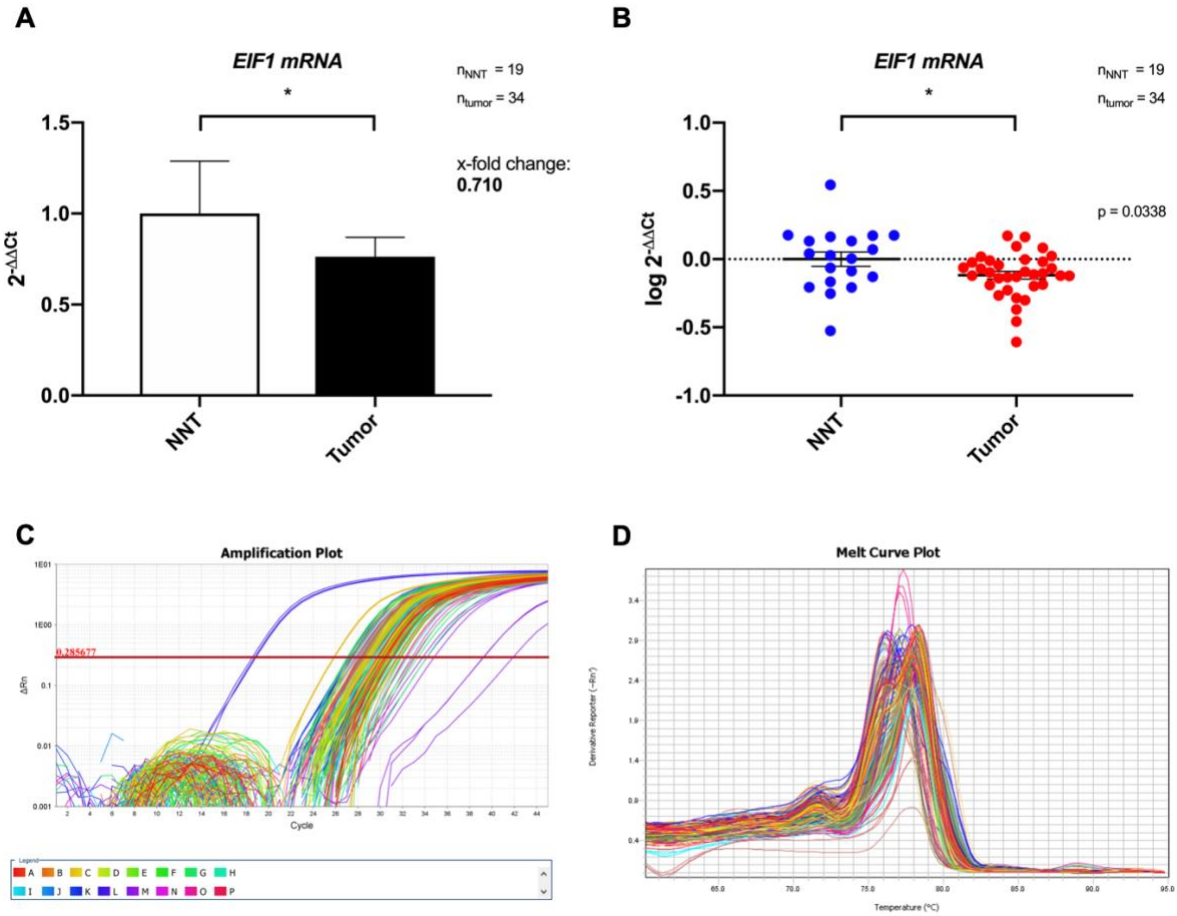


***Figure 25: qRT-PCR analysis of EIF1 mRNA expression in PDAC.***

**(A)** *EIF1* mRNA expression analyzed by $2^{-\Delta\Delta Ct}$-method. A 0.710-fold decrease is seen in PDAC (n = 34) compared to NNT (n = 19) **(B)** Log-transformed data analyzed by t-test. Significantly lower amounts of *EIF1* mRNA was present in PDAC compared to NNT, p = 0.0338. **(C)** Amplification plot of analyzed samples. **(D)** Melt curve plot of analyzed samples. The amplicon peaks are present at around 77°C.

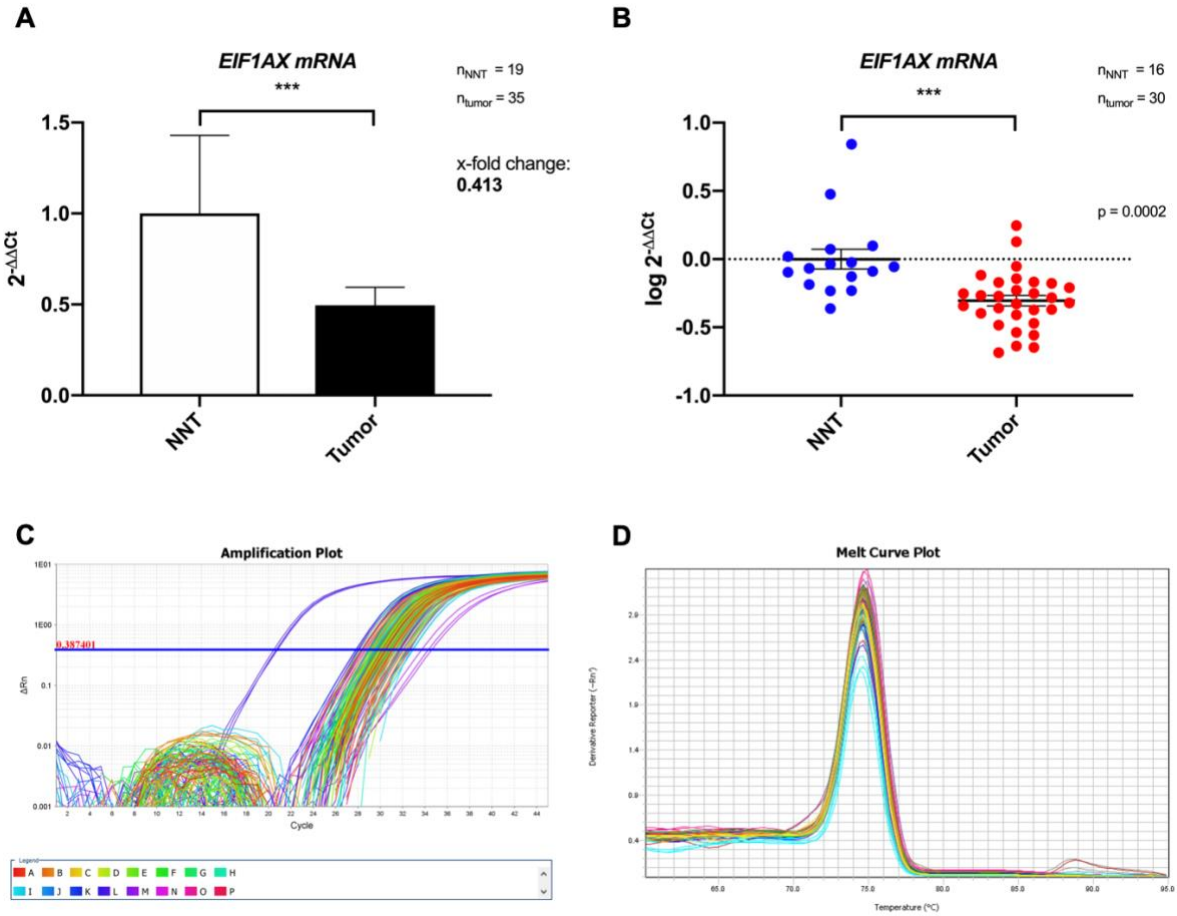


***Figure 26: qRT-PCR analysis of EIF1AX mRNA expression in PDAC.***

**(A)** *EIF1AX* mRNA expression analyzed by $2^{-\Delta\Delta Ct}$-method. A 0.413-fold decrease is seen in PDAC (n = 30) compared to NNT (n = 16) **(B)** Log-transformed data analyzed by t-test. Significantly lower amounts of *EIF1AX* mRNA was present in PDAC compared to NNT, p = 0.0002. **(C)** Amplification plot of analyzed samples. **(D)** Melt curve plot of analyzed samples. The amplicon-specific peak is present at around 75°C.

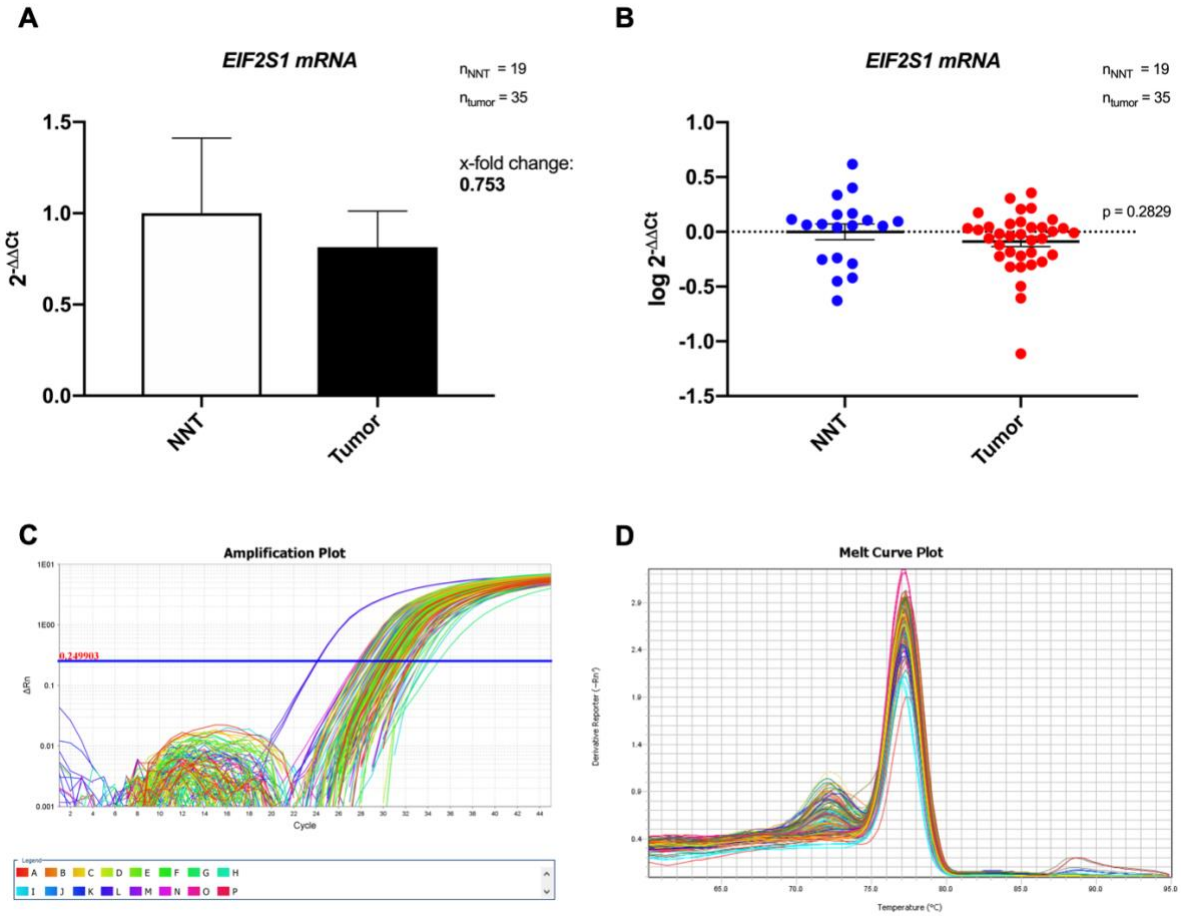


***Figure 27: qRT-PCR analysis of EIF2S1 mRNA expression in PDAC.***

**(A)** *EIF2S1* mRNA expression analyzed by $2^{-\Delta\Delta Ct}$-method. A 0.753-fold decrease is seen in PDAC (n = 35) compared to NNT (n = 19) **(B)** Log-transformed data analyzed by t-test. No significant decrease is seen in PDAC compared to NNT, p = 0.2829. **(C)** Amplification plot of analyzed samples. **(D)** Melt curve plot of analyzed samples. The amplicon-specific peak is present at 77°C. A smaller primer dimer peak is present at 72°C.

## 3.3 Clinical relevance of eIF expression – survival analysis

### 3.3.1 Survival analysis with protein data

Kaplan-Meier curves were generated for patients of the IHC cohort where survival data was available (n = 155). Groups were first stratified by eIF expression (low (0 and 1) vs. high (2 and 3) expression) and the log-rank test was applied. Furthermore, groups were sub-stratified by grading into 4 distinct groups (G1/2 with low eIF vs. G1/2 with high eIF vs. G3 with low eIF vs. G3 with high eIF) and analyzed with the log-rank test.

#### 3.3.1.1 eIF2α

Patients with high eIF2α expression showed significantly poorer outcome compared to patients with low expression (n = 148, p = 0.0401, Figure 28A). The median overall survival in the low expression group was 532 days compared to 370 days in the high expression group. Sub-stratification by grading showed significant differences in overall survival, with the worst outcome for patients with high eIF2α and poor differentiation (p = 0.0443, Figure 28B). Median overall survival was 611 (G1/2 and low eIF2α), 434 (G1/2 and high eIF2α), 448 (G3 and low eIF2α) and 268 (G3 and high eIF2α) days, respectively.

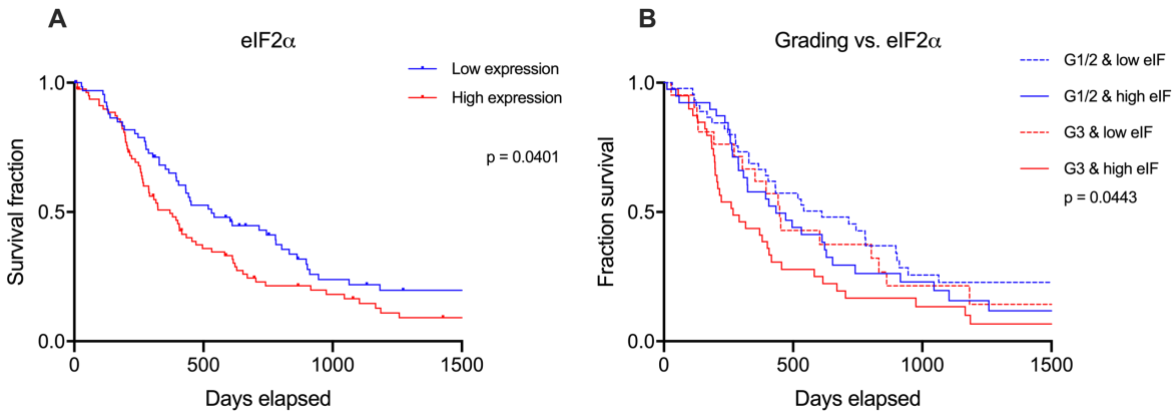


***Figure 28: Survival analysis of PDAC patients stratified by eIF2α expression.***

**(A)** Significant difference in overall survival is present between patients with low versus high eIF2α expression, p = 0.0401. **(B)** Sub-stratification by tumor grade. Patients with high eIF2α and poor differentiation (G3) show the worst outcome.

3.3.1.2 eIFs without significant influence on survival on protein level

Additional eIFs were stratified into low and high expression and analyzed for their effect on overall survival. No significant influence on patient survival was found for eIF3A (p = 0.6168), eIF3C (p = 0.2073), eIF4E (p = 0.6721), eIF4G (p = 0.5172), eIF5 (p = 0.8686) and eIF6 (p = 0.2041) (Figures 29 and 30). Median overall survival is given in Table 11. Further stratification by tumor grade showed no significant influences on overall survival (Figures 29 and 30).

***Table 11: Median overall survival (days) of patients stratified by eIF expression.***

| | **eIF3A** | **eIF3C** | **eIF4E** | **eIF4G** | **eIF5** | **eIF6** |
|---|---|---|---|---|---|---|
| Low eIF | 432 | 452 | 434 | 386 | 404 | 532 |
| High eIF | 431 | 308 | 348 | 452 | 612 | 406 |

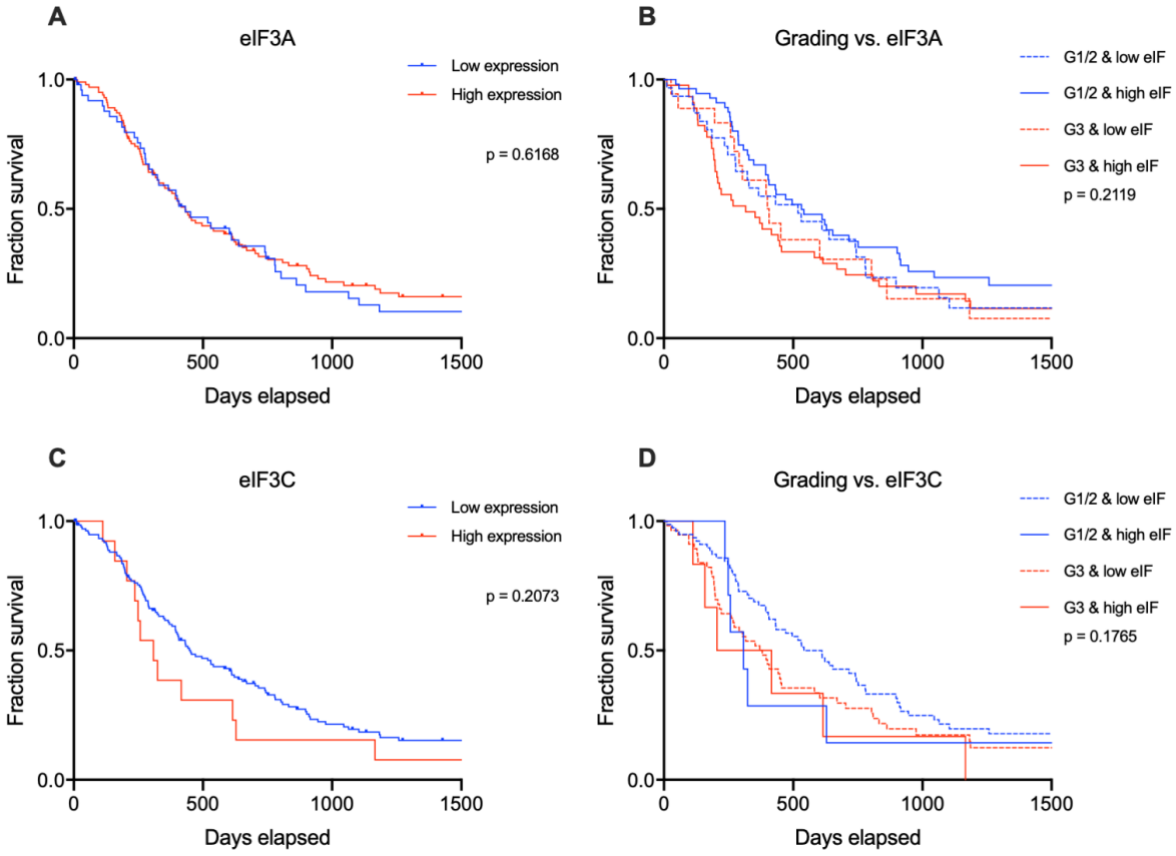


***Figure 29: Survival analysis of PDAC patients stratified by eIF3A and eIF3C expression.***

**(A + C)** Survival analysis stratified by eIF3A and eIF3C expression. No significant differences were observed.
**(B + D)** Survival analysis stratified by eIF expression and tumor grade. No significant differences were observed.

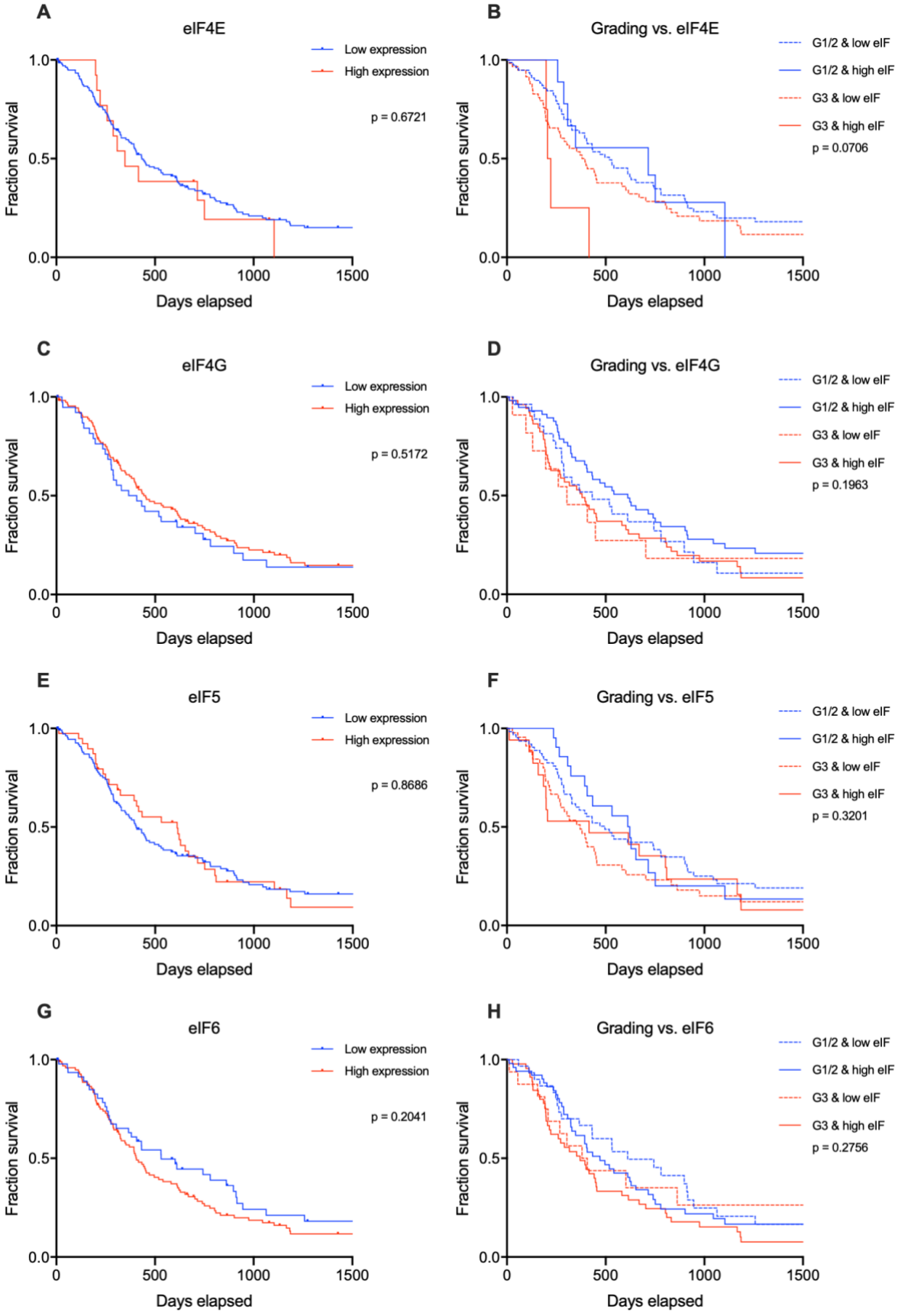


***Figure 30: Survival analysis of PDAC patients stratified by eIF4E, eIF4G, eIF5 and eIF6 expression.***

**(A, C, E, G)** Survival analysis stratified by eIF expression. No significant differences were observed. **(B, D, F, H)** Stratification by eIF expression and tumor grade. No significant differences were observed.

### 3.3.2 *In silico* survival analysis with mRNA data

Survival analysis on mRNA level was performed for patient data available on the TCGA data bank (n = 125). Significant influence on overall survival was found for *EIF1*, *EIF2A* and *EIF3C*.

#### 3.3.2.1 *EIF1*

Higher levels of *EIF1* mRNA correlated with better overall survival compared to tumors expressing low levels of *EIF1* mRNA (p = 0.048, Figure 31).

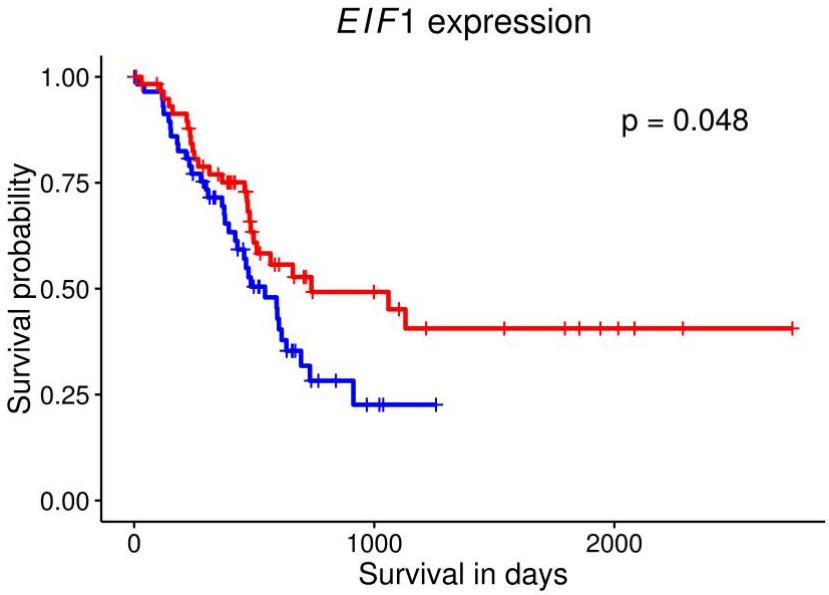


***Figure 31: Survival analysis of TCGA patient data, stratified by EIF1 mRNA level.***
Patients with high *EIF1* mRNA level (red) show better overall survival compared to patients with low *EIF1* mRNA level (blue), p = 0.048, n = 125.

#### 3.3.2.2 *EIF2A*

Low levels of *EIF2A* mRNA (encoding eIF2A, not eIF2α whose mRNA is termed *EIF2S1*) correlated with better overall survival compared to tumors expressing high levels of *EIF2A* mRNA (p = 0.002, Figure 32).

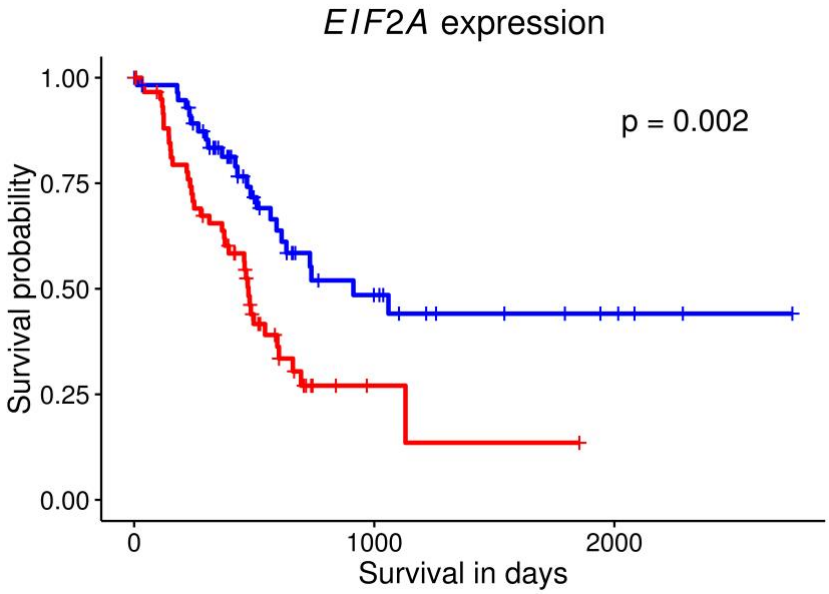


***Figure 32: Survival analysis of TCGA patient data, stratified by EIF2A mRNA level.***

Patients with low *EIF2A* mRNA level (blue) show better overall survival compared to patients with high *EIF2A* mRNA level (red), p = 0.002, n = 125.

#### 3.3.2.3 *EIF3C*

Low levels of *EIF3C* mRNA correlated with better overall survival compared to tumors expressing high levels of *EIF3C* mRNA (p = 0.026, Figure 33).

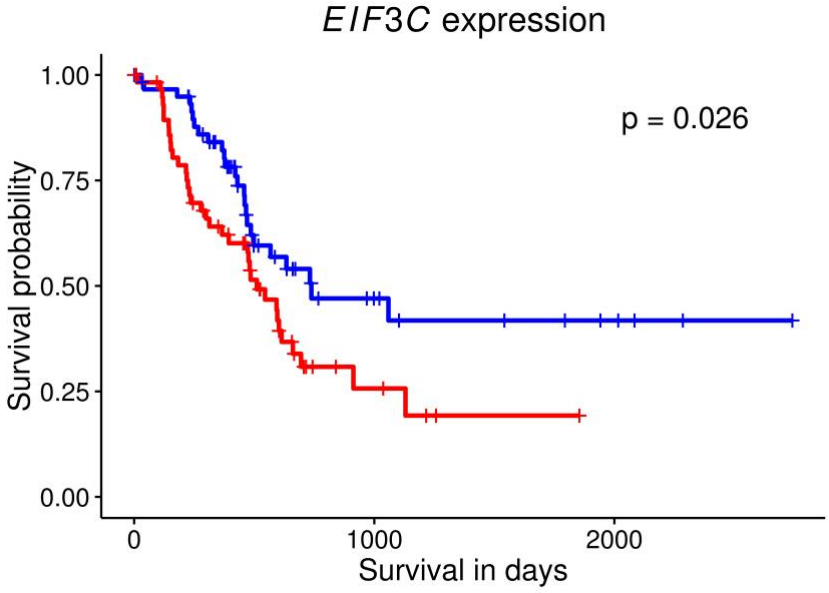


***Figure 33: Survival analysis of TCGA patient data, stratified by EIF3C mRNA level.***

Patients with low *EIF3C* mRNA level (blue) show better overall survival compared to patients with high *EIF3C* mRNA level (red), p = 0.026, n = 125.

3.3.2.4 eIFs without significant influence on survival on mRNA level

mRNA levels of additional eIFs were analyzed for their influence on patient survival. No significant influence on overall survival was found for *EIF1AX* (p = 0.187), *EIF3A* (p = 0.280), *EIF4E* (p = 0.361), *EIF4G1* (p = 0.058), *EIF5* (p = 0.661) and *EIF6* (p = 0.132) mRNA levels (Figure 34).

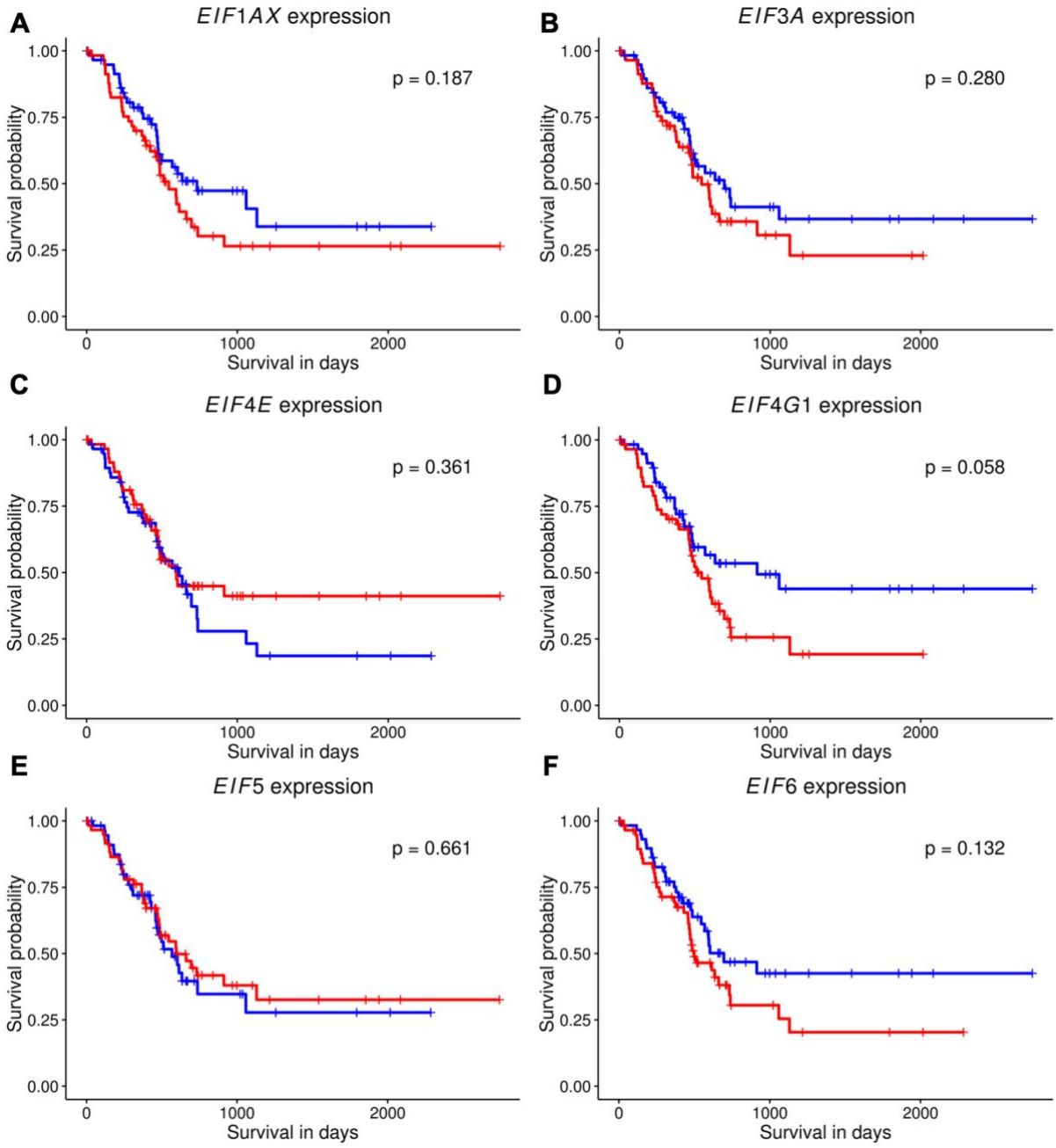


***Figure 34: Survival analysis of TCGA patient data, stratified by EIF1AX, EIF3A, EIF4E, EIF4G1, EIF5 and EIF6 mRNA levels.***

**(A – F)** No significant influences on overall survival were observed for **(A)** *EIF1A*, **(B)** *EIF3A*, **(C)***EIF4E*, **(D)** *EIF4G1*, **(E)** *EIF5* and **(F)** *EIF6* mRNA levels.

# 4 Discussion

Understanding tumor biology on a molecular level and dysregulation of cellular processes is of great importance to improve patient outcome in the future. Thus, developing novel tailored therapies and prognostic models based on biomarkers is crucially depending on continuous research efforts elucidating pathways and therapeutic targets, especially in entities with such dismal prognosis as PDAC.

In this study, evidence is presented hinting to differential expression of various eIFs in PDAC, adding to previous research implicating eIFs in tumor biology in many other entities. Additionally, prognostic relevance of some eIFs was found, providing potential novel tools for identification of subgroups of patients with either more or less favorable prognosis.

## 4.1 Methodological limitations

First, the subset of analyzed cells differs from method to method. In the Immunoblot and qRT-PCR, whole tissue samples are analyzed after tissue homogenization. Therefore, the measured protein and mRNA levels are also influenced by all tumor stromal cells such as infiltrating immune cells, endothelial cells and connective tissue cells. As pancreatic cancer shows especially dense and multifaceted stromal reactions (155), caution is warranted when interpreting the results. To properly account for this issue, IHC results are of great use, as they allow for tumor cell-specific analysis of expression. Interpretation is therefore done as synopsis of all methods.

Second, the presented data are solely descriptive. As no definitive molecular mechanism for the obtained results is currently available, it remains unknown if the described findings are causatively implicated in pancreatic carcinogenesis or if they are bystander products resulting from other primarily affected pathways. Exemplarily, for the downregulated factors, further research might focus on generating an overexpression model and analyzing if tumor biology is thereby affected.

Last, inter-tumor heterogeneity poses a tremendously hard factor to account for. As mentioned above, genetic diversity of tumors that all histologically appear as PDAC

is utterly complex (62). Such genetic sub-classifications have not been considered here, analyzing all PDAC samples in one group (except for stratification by tumor grade) as if they were biologically the same entity. It is therefore likely, that generalized statements made here concerning PDAC do not apply for all biologically distinct subgroups.

## 4.2 eIF expression patterns in PDAC

eIF1 was found downregulated in tumor tissue on protein level (IHC, Immunoblot) and on mRNA level (qRT-PCR). Interestingly, the immunohistochemical analysis shows total loss of eIF1 expression in all but one sample. The finding, that eIF1 seems present in the Immunoblot and qRT-PCR, albeit at low levels, might be attributable to stromal cells, as indicated above. The rationale underlying this loss or downregulation may be found in the protein´s function. As described above, eIF1 functions to ensure start codon recognition fidelity (82) and was initially described as translation initiation inhibitor *sui1* in yeast (156). Overexpression of *EIF1* (hu-*sui1*) was performed in hepatocellular carcinoma cells (HepG2) and caused effective suppression of growth (157), further underlining its tumor-suppressive powers. Additional recent data demonstrated that eIF1 deprivation and the consecutive imprecise initiation codon recognition substantially affects translational control of at least 245 different transcripts by enhancing expression of their respective upstream open reading frames (uORFs) in the 5´UTR (158). The same study also associated eIF1 deprivation with downregulation of eIF2$\alpha$. Generally, eIF1 might, through the mechanisms mentioned above, lead to alteration of expression of both growth-stimulatory genes and tumor-suppressive genes, ultimately contributing to cancerous phenotype. In line with these suggestions were the findings in this study, that high levels of *EIF1* mRNA are associated with better outcome and vice versa. Downregulation was also found for eIF1A on both protein and mRNA levels. As eIF1A is functionally similar to eIF1, this may be due to the very same, abovementioned reasons. Furthermore, eIF2$\alpha$ was found downregulated on protein level, both in IHC and the Immunoblot. This finding may be attributable to the fact, that almost all NNTs used as comparison showed an intense expression of eIF2$\alpha$, leading to detection of relative downregulation in the PDAC samples. Nonetheless, PDAC samples also demonstrated considerable

expression of eIF2α. However, this difference was not seen on mRNA level. Therefore, the detected relative downregulation of eIF2α may be primarily caused by translational or posttranslational regulation. As described above, eIF1 loss coincides with downregulation of eIF2α (158), even though the extent of eIF2α downregulation here exceeds the reported quantity. Regarding functional aspects, eIF2α was shown to be a regulator of global protein synthesis, making its downregulation in tumor cells rather unexpected. Notably, eIF2α activity is tightly regulated, which is achieved by phosphorylation (159). Hence, the additional finding described here, that the phosphorylated form of eIF2α is also less abundant in PDAC might diminish the effect or even abolish the expected translational inhibition caused by eIF2α downregulation. However, as the phosphorylation of eIF2α also represents an important survival mechanism under hypoxic and anoxic conditions (160) (as it is commonly encountered in PDAC and is associated with tumor aggressiveness (161)), this axis should be further investigated and might reveal promising findings. Limitations to the abovementioned statements result from the fact, that p-eIF2α expression was only analyzed via immunoblot in this study. Therefore, experiments confirming these findings with other methods are still pending. Besides overall expression, analysis of different tumor grades revealed higher eIF2α expression in poorly differentiated tumors compared to well and moderately differentiated tumors. This may reflect its role as oncoprotein found in most other entities, with higher expression rates accompanying successive dedifferentiation. Besides eIF1 and eIF2α, relevant alterations were also found for eIF3C and eIF6. Relatively little is known about eIF3C in tumor biology so far, but reports have implicated it as oncoprotein in breast cancer cell lines (BT474 and MDA-MB-231) (162) and as contributing factor to drug resistance in lung cancer cell lines (PC9/ER) (163), somewhat contrasting the downregulation of eIF3C reported here. However, the abovementioned reports were done *in vitro* only. Interestingly, another study reported differential expression of eIF3C in meningioma, with eIF3C expression depending on cellular contexts: samples where expression of the eIF3C interaction partner schwannomin, a tumor suppressor, was lost showed increased eIF3C expression, whereas tumors with intact schwannomin showed decreased eIF3C expression (164). A similar, context-dependent expression of eIF3C in PDAC might be possible. Therefore, further studies elucidating interaction partners of

eIF3C and their functions might explain these findings. The function of eIF6 on the other hand, is much better understood. The cytoplasmic function is to prevent premature ribosomal subunit joining and eIF6 overexpression has been found in a variety of tumors (165), such as colorectal cancer (138), non-small cell lung cancer (166) and head and neck cancer (140). Its downregulation in PDAC compared to healthy pancreatic tissue might therefore be the result of the very high baseline expression in the control tissue rather than a carcinogenetic necessity. Nonetheless, the molecular mechanisms causing this expression shift might reveal novel pathways and therefore deserves attention. Lastly, eIF3A was found to be overexpressed in PDAC in IHC. However, this has already been described (146) and confirms the reported findings.

Besides dissecting the findings factor by factor, a possible explanation might help interpret this almost global eIF downregulation. PDAC, as described in the introduction, arises from a variety of precursor lesions, with one model hinting to the acinar cell as its most common cell of origin (65). Thus, PDAC is a result of successive dedifferentiation of acinar cells, which constitute an exocrine cell type physiologically producing vast amounts of proteins such as digestion enzymes. Consequently, the almost global downregulation of eIFs in neoplastic pancreatic tissue described in this study might be the result of relative loss of eIF expression through mutational or epigenetic strikes occurring during pancreatic tumorigenesis. However, to confirm these hypotheses further research is needed. As novel single-cell approaches allow for detailed characterization of cell-type specific protein and gene expression, this might be possible in the near future. Additionally, in this study the cell of origin yielding the respective tumor was not taken into account. If duct cell-derived tumors and acinar cell-derived tumors were analyzed separately and compared to their respective cell of origin, one might indeed find divergent regulations of eIF expression.

## 4.3 Clinical potential of eIFs in PDAC

eIFs were shown to be of possible clinical interest as prognostic biomarkers, as eIF2$\alpha$ expression in IHC and *EIF2A*, *EIF1* and *EIF3C* mRNA expression significantly correlated with overall survival. Specifically, *EIF2A* and *EIF3C* mRNA levels as well as eIF2$\alpha$ protein levels were found to be unfavorable prognostic factors. In contrast, *EIF1*, whose expression level was also found to be downregulated in PDAC, was found to be a favorable prognostic factor. Besides measuring mRNA or protein levels of the indicated factors in the primary tumor tissue, another possible application might result from quantifying their presence in patient blood via circulating tumor cells. If such tests yield significant prognostic parameters remains to be investigated, though. Hence, to evaluate their applicability, prospective studies would be of great use. Last, therapeutic potential of inhibiting eIFs in PDAC needs to be addressed. Generally, the observed relative downregulation must not necessarily indicate, that inhibitory approaches are not useful in this entity. As discussed for some factors such as eIF2$\alpha$, the expression is still considerably high, making therapeutic inhibition a possibility. If the effects of inhibition will be as promising as in other entities remains to be seen. However, targeting the translation machinery shows rapid advancements in preclinical tests (167) which should not spare PDAC.

## 4.4 Conclusion

In summary, this study demonstrates that the expression of various eIF subunits is altered in PDAC and that some of these changes correlate with clinical outcome. However, mechanistic insights into the underlying causes are yet pending. Consequently, eIFs might be regarded as important players in PDAC carcinogenesis and should receive further attention in future research.

# 5 References


1. Ferlay J, Colombet M, Soerjomataram I, Dyba T, Randi G, Bettio M, et al. Cancer incidence and mortality patterns in Europe: Estimates for 40 countries and 25 major cancers in 2018. Eur J Cancer. 2018 Nov;103:356–87.
2. Siegel RL, Miller KD, Jemal A. Cancer statistics, 2018. CA Cancer J Clin. 2018 Jan;68(1):7–30.
3. Malvezzi M, Carioli G, Bertuccio P, Boffetta P, Levi F, La Vecchia C, et al. European cancer mortality predictions for the year 2018 with focus on colorectal cancer. Ann Oncol. 2018 Apr 1;29(4):1016–22.
4. Bray F, Ferlay J, Soerjomataram I, Siegel RL, Torre LA, Jemal A. Global cancer statistics 2018: GLOBOCAN estimates of incidence and mortality worldwide for 36 cancers in 185 countries. CA Cancer J Clin. 2018 Nov;68(6):394–424.
5. Yeo TP. Demographics, epidemiology, and inheritance of pancreatic ductal adenocarcinoma. Semin Oncol. 2015 Feb;42(1):8–18.
6. Midha S, Chawla S, Garg PK. Modifiable and non-modifiable risk factors for pancreatic cancer: A review. Cancer Lett. 2016 Oct 10;381(1):269–77.
7. Lowenfels AB, Maisonneuve P. Epidemiology and risk factors for pancreatic cancer. Best Pract Res Clin Gastroenterol. 2006 Apr;20(2):197–209.
8. Yuan C, Morales-Oyarvide V, Babic A, Clish CB, Kraft P, Bao Y, et al. Cigarette Smoking and Pancreatic Cancer Survival. J Clin Oncol. American Society of Clinical Oncology; 2017 Jun 1;35(16):1822–8.
9. Maisonneuve P, Lowenfels AB. Risk factors for pancreatic cancer: a summary review of meta-analytical studies. Int J Epidemiol. 2015 Feb 1;44(1):186–98.
10. Carrera S, Sancho A, Azkona E, Azkuna J, Lopez-Vivanco G. Hereditary pancreatic cancer: related syndromes and clinical perspective. Hered Cancer Clin Pract. BioMed Central; 2017;15:9.
11. Matsubayashi H, Takaori K, Morizane C, Maguchi H, Mizuma M, Takahashi H, et al. Familial pancreatic cancer: Concept, management and issues. World J Gastroenterol. Baishideng Publishing Group Inc; 2017 Feb 14;23(6):935–48.
12. Hackeng WM, Hruban RH, Offerhaus GJA, Brosens LAA. Surgical and

molecular pathology of pancreatic neoplasms. Diagn Pathol. BioMed Central; 2016 Jun 7;11(1):47.

13. Hruban RH, Klimstra DS. Adenocarcinoma of the pancreas. Semin Diagn Pathol. NIH Public Access; 2014 Nov;31(6):443–51.
14. Maitra A, Hruban RH. Pancreatic cancer. Annu Rev Pathol. NIH Public Access; 2008;3:157–88.
15. Luchini C, Capelli P, Scarpa A. Pancreatic Ductal Adenocarcinoma and Its Variants. Surg Pathol Clin. 2016 Dec;9(4):547–60.
16. Cioc AM, Ellison EC, Proca DM, Lucas JG, Frankel WL. Frozen section diagnosis of pancreatic lesions. Arch Pathol Lab Med. 2002 Oct;126(10):1169–73.
17. Winter JM, Cameron JL, Campbell KA, Arnold MA, Chang DC, Coleman J, et al. 1423 pancreaticoduodenectomies for pancreatic cancer: A single-institution experience. J Gastrointest Surg. 2006 Nov;10(9):1199-210; discussion 1210-1.
18. Sierzega M, Młynarski D, Tomaszewska R, Kulig J. Semiquantitative immunohistochemistry for mucin (MUC1, MUC2, MUC3, MUC4, MUC5AC, and MUC6) profiling of pancreatic ductal cell adenocarcinoma improves diagnostic and prognostic performance. Histopathology. 2016 Oct;69(4):582–91.
19. Real FX, Vilá MR, Skoudy A, Ramaekers FC, Corominas JM. Intermediate filaments as differentiation markers of exocrine pancreas. II. Expression of cytokeratins of complex and stratified epithelia in normal pancreas and in pancreas cancer. Int J cancer. 1993 Jul 9;54(5):720–7.
20. Ballehaninna UK, Chamberlain RS. Biomarkers for pancreatic cancer: promising new markers and options beyond CA 19-9. Tumor Biol. 2013 Dec 17;34(6):3279–92.
21. Oshima M, Okano K, Muraki S, Haba R, Maeba T, Suzuki Y, et al. Immunohistochemically Detected Expression of 3 Major Genes (CDKN2A/p16, TP53, and SMAD4/DPC4) Strongly Predicts Survival in Patients With Resectable Pancreatic Cancer. Ann Surg. 2013 Aug;258(2):336–46.
22. Wilentz RE, Goggins M, Redston M, Marcus VA, Adsay N V, Sohn TA, et al. Genetic, immunohistochemical, and clinical features of medullary carcinoma

of the pancreas: A newly described and characterized entity. Am J Pathol. American Society for Investigative Pathology; 2000 May;156(5):1641–51.

23. Kuo P-C, Chen S-C, Shyr Y-M, Kuo Y-J, Lee R-C, Wang S-E. Hepatoid carcinoma of the pancreas. World J Surg Oncol. BioMed Central; 2015 May 20;13:185.
24. Temesgen WM, Wachtel M, Dissanaike S. Osteoclastic giant cell tumor of the pancreas. Int J Surg Case Rep. Elsevier; 2014;5(4):175–9.
25. Borazanci E, Millis SZ, Korn R, Han H, Whatcott CJ, Gatalica Z, et al. Adenosquamous carcinoma of the pancreas: Molecular characterization of 23 patients along with a literature review. World J Gastrointest Oncol. Baishideng Publishing Group Inc; 2015 Sep 15;7(9):132–40.
26. Hoshimoto S, Matsui J, Miyata R, Takigawa Y, Miyauchi J. Anaplastic carcinoma of the pancreas: Case report and literature review of reported cases in Japan. World J Gastroenterol. Baishideng Publishing Group Inc; 2016 Oct 14;22(38):8631–7.
27. Liszka Ł, Zielińska-Pajak E, Pajak J, Gołka D. Colloid carcinoma of the pancreas: review of selected pathological and clinical aspects. Pathology. 2008 Dec;40(7):655–63.
28. Sakai T, Koshita S, Ito K, Kanno Y, Ogawa T, Kusunose H, et al. Signet-ring Cell Carcinoma Derived from a Main Duct-type Intraductal Papillary Mucinous Neoplasm of the Pancreas: A Case Report with Long-term Follow-up. Intern Med. 2018 Apr 15;57(8):1093–9.
29. Fearon ER, Vogelstein B. A genetic model for colorectal tumorigenesis. Cell. 1990 Jun 1;61(5):759–67.
30. Hruban RH, Goggins M, Parsons J, Kern SE. Progression model for pancreatic cancer. Clin Cancer Res. 2000 Aug;6(8):2969–72.
31. Pittman ME, Rao R, Hruban RH. Classification, Morphology, Molecular Pathogenesis, and Outcome of Premalignant Lesions of the Pancreas. Arch Pathol Lab Med. 2017 Dec;141(12):1606–14.
32. Esposito I, Konukiewitz B, Schlitter AM, Klöppel G. Pathology of pancreatic ductal adenocarcinoma: facts, challenges and future developments. World J Gastroenterol. Baishideng Publishing Group Inc; 2014 Oct 14;20(38):13833–41.
33. Yamaguchi H, Shimizu M, Ban S, Koyama I, Hatori T, Fujita I, et al. Intraductal

tubulopapillary neoplasms of the pancreas distinct from pancreatic intraepithelial neoplasia and intraductal papillary mucinous neoplasms. Am J Surg Pathol. 2009 Aug;33(8):1164–72.

34. Basturk O, Hong S-M, Wood LD, Adsay NV, Albores-Saavedra J, Biankin A V, et al. A Revised Classification System and Recommendations From the Baltimore Consensus Meeting for Neoplastic Precursor Lesions in the Pancreas. Am J Surg Pathol. NIH Public Access; 2015 Dec;39(12):1730–41.
35. Konstantinidis IT, Vinuela EF, Tang LH, Klimstra DS, D'Angelica MI, DeMatteo RP, et al. Incidentally Discovered Pancreatic Intraepithelial Neoplasia: What Is Its Clinical Significance? Ann Surg Oncol. 2013 Oct 8;20(11):3643–7.
36. Hruban RH, Adsay N V, Albores-Saavedra J, Compton C, Garrett ES, Goodman SN, et al. Pancreatic intraepithelial neoplasia: a new nomenclature and classification system for pancreatic duct lesions. Am J Surg Pathol. 2001 May;25(5):579–86.
37. Kanda M, Matthaei H, Wu J, Hong S-M, Yu J, Borges M, et al. Presence of somatic mutations in most early-stage pancreatic intraepithelial neoplasia. Gastroenterology. NIH Public Access; 2012 Apr;142(4):730–733.e9.
38. Koorstra J-BM, Feldmann G, Habbe N, Maitra A. Morphogenesis of pancreatic cancer: role of pancreatic intraepithelial neoplasia (PanINs). Langenbeck's Arch Surg. NIH Public Access; 2008 Jul;393(4):561–70.
39. Sessa F, Solcia E, Capella C, Bonato M, Scarpa A, Zamboni G, et al. Intraductal papillary-mucinous tumours represent a distinct group of pancreatic neoplasms: an investigation of tumour cell differentiation and K-ras, p53 and c-erbB-2 abnormalities in 26 patients. Virchows Arch. 1994;425(4):357–67.
40. Hruban RH, Takaori K, Klimstra DS, Adsay NV, Albores-Saavedra J, Biankin A V, et al. An illustrated consensus on the classification of pancreatic intraepithelial neoplasia and intraductal papillary mucinous neoplasms. Am J Surg Pathol. 2004 Aug;28(8):977–87.
41. Tanaka M, Fernández-del Castillo C, Kamisawa T, Jang JY, Levy P, Ohtsuka T, et al. Revisions of international consensus Fukuoka guidelines for the management of IPMN of the pancreas. Pancreatology. 2017 Sep;17(5):738–53.

42. Ban S, Naitoh Y, Mino-Kenudson M, Sakurai T, Kuroda M, Koyama I, et al. Intraductal papillary mucinous neoplasm (IPMN) of the pancreas: its histopathologic difference between 2 major types. Am J Surg Pathol. 2006 Dec;30(12):1561–9.
43. Zhang X-M, Mitchell DG, Dohke M, Holland GA, Parker L. Pancreatic cysts: depiction on single-shot fast spin-echo MR images. Radiology. 2002 May;223(2):547–53.
44. Wu J, Matthaei H, Maitra A, Dal Molin M, Wood LD, Eshleman JR, et al. Recurrent GNAS mutations define an unexpected pathway for pancreatic cyst development. Sci Transl Med. NIH Public Access; 2011 Jul 20;3(92):92ra66.
45. Paini M, Crippa S, Partelli S, Scopelliti F, Tamburrino D, Baldoni A, et al. Molecular pathology of intraductal papillary mucinous neoplasms of the pancreas. World J Gastroenterol. Baishideng Publishing Group Inc; 2014 Aug 7;20(29):10008–23.
46. Ren B, Liu X, Suriawinata AA. Pancreatic Ductal Adenocarcinoma and Its Precursor Lesions. Am J Pathol. 2019 Jan;189(1):9–21.
47. Hruban RH, Maitra A, Kern SE, Goggins M. Precursors to pancreatic cancer. Gastroenterol Clin North Am. NIH Public Access; 2007 Dec;36(4):831–49, vi.
48. Le Borgne J, de Calan L, Partensky C, Association the FS. Cystadenomas and cystadenocarcinomas of the pancreas: a multiinstitutional retrospective study of 398 cases. French Surgical Association. Ann Surg. Lippincott, Williams, and Wilkins; 1999 Aug;230(2):152–61.
49. Wilentz RE, Albores-Saavedra J, Zahurak M, Talamini MA, Yeo CJ, Cameron JL, et al. Pathologic examination accurately predicts prognosis in mucinous cystic neoplasms of the pancreas. Am J Surg Pathol. 1999 Nov;23(11):1320–7.
50. Kim H, Ro JY. Intraductal Tubulopapillary Neoplasm of the Pancreas: An Overview. Arch Pathol Lab Med. 2018 Mar;142(3):420–3.
51. Basturk O, Berger MF, Yamaguchi H, Adsay V, Askan G, Bhanot UK, et al. Pancreatic intraductal tubulopapillary neoplasm is genetically distinct from intraductal papillary mucinous neoplasm and ductal adenocarcinoma. Mod Pathol. 2017 Dec 4;30(12):1760–72.
52. Yamaguchi H, Kuboki Y, Hatori T, Yamamoto M, Shiratori K, Kawamura S, et al. Somatic Mutations in PIK3CA and Activation of AKT in Intraductal

Tubulopapillary Neoplasms of the Pancreas. Am J Surg Pathol. 2011 Dec;35(12):1812–7.

53. Jones S, Zhang X, Parsons DW, Lin JC-H, Leary RJ, Angenendt P, et al. Core signaling pathways in human pancreatic cancers revealed by global genomic analyses. Science. 2008 Sep 26;321(5897):1801–6.
54. Shi C, Daniels JA, Hruban RH. Molecular characterization of pancreatic neoplasms. Adv Anat Pathol. 2008 Jul;15(4):185–95.
55. Hruban RH, van Mansfeld AD, Offerhaus GJ, van Weering DH, Allison DC, Goodman SN, et al. K-ras oncogene activation in adenocarcinoma of the human pancreas. A study of 82 carcinomas using a combination of mutant-enriched polymerase chain reaction analysis and allele-specific oligonucleotide hybridization. Am J Pathol. 1993 Aug;143(2):545–54.
56. Moskaluk CA, Hruban RH, Kern SE. p16 and K-ras gene mutations in the intraductal precursors of human pancreatic adenocarcinoma. Cancer Res. 1997 Jun 1;57(11):2140–3.
57. Hingorani SR, Petricoin EF, Maitra A, Rajapakse V, King C, Jacobetz MA, et al. Preinvasive and invasive ductal pancreatic cancer and its early detection in the mouse. Cancer Cell. 2003 Dec;4(6):437–50.
58. Mann KM, Ying H, Juan J, Jenkins NA, Copeland NG. KRAS-related proteins in pancreatic cancer. Pharmacol Ther. 2016 Dec;168:29–42.
59. Eser S, Schnieke A, Schneider G, Saur D. Oncogenic KRAS signalling in pancreatic cancer. Br J Cancer. 2014 Aug 22;111(5):817–22.
60. Hruban RH, Offerhaus GJ, Kern SE, Goggins M, Wilentz RE, Yeo CJ. Tumor-suppressor genes in pancreatic cancer. J Hepatobiliary Pancreat Surg. 1998;5(4):383–91.
61. Waddell N, Pajic M, Patch A-M, Chang DK, Kassahn KS, Bailey P, et al. Whole genomes redefine the mutational landscape of pancreatic cancer. Nature. NIH Public Access; 2015 Feb 26;518(7540):495–501.
62. Bailey P, Chang DK, Nones K, Johns AL, Patch A-M, Gingras M-C, et al. Genomic analyses identify molecular subtypes of pancreatic cancer. Nature. 2016 Mar 3;531(7592):47–52.
63. Yamaguchi J, Yokoyama Y, Kokuryo T, Ebata T, Nagino M. Cells of origin of pancreatic neoplasms. Surg Today. 2018 Jan 4;48(1):9–17.
64. Cubilla AL, Fitzgerald PJ. Morphological lesions associated with human

primary invasive nonendocrine pancreas cancer. Cancer Res. 1976 Jul;36(7 PT 2):2690–8.

65. Ferreira RMM, Sancho R, Messal HA, Nye E, Spencer-Dene B, Stone RK, et al. Duct- and Acinar-Derived Pancreatic Ductal Adenocarcinomas Show Distinct Tumor Progression and Marker Expression. Cell Rep. Elsevier; 2017 Oct 24;21(4):966–78.
66. Kopp JL, von Figura G, Mayes E, Liu F-F, Dubois CL, Morris JP, et al. Identification of Sox9-dependent acinar-to-ductal reprogramming as the principal mechanism for initiation of pancreatic ductal adenocarcinoma. Cancer Cell. NIH Public Access; 2012 Dec 11;22(6):737–50.
67. Habbe N, Shi G, Meguid RA, Fendrich V, Esni F, Chen H, et al. Spontaneous induction of murine pancreatic intraepithelial neoplasia (mPanIN) by acinar cell targeting of oncogenic Kras in adult mice. Proc Natl Acad Sci U S A. National Academy of Sciences; 2008 Dec 2;105(48):18913–8.
68. Morris JP, Wang SC, Hebrok M. KRAS, Hedgehog, Wnt and the twisted developmental biology of pancreatic ductal adenocarcinoma. Nat Rev Cancer. 2010 Oct 3;10(10):683–95.
69. von Figura G, Morris JP, Wright CVE, Hebrok M. Nr5a2 maintains acinar cell differentiation and constrains oncogenic Kras-mediated pancreatic neoplastic initiation. Gut. 2014 Apr;63(4):656–64.
70. Houbracken I, de Waele E, Lardon J, Ling Z, Heimberg H, Rooman I, et al. Lineage Tracing Evidence for Transdifferentiation of Acinar to Duct Cells and Plasticity of Human Pancreas. Gastroenterology. 2011 Aug;141(2):731–741.e4.
71. von Figura G, Fukuda A, Roy N, Liku ME, Morris IV JP, Kim GE, et al. The chromatin regulator Brg1 suppresses formation of intraductal papillary mucinous neoplasm and pancreatic ductal adenocarcinoma. Nat Cell Biol. 2014 Mar 23;16(3):255–67.
72. Bailey JM, Hendley AM, Lafaro KJ, Pruski MA, Jones NC, Alsina J, et al. p53 mutations cooperate with oncogenic Kras to promote adenocarcinoma from pancreatic ductal cells. Oncogene. 2016 Aug 23;35(32):4282–8.
73. Amin, M.B., Edge, S., Greene, F., Byrd, D.R., Brookland, R.K., Washington, M.K., Gershenwald, J.E., Compton, C.C., Hess, K.R., Sullivan, D.C., Jessup, J.M., Brierley, J.D., Gaspar, L.E., Schilsky, R.L., Balch, C.M., Winchester,

D.P., Asare, E.A., Madera, LR (Eds. . AJCC Cancer Staging Manual (8th edition). Eighth Edi. American Joint Commission on Cancer; 2017.

74. Kamisawa T, Wood LD, Itoi T, Takaori K. Pancreatic cancer. Lancet. 2016 Jul 2;388(10039):73–85.
75. Keane MG, Horsfall L, Rait G, Pereira SP. A case–control study comparing the incidence of early symptoms in pancreatic and biliary tract cancer. BMJ Open. 2014 Nov 19;4(11):e005720.
76. Ducreux M, Cuhna AS, Caramella C, Hollebecque A, Burtin P, Goéré D, et al. Cancer of the pancreas: ESMO Clinical Practice Guidelines for diagnosis, treatment and follow-up. Ann Oncol. Oxford University Press; 2015 Sep 26;26(suppl 5):v56–68.
77. Kamarajah SK, Burns WR, Frankel TL, Cho CS, Nathan H. Validation of the American Joint Commission on Cancer (AJCC) 8th Edition Staging System for Patients with Pancreatic Adenocarcinoma: A Surveillance, Epidemiology and End Results (SEER) Analysis. Ann Surg Oncol. 2017 Jul;24(7):2023–30.
78. Bilimoria KY, Bentrem DJ, Ko CY, Ritchey J, Stewart AK, Winchester DP, et al. Validation of the 6th edition AJCC Pancreatic Cancer Staging System: report from the National Cancer Database. Cancer. 2007 Aug 15;110(4):738–44.
79. Crick F. Central dogma of molecular biology. Nature. 1970 Aug 8;227(5258):561–3.
80. Jacob F, Monod J. Genetic regulatory mechanisms in the synthesis of proteins. J Mol Biol. Academic Press; 1961 Jun 1;3(3):318–56.
81. Ruggero D. Translational Control in Cancer Etiology. Cold Spring Harb Perspect Biol. 2013 Feb 1;5(2):a012336–a012336.
82. Jackson RJ, Hellen CUT, Pestova T V. The mechanism of eukaryotic translation initiation and principles of its regulation. Nat Rev Mol Cell Biol. NIH Public Access; 2010 Feb;11(2):113–27.
83. Silvera D, Formenti SC, Schneider RJ. Translational control in cancer. Nat Rev Cancer. 2010 Apr;10(4):254–66.
84. Guca E, Hashem Y. Major structural rearrangements of the canonical eukaryotic translation initiation complex. Curr Opin Struct Biol. 2018 Dec;53:151–8.
85. Aitken CE, Lorsch JR. A mechanistic overview of translation initiation in

eukaryotes. Nat Struct Mol Biol. 2012 Jun 5;19(6):568–76.

86. Schmitt E, Naveau M, Mechulam Y. Eukaryotic and archaeal translation initiation factor 2: A heterotrimeric tRNA carrier. FEBS Lett. 2010 Jan 21;584(2):405–12.
87. Kimball SR, Fabian JR, Pavitt GD, Hinnebusch AG, Jefferson LS. Regulation of guanine nucleotide exchange through phosphorylation of eukaryotic initiation factor eIF2alpha. Role of the alpha- and delta-subunits of eiF2b. J Biol Chem. 1998 May 22;273(21):12841–5.
88. Baird TD, Wek RC. Eukaryotic initiation factor 2 phosphorylation and translational control in metabolism. Adv Nutr. American Society for Nutrition; 2012 May 1;3(3):307–21.
89. Majumdar R, Bandyopadhyay A, Maitra U. Mammalian translation initiation factor eIF1 functions with eIF1A and eIF3 in the formation of a stable 40 S preinitiation complex. J Biol Chem. 2003 Feb 21;278(8):6580–7.
90. Asano K, Shalev A, Phan L, Nielsen K, Clayton J, Valásek L, et al. Multiple roles for the C-terminal domain of eIF5 in translation initiation complex assembly and GTPase activation. EMBO J. 2001 May 1;20(9):2326–37.
91. Gallie DR. The cap and poly(A) tail function synergistically to regulate mRNA translational efficiency. Genes Dev. 1991 Nov;5(11):2108–16.
92. Gingras A-C, Raught B, Sonenberg N. eIF4 Initiation Factors: Effectors of mRNA Recruitment to Ribosomes and Regulators of Translation. Annu Rev Biochem. 1999 Jun;68(1):913–63.
93. Berset C, Zurbriggen A, Djafarzadeh S, Altmann M, Trachsel H. RNA-binding activity of translation initiation factor eIF4G1 from Saccharomyces cerevisiae. RNA. Cold Spring Harbor Laboratory Press; 2003 Jul;9(7):871–80.
94. Wells SE, Hillner PE, Vale RD, Sachs AB. Circularization of mRNA by eukaryotic translation initiation factors. Mol Cell. 1998 Jul;2(1):135–40.
95. Morley SJ, Curtis PS, Pain VM. eIF4G: translation's mystery factor begins to yield its secrets. RNA. Cold Spring Harbor Laboratory Press; 1997 Oct;3(10):1085–104.
96. Kahvejian A, Roy G, Sonenberg N. The mRNA closed-loop model: the function of PABP and PABP-interacting proteins in mRNA translation. Cold Spring Harb Symp Quant Biol. 2001;66:293–300.
97. Villa N, Do A, Hershey JWB, Fraser CS. Human eukaryotic initiation factor 4G

(eIF4G) protein binds to eIF3c, -d, and -e to promote mRNA recruitment to the ribosome. J Biol Chem. American Society for Biochemistry and Molecular Biology; 2013 Nov 15;288(46):32932–40.

98. Thoreen CC, Chantranupong L, Keys HR, Wang T, Gray NS, Sabatini DM. A unifying model for mTORC1-mediated regulation of mRNA translation. Nature. 2012 May 3;485(7396):109–13.
99. Damoc E, Fraser CS, Zhou M, Videler H, Mayeur GL, Hershey JWB, et al. Structural Characterization of the Human Eukaryotic Initiation Factor 3 Protein Complex by Mass Spectrometry. Mol Cell Proteomics. 2007 Jul;6(7):1135–46.
100. Kozak M, Shatkin AJ. Migration of 40 S ribosomal subunits on messenger RNA in the presence of edeine. J Biol Chem. 1978 Sep 25;253(18):6568–77.
101. Hinnebusch AG. Structural Insights into the Mechanism of Scanning and Start Codon Recognition in Eukaryotic Translation Initiation. Trends Biochem Sci. 2017 Aug;42(8):589–611.
102. Martin-Marcos P, Nanda JS, Luna RE, Zhang F, Saini AK, Cherkasova VA, et al. Enhanced eIF1 binding to the 40S ribosome impedes conformational rearrangements of the preinitiation complex and elevates initiation accuracy. RNA. 2014 Feb 1;20(2):150–67.
103. Cheung Y-N, Maag D, Mitchell SF, Fekete CA, Algire MA, Takacs JE, et al. Dissociation of eIF1 from the 40S ribosomal subunit is a key step in start codon selection in vivo. Genes Dev. 2007 May 15;21(10):1217–30.
104. Algire MA, Maag D, Lorsch JR. Pi Release from eIF2, Not GTP Hydrolysis, Is the Step Controlled by Start-Site Selection during Eukaryotic Translation Initiation. Mol Cell. 2005 Oct 28;20(2):251–62.
105. Brina D, Grosso S, Miluzio A, Biffo S. Translational control by 80S formation and 60S availability: The central role of eIF6, a rate limiting factor in cell cycle progression and tumorigenesis. Cell Cycle. 2011 Oct 15;10(20):3441–6.
106. Unbehaun A, Marintchev A, Lomakin IB, Didenko T, Wagner G, Hellen CUT, et al. Position of eukaryotic initiation factor eIF5B on the 80S ribosome mapped by directed hydroxyl radical probing. EMBO J. European Molecular Biology Organization; 2007 Jul 11;26(13):3109–23.
107. Acker MG, Shin B-S, Nanda JS, Saini AK, Dever TE, Lorsch JR. Kinetic Analysis of Late Steps of Eukaryotic Translation Initiation. J Mol Biol. 2009

Jan 16;385(2):491–506.

108. Spilka R, Ernst C, Mehta AK, Haybaeck J. Eukaryotic translation initiation factors in cancer development and progression. Cancer Lett. 2013 Oct;340(1):9–21.
109. Ali MU, Ur Rahman MS, Jia Z, Jiang C. Eukaryotic translation initiation factors and cancer. Tumor Biol. 2017 Jun 27;39(6):101042831770980.
110. Fletcher CM, Pestova T V., Hellen CUT, Wagner G. Structure and interactions of the translation initiation factor eIF1. EMBO J. 1999 May 4;18(9):2631–7.
111. Sheikh MS, Fornace AJ. Regulation of translation initiation following stress. Oncogene. 1999 Nov 4;18(45):6121–8.
112. Yi T, Arthanari H, Akabayov B, Song H, Papadopoulos E, Qi HH, et al. eIF1A augments Ago2-mediated Dicer-independent miRNA biogenesis and RNA interference. Nat Commun. 2015 May 28;6(1):7194.
113. Harding HP, Zhang Y, Zeng H, Novoa I, Lu PD, Calfon M, et al. An integrated stress response regulates amino acid metabolism and resistance to oxidative stress. Mol Cell. 2003 Mar;11(3):619–33.
114. Tuval-Kochen L, Paglin S, Keshet G, Lerenthal Y, Nakar C, Golani T, et al. Eukaryotic Initiation Factor 2α - a Downstream Effector of Mammalian Target of Rapamycin - Modulates DNA Repair and Cancer Response to Treatment. Glinskii VV, editor. PLoS One. 2013 Oct 25;8(10):e77260.
115. Lobo M V, Martín ME, Pérez MI, Alonso FJ, Redondo C, Alvarez MI, et al. Levels, phosphorylation status and cellular localization of translational factor eIF2 in gastrointestinal carcinomas. Histochem J. 2000 Mar;32(3):139–50.
116. Perkins DJ, Barber GN. Defects in translational regulation mediated by the alpha subunit of eukaryotic initiation factor 2 inhibit antiviral activity and facilitate the malignant transformation of human fibroblasts. Mol Cell Biol. American Society for Microbiology (ASM); 2004 Mar;24(5):2025–40.
117. Benne R, Hershey JW. Purification and characterization of initiation factor IF-E3 from rabbit reticulocytes. Proc Natl Acad Sci U S A. 1976 Sep;73(9):3005–9.
118. Haybaeck J, O'Connor T, Spilka R, Spizzo G, Ensinger C, Mikuz G, et al. Overexpression of p150, a part of the large subunit of the eukaryotic translation initiation factor 3, in colon cancer. Anticancer Res. 2010 Apr;30(4):1047–55.

119. Pincheira R, Chen Q, Zhang J-T. Identification of a 170-kDa protein over-expressed in lung cancers. Br J Cancer. 2001 Jun 5;84(11):1520–7.
120. Spilka R, Ernst C, Bergler H, Rainer J, Flechsig S, Vogetseder A, et al. eIF3a is over-expressed in urinary bladder cancer and influences its phenotype independent of translation initiation. Cell Oncol. 2014 Aug 29;37(4):253–67.
121. Loftus BJ, Kim UJ, Sneddon VP, Kalush F, Brandon R, Fuhrmann J, et al. Genome duplications and other features in 12 Mb of DNA sequence from human chromosome 16p and 16q. Genomics. 1999 Sep 15;60(3):295–308.
122. Zhang L, Pan X, Hershey JWB. Individual Overexpression of Five Subunits of Human Translation Initiation Factor eIF3 Promotes Malignant Transformation of Immortal Fibroblast Cells. J Biol Chem. 2007 Feb 23;282(8):5790–800.
123. Piserà A, Campo A, Campo S. Structure and functions of the translation initiation factor eIF4E and its role in cancer development and treatment. J Genet Genomics. 2018 Jan 20;45(1):13–24.
124. Feoktistova K, Tuvshintogs E, Do A, Fraser CS. Human eIF4E promotes mRNA restructuring by stimulating eIF4A helicase activity. Proc Natl Acad Sci. 2013 Aug 13;110(33):13339–44.
125. De Benedetti A, Graff JR. eIF-4E expression and its role in malignancies and metastases. Oncogene. 2004 Apr 19;23(18):3189–99.
126. Haghighat A, Mader S, Pause A, Sonenberg N. Repression of cap-dependent translation by 4E-binding protein 1: competition with p220 for binding to eukaryotic initiation factor-4E. EMBO J. 1995 Nov 15;14(22):5701–9.
127. Kim SH, Miller FR, Tait L, Zheng J, Novak RF. Proteomic and phosphoproteomic alterations in benign, premalignant and tumor human breast epithelial cells and xenograft lesions: Biomarkers of progression. Int J Cancer. 2009 Jun 15;124(12):2813–28.
128. Graff JR, Konicek BW, Lynch RL, Dumstorf CA, Dowless MS, McNulty AM, et al. eIF4E Activation Is Commonly Elevated in Advanced Human Prostate Cancers and Significantly Related to Reduced Patient Survival. Cancer Res. 2009 May 1;69(9):3866–73.
129. Buxade M, Parra-Palau JL, Proud CG. The Mnks: MAP kinase-interacting kinases (MAP kinase signal-integrating kinases). Front Biosci. 2008 May 1;13:5359–73.
130. Carter JH, Deddens JA, Spaulding IV NR, Lucas D, Colligan BM, Lewis TG,

et al. Phosphorylation of eIF4E serine 209 is associated with tumour progression and reduced survival in malignant melanoma. Br J Cancer. 2016 Feb 4;114(4):444–53.

131. Robichaud N, del Rincon S V, Huor B, Alain T, Petruccelli LA, Hearnden J, et al. Phosphorylation of eIF4E promotes EMT and metastasis via translational control of SNAIL and MMP-3. Oncogene. 2015 Apr 9;34(16):2032–42.
132. Proud CG. Mnks, eIF4E phosphorylation and cancer. Biochim Biophys Acta - Gene Regul Mech. 2015 Jul;1849(7):766–73.
133. Bauer C, Brass N, Diesinger I, Kayser K, Grässer FA, Meese E. Overexpression of the eukaryotic translation initiation factor 4G (eIF4G-1) in squamous cell lung carcinoma. Int J cancer. 2002 Mar 10;98(2):181–5.
134. Braunstein S, Karpisheva K, Pola C, Goldberg J, Hochman T, Yee H, et al. A hypoxia-controlled cap-dependent to cap-independent translation switch in breast cancer. Mol Cell. 2007 Nov 9;28(3):501–12.
135. Badura M, Braunstein S, Zavadil J, Schneider RJ. DNA damage and eIF4G1 in breast cancer cells reprogram translation for survival and DNA repair mRNAs. Proc Natl Acad Sci U S A. 2012 Nov 13;109(46):18767–72.
136. Si K, Das K, Maitra U. Characterization of multiple mRNAs that encode mammalian translation initiation factor 5 (eIF-5). J Biol Chem. 1996 Jul 12;271(28):16934–8.
137. Kozel C, Thompson B, Hustak S, Moore C, Nakashima A, Singh CR, et al. Overexpression of eIF5 or its protein mimic 5MP perturbs eIF2 function and induces *ATF4* translation through delayed re-initiation. Nucleic Acids Res. 2016 Oct 14;44(18):8704–13.
138. Golob-Schwarzl N, Schweiger C, Koller C, Krassnig S, Gogg-Kamerer M, Gantenbein N, et al. Separation of low and high grade colon and rectum carcinoma by eukaryotic translation initiation factors 1, 5 and 6. Oncotarget. Impact Journals, LLC; 2017 Nov 24;8(60):101224–43.
139. Miluzio A, Beugnet A, Volta V, Biffo S. Eukaryotic initiation factor 6 mediates a continuum between 60S ribosome biogenesis and translation. EMBO Rep. 2009 May 17;10(5):459–65.
140. Rosso P, Cortesina G, Sanvito F, Donadini A, Di Benedetto B, Biffo S, et al. Overexpression of p27BBP in head and neck carcinomas and their lymph node metastases. Head Neck. 2004 May;26(5):408–17.

141. Sanvito F, Vivoli F, Gambini S, Santambrogio G, Catena M, Viale E, et al. Expression of a highly conserved protein, p27BBP, during the progression of human colorectal cancer. Cancer Res. 2000 Feb 1;60(3):510–6.
142. Ceci M, Gaviraghi C, Gorrini C, Sala LA, Offenhäuser N, Marchisio PC, et al. Release of eIF6 (p27BBP) from the 60S subunit allows 80S ribosome assembly. Nature. 2003 Dec 4;426(6966):579–84.
143. Gandin V, Miluzio A, Barbieri AM, Beugnet A, Kiyokawa H, Marchisio PC, et al. Eukaryotic initiation factor 6 is rate-limiting in translation, growth and transformation. Nature. 2008 Oct 2;455(7213):684–8.
144. Chendrimada TP, Finn KJ, Ji X, Baillat D, Gregory RI, Liebhaber SA, et al. MicroRNA silencing through RISC recruitment of eIF6. Nature. 2007 Jul 16;447(7146):823–8.
145. Flavin RJ, Smyth PC, Finn SP, Laios A, O'Toole SA, Barrett C, et al. Altered eIF6 and Dicer expression is associated with clinicopathological features in ovarian serous carcinoma patients. Mod Pathol. 2008 Jun 7;21(6):676–84.
146. Wang S, Liu Y, Yao M, Jin J. Eukaryotic Translation Initiation Factor 3a (eIF3a) Promotes Cell Proliferation and Motility in Pancreatic Cancer. J Korean Med Sci. 2016 Oct;31(10):1586.
147. Yu Y, Tian L, Feng X, Cheng J, Gong Y, Liu X, et al. eIF4E-phosphorylation-mediated Sox2 upregulation promotes pancreatic tumor cell repopulation after irradiation. Cancer Lett. 2016 May 28;375(1):31–8.
148. Kumar K, Chow CR, Ebine K, Arslan AD, Kwok B, Bentrem DJ, et al. Differential Regulation of ZEB1 and EMT by MAPK-Interacting Protein Kinases (MNK) and eIF4E in Pancreatic Cancer. Mol Cancer Res. 2016 Feb 1;14(2):216–27.
149. Martineau Y, Azar R, Müller D, Lasfargues C, El Khawand S, Anesia R, et al. Pancreatic tumours escape from translational control through 4E-BP1 loss. Oncogene. Nature Publishing Group; 2014 Mar 13;33(11):1367–74.
150. Fujimura K, Wright T, Strnadel J, Kaushal S, Metildi C, Lowy AM, et al. A Hypusine-eIF5A-PEAK1 Switch Regulates the Pathogenesis of Pancreatic Cancer. Cancer Res. 2014 Nov 15;74(22):6671–81.
151. Fujimura K, Choi S, Wyse M, Strnadel J, Wright T, Klemke R. Eukaryotic Translation Initiation Factor 5A (EIF5A) Regulates Pancreatic Cancer Metastasis by Modulating RhoA and Rho-associated Kinase (ROCK) Protein

Expression Levels. J Biol Chem. 2015 Dec 11;290(50):29907–19.
152. Strnadel J, Choi S, Fujimura K, Wang H, Zhang W, Wyse M, et al. eIF5A-PEAK1 Signaling Regulates YAP1/TAZ Protein Expression and Pancreatic Cancer Cell Growth. Cancer Res. 2017 Apr 15;77(8):1997–2007.
153. Doldan A, Chandramouli A, Shanas R, Bhattacharyya A, Cunningham JT, Nelson MA, et al. Loss of the eukaryotic initiation factor 3f in pancreatic cancer. Mol Carcinog. 2008 Mar;47(3):235–44.
154. Shi J, Kahle A, Hershey JWB, Honchak BM, Warneke JA, Leong SPL, et al. Decreased expression of eukaryotic initiation factor 3f deregulates translation and apoptosis in tumor cells. Oncogene. 2006 Aug 10;25(35):4923–36.
155. Ansari D, Carvajo M, Bauden M, Andersson R. Pancreatic cancer stroma: controversies and current insights. Scand J Gastroenterol. 2017 Jul 3;52(6–7):641–6.
156. Castilho-Valavicius B, Yoon H, Donahue TF. Genetic characterization of the Saccharomyces cerevisiae translational initiation suppressors sui1, sui2 and SUI3 and their effects on HIS4 expression. Genetics. 1990;124(3).
157. Lian Z, Pan J, Liu J, Zhang S, Zhu M, Arbuthnot P, et al. The translation initiation factor, hu-Sui1 may be a target of hepatitis B X antigen in hepatocarcinogenesis. Oncogene. 1999 Mar 4;18(9):1677–87.
158. Fijalkowska D, Verbruggen S, Ndah E, Jonckheere V, Menschaert G, Van Damme P. eIF1 modulates the recognition of suboptimal translation initiation sites and steers gene expression via uORFs. Nucleic Acids Res. Oxford University Press; 2017 Jul 27;45(13):7997–8013.
159. Baird TD, Wek RC. Eukaryotic initiation factor 2 phosphorylation and translational control in metabolism. Adv Nutr. 2012 May 1;3(3):307–21.
160. Koritzinsky M, Rouschop KMA, van den Beucken T, Magagnin MG, Savelkouls K, Lambin P, et al. Phosphorylation of eIF2α is required for mRNA translation inhibition and survival during moderate hypoxia. Radiother Oncol. 2007 Jun;83(3):353–61.
161. Erkan M, Kurtoglu M, Kleeff J. The role of hypoxia in pancreatic cancer: a potential therapeutic target? Expert Rev Gastroenterol Hepatol. 2016 Mar 3;10(3):301–16.
162. Zhao W, Li X, Wang J, Wang C, Jia Y, Yuan S, et al. Decreasing Eukaryotic Initiation Factor 3C (EIF3C) Suppresses Proliferation and Stimulates

Apoptosis in Breast Cancer Cell Lines Through Mammalian Target of Rapamycin (mTOR) Pathway. Med Sci Monit. 2017 Aug 30;23:4182–91.

163. Shintani T, Higashisaka K, Maeda M, Hamada M, Tsuji R, Kurihara K, et al. Eukaryotic translation initiation factor 3 subunit C is associated with acquired resistance to erlotinib in non-small cell lung cancer. Oncotarget. 2018 Dec 25;9(101):37520–33.
164. Scoles DR, Yong WH, Qin Y, Wawrowsky K, Pulst SM. Schwannomin inhibits tumorigenesis through direct interaction with the eukaryotic initiation factor subunit c (eIF3c). Hum Mol Genet. 2006 Apr 1;15(7):1059–70.
165. Zhu W, Li GX, Chen HL, Liu XY. The role of eukaryotic translation initiation factor 6 in tumors. Oncol Lett. Spandidos Publications; 2017 Jul;14(1):3–9.
166. Gantenbein N, Bernhart E, Anders I, Golob-Schwarzl N, Krassnig S, Wodlej C, et al. Influence of eukaryotic translation initiation factor 6 on non–small cell lung cancer development and progression. Eur J Cancer. 2018 Sep;101:165–80.
167. Bhat M, Robichaud N, Hulea L, Sonenberg N, Pelletier J, Topisirovic I. Targeting the translation machinery in cancer. Nat Rev Drug Discov. 2015 Mar 6;14(4):261–78.